Palestine Polytechnic University

Deanship of Graduate Studies and Scientific Research

Master of Civil Engineering

Forensic Structural Assessment and Rehabilitation of an Existing Steel Truss Industrial Building: A Case Study

Student Name:

Mohammed Ahmed ALBASHA

Supervisor:

Dr. Belal Almassri

Thesis submitted in partial fulfillment of requirements of the degree

Master of Civil Engineering

May 2026

The undersigned hereby certify that they have read, examined and recommended to the Deanship of Graduate Studies and Scientific Research at Palestine Polytechnic University:

Forensic Structural Assessment and Rehabilitation of an Existing Steel Truss Industrial Building: A Case Study

Mohammed Ahmed ALBASHA

in partial fulfillment of the requirements for the degree of Master in Civil Engineering.

Graduate Advisory Committee:

Prof./Dr. ……,……..

(Supervisor), University (typed)

Signature: _____ Date: _____

Prof./ Dr. ……, ……..

(Co-supervisor), University (typed)

Signature: _____ Date: _____

Prof./Dr……,……..

(Internal committee member), University (typed).

Signature: _____ Date: _____

Prof./Dr. ……,……..

(External committee member), University (typed).

Signature: _____ Date: _____

Thesis Approved by:

Name:

Dean of Graduate Studies & Scientific Research

Palestine Polytechnic University

Signature:……...……

Date:…..……...……

DECLARATION

I declare that the Master Thesis entitled " **Forensic Structural Assessment and Rehabilitation of an Existing Steel Truss Industrial Building** " is my own original work, and I hereby certify that unless stated, all work contained within this thesis is my own independent research and has not been submitted for the award of any other degree at any institution, except where due acknowledgement is made in the text.

Student Name…….

Signature: ———————————— Date:————————

DEDICATION

To the ones who sparked our curiosity,
and maneuvered our minds towards the direction of exploring, questioning, and finally discovering...

To the sagacious mentors and the educators who transformed every obstacle into a lesson, and every uncertainty into an avenue for personal development and self-improvement...

To the ones who not only facilitated our understanding but also our development, motivating us to exceed the limits we previously deemed unbreakable...

To the loved ones, whose constant affection, endurance, and help
uplifted us in the toughest times...

This research is a modest recognition of your direction, sacrifices, and motivation,
a sincere recognition to those who illuminate the way for others,
bringing dreams to life and turning aspirations into reality.

ACKNOWLEDGEMENT

I extend my deepest gratitude to **Palestine Polytechnic University, College of Engineering, Civil Engineering Department**, and to all the esteemed faculty members, whose guidance and support created a fertile environment for knowledge and excellence.
My heartfelt appreciation goes to my supervisor, **Dr. Belal Almassri**, who has been a guiding light at every step of this journey, inspiring me to overcome challenges, and generously sharing his wisdom and expertise.

I would also like to thank all my instructors, who illuminated my path with their knowledge, shared their invaluable experiences, and inspired me to grow into a confident engineer ready to face the future.

Finally, I dedicate my sincerest gratitude to my beloved family, whose patience, unwavering support, and constant presence provided me with the strength and inspiration to complete this academic journey. Without them, this work would not have been possible.

Table of Contents

ABSTRACT ..... **i**
DEDICATION ..... **ii**
ACKNOWLEDGEMENT ..... **iii**
CONTENTS ..... **iv**
LIST OF FIGURES ..... **vi**
LIST OF TABLES ..... **vii**
CHAPTER 1: INTRODUCTION 1
1.1 Background 1
1.2 Problem Statement 3
1.3 Research Objectives and Methodology 5
1.3.1 Research Objectives 5
1.3.2 Research Methodology 6
1.4 Scope of the Research 6
1.5 Significance and Impact of the Research 7
1.6 Research Contributions 8
CHAPTER 2: ADVANCED LITERATURE REVIEW 9
2.1 Introduction: The Forensic Engineering Paradigm 9
2.2 Stability Methodologies: The Forensic Application of ELM in Non-Engineered Contexts 10
2.2.1 Traditional Literature: The Idealized Approach 10
2.2.2 Comparative Analysis of Stability Frameworks 11
2.2.3 Discussion of Methodological Divergence 11
2.3 Research Gaps and Scientific Novelty 12
2.3.1 Comparative Matrix of Research Dimensions 12
2.3.2 Synthesizing the Forensic Approach 13
2.4 The Methodology of Structural Mirroring in As-Built Reconstruction 13
2.4.1 Comparison with Conventional Modeling Approaches 13
2.4.2 Comparative Advantages of the Mirroring Approach 14
2.4.3 Supporting the Recovery Plan 14
2.5 Impact of Atmospheric Corrosion on Residual Structural Capacity 15
2.6 Wind Topographic Amplification and Internal Pressure Dynamics in Mountainous Regions 16
2.7 Structural Mechanics of Non-Standard Hand-Welded and Semi-Rigid Connections 17
2.8 Structural Mechanics and Capacity Enhancement of Built-up Laced Columns 18
2.9 Comparative Review of Previous Studies 19
2.10 Literature on In-Situ Structural Retrofitting, Analytical Formulations, and Strengthening Techniques 20
2.10.1 Built-up and Laced Column Upgrading 20
2.10.2 Strengthening and Steel Sleeving (Jacketing) of Deteriorated Tubular (CHS) Members 22
2.10.3 Integration of Lateral Bracing Systems and Stiffness Demand 24
2.10.4 Purlin System Rectification and Combined Axial-Flexural Interaction 25
2.10.5 Substructure Anchorage and Base Plate Remediations 26
CHAPTER 3: FIELD INVESTIGATION, STRUCTURAL ASSESSMENT, AND LOADING ANALYSIS 29
3.1 Description of the Studied Industrial Steel Building 29
3.2 Structural Assessment and Causes of Deterioration in Steel Structures 30
3.2.1 Causes of Deterioration in Steel Structures 31
3.2.2 Steel Structure Assessment Procedure 33
3.3 Existing Structural Deficiencies and Performance Issues 33
3.4 Field Inspection Results 34
3.5 Structural System Idealization and Modeling Assumptions 41
3.6 Load Calculation 42

3.6.1 Dead Loads 42
3.6.2 Live Loads 43
3.6.3 Rain Load 47
3.6.4 Snow Load 47
3.6.5 Wind Loads 49
3.6.5.1 Introduction 49
3.6.5.2 Design Wind Speed 49
3.6.5.3 Exposure Category 50
3.6.5.4 Building Height and Elevation-Dependent Factors 50
3.6.5.5 Velocity Pressure Calculation 52
3.6.5.6 External Pressure Coefficients for the Roof 52
3.6.5.7 Internal Pressure Coefficient 53
3.6.5.8 Wind Pressure Coefficients and Roof Angle Interpolation 54
3.6.5.9 Design Wind Pressure Evaluation 56
3.6.6 Seismic Analysis 59
3.6.6.1 Introduction 60
3.6.6.2 Seismic Hazard Parameters 60
3.6.6.3 Site Coefficients and Design Spectrum 60
3.6.6.4 Seismic Force Resisting System 61
3.6.6.5 Fundamental Period Calculation 62
3.6.6.5.1 Steel System Not Specifically Detailed for Seismic Resistance 62
3.6.6.6 Seismic Response Coefficient 63
3.6.6.6.1 Moment-Resisting Frame 63
3.6.6.7 Base Shear Calculation 63
3.6.7 Wind–Seismic Load Comparison and Governing Load Case 63
CHAPTER 4: STRUCTURAL ASSESSMENT AND DESIGN VERIFICATION 64
4.1 Introduction 64
4.2 Development of the Structural Model 65
4.2.1 Structural Sections and Profile Assignments 66
4.3 Modeling Assumptions and Simplifications 67
4.4 Parametric Study on Section Loss and Column Inclination 68
4.4.1 Scientific Basis for Considering Section Loss 69
4.4.2 Effect of Section Loss 69
4.4.3 Scientific Basis for Considering Column Inclination 71
4.4.4 Effect of Column Inclination 71
4.4.5 Interaction Between Section Loss and Column Inclination 73
4.4.6 Summary of Parametric Study 73
4.5 Structural Observations Based on Site Inspection 74
4.5.1 Wind Load Classification 74
4.5.2 Truss Configuration and Load Transfer Deficiencies 75
4.5.3 Absence and Discontinuity of the Bracing System 75
4.6 Load Application and Combinations 76
4.7 Structural Analysis Results and Design Verification 78
4.7.1 Phase I: Internal Force Distribution and Structural Behavior 78
4.7.2 Failure Analysis and Discussion 80
4.7.3 Detailed Member Design Checks 81
4.8 Summary of Analytical Findings 83
CHAPTER 5: PROPOSED STRUCTURAL SOLUTIONS, REHABILITATION STRATEGY, AND LIFE-CYCLE COST ANALYSIS 85
5.1 Introduction and Overview of Solutions 85
5.2 Option 1: Full Structural Replacement with Rigid Portal Frame System 87
5.3 Option 2: In-Situ Structural Rehabilitation and Strengthening of the Existing Truss System 90
5.3.1 Engineered Column-Trussing Retrofitting Scheme 90
5.3.2 Design Basis, Structural Mechanics, and Code Compliance 92

5.3.3 Roof Truss Component Optimization and Purlin Modification 93
5.3.4 Substructure Anchorage and Connection Remediation 94
5.3.5 Finite Element Numerical Verification of the Retrofitted Framework 96
5.3.6 Phase I: Post-Retrofitting Internal Force Distribution and Structural Behavior 99
5.3.7 Phase II: Global Capacity Re-Verification and Stress Ratio Envelope 102
5.3.8 Advanced Numerical Verification of Critical Connections 103
5.4 Comparison of the Structure Before and After Rehabilitation 105
5.5 Technical and Economic Evaluation: Retrofitting vs. Replacement 107
5.6 Life-Cycle Cost Analysis 108
5.6.1 Cost Components of Full Structural Replacement 110
5.6.2 Cost Components of In-Situ Rehabilitation 111
5.6.3 LCCA Comparison Between Replacement and Rehabilitation 112
5.6.4 Adopted Service Life for LCCA 113
5.7 Technical and Economic Evaluation 114
5.8 Chapter Summary 116
CHAPTER 6: CONCLUSIONS AND RECOMMENDATIONS 119
6.1 Introduction 119
6.2 Main Conclusions 119
6.2.1 Forensic Diagnostic and Legacy Condition Conclusions 119
6.2.2 Numerical Re-Verification and Retrofitting Conclusions 120
6.2.3 Technical and Economic Conclusions 121
6.3 Recommendations for Engineering Practice 122
6.4 Future Research Horizons 123
REFERENCE LIST 124

List of Abbreviations

ACI	American Concrete Institute
AISC	American Institute of Steel Construction
AISI	American Iron and Steel Institute
ASCE	American Society of Civil Engineers
AWS	American Welding Society
CBFEM	Component-Based Finite Element Method
CFD	Computational Fluid Dynamics
CHS	Circular Hollow Section
D/C	Demand-to-Capacity Ratio
DAM	Direct Analysis Method
ELM	Effective Length Method
FEM	Finite Element Method
FEA	Finite Element Analysis
GMNA	Geometrically and Materially Nonlinear Analysis
LCCA	Life-Cycle Cost Analysis
LFRS	Lateral Force-Resisting System
LRFD	Load and Resistance Factor Design
NDT	Non-Destructive Testing
PEB	Pre-Engineered Building
RHS	Rectangular Hollow Section
STAAD.Pro	Structural Analysis and Design Software
ULS	Ultimate Limit State
WPS	Welding Procedure Specification

List of Figures

Figure 2.1: Mechanical transformation, web lattice activation, and geometric parameters of the engineered built-up laced column retrofitting scheme for legacy CHS members (Adapted from Ziemian, 2010; AISC 360-16; Dar et al., 2018). 22
Figure 2.2: Geometric configuration, dimensions (Ø89.1 × 3.2 mm), and artificial pitting corrosion damage parameters (H ×W) on circular hollow steel (CHS) tubular test specimens (Source: Ahn et al., 2018). 23
Figure 2.3: Experimental configuration versus Finite Element Analysis (FEA) Von Mises stress distributions and progressive local/lateral buckling failure modes of locally corroded CHS tubular columns: (a) initial elastic state, (b) intermediate localized yielding, and (c) ultimate failure under axial compression (Source: Ahn et al., 2018). 24
Figure 2.4: Typical engineered purlin cleat connection detail and arched truss configuration demonstrating nodal load transfer mechanisms to eliminate secondary bending moments. 26
Figure 3.1: Field inspection and site survey conducted to document the as-built geometry of the existing industrial building 30
Figure 3.2: Non-engineered mid-height welded splice in a circular hollow steel column, showing local deformation, surface indentation, and coating damage 36
Figure 3.3: Deficient column-base connection showing inadequate anchor bolt arrangement, poor base plate detailing, and lack of proper grout finishing.....37
Figure 3.4: Local coating damage and surface corrosion observed on a circular hollow steel column 38
Figure 3.5: Local impact damage and surface indentation observed on a circular hollow steel column, accompanied by coating deterioration 39
Figure 3.6: Field survey process showing discontinuous X-bracing in the background of the industrial steel building 40
Figure 3.7: Determination of site elevation using a surveying instrument for the calculation of the basic ground snow load 48
Figure 3.8: Ground snow load calculation and sloped roof shape coefficients 49
Figure 4.1: 3D analytical model of the industrial building generated in STAAD.Pro, highlighting the proposed longitudinal bracing system and end-wall column extensions (in red) required for global stability 65
Figure 4.2: Three-dimensional analytical wireframe model of the existing steel truss building developed in STAAD.Pro based on field measurements 66
Figure 4.3: Transverse cross-section of the existing steel warehouse showing overall geometry and structural member sizes 66
Figure 4.4: Axial force diagram for the main truss and column frame 78
Figure 4.5: Shear force diagram for the primary structural frame 79
Figure 4.6: Bending moment diagram showing the locations of maximum stress 79
Figure 4.7: Detailed numerical stress ratios for the structural frame, where members with a ratio greater than 1.0 indicate structural failure 80
Figure 4.8: Design check report snippet for the critical primary column, indicating insufficient capacity under governing loads 81
Figure 4.9: Detailed design check for the truss top chord member failing under combined axial compression and bending 82
Figure 4.10: Detailed design check for a truss diagonal web member successfully passing the code requirements 82
Figure 4.11: Detailed design verification for the truss top chord member failing under combined axial

compression and bending 83
Figure 5.1: Three-dimensional analytical finite element model illustrating the engineered column-trussing retrofitting scheme 90
Figure 5.2: Engineered retrofitted hollow base plate and anchorage assembly..... 93
Figure 5.3: STAAD.Pro post-retrofitting design check report for Beam No. 1106..... 95
Figure 5.4: STAAD.Pro post-retrofitting design check report for Beam No. 830 95
Figure 5.5: STAAD.Pro post-retrofitting design check report for Beam No. 990..... 96
Figure 5.6: STAAD.Pro post-retrofitting design check report for Beam No. 1127..... 97
Figure 5.7: STAAD.Pro post-retrofitting design check report for Beam No. 1150..... 97
Figure 5.8: STAAD.Pro post-retrofitting design check report for Beam No. 1170.....98
Figure 5.9: Axial force diagram for the retrofitted main truss and column frame 99
Figure 5.10: Shear force diagram for the retrofitted primary structural frame.....99
Figure 5.11: Bending moment diagram for the retrofitted structural frame.....100
Figure 5.12: Global frame stress-ratio envelope after retrofitting.....101
Figure 5.13: CBFEM numerical evaluation of the retrofitted truss apex connection.....104

List of Tables

Table 2.1: Comparison of stability methodologies and structural contexts in industrial steel research 11
Table 2.2: Research gaps and scientific novelty of the current study 12
Table 2.3: Comparative advantages of structural mirroring versus idealized modeling 14
Table 2.4: Impact of localized 10% section loss on mechanical properties 15
Table 2.5: Comparison of boundary condition idealizations and forensic risks 17
Table 2.6: Comparative summary of previous studies and research gaps 19
Table 2.7: Summary of Literature-Based Retrofitting Techniques, Governing Equations, and Application to the Case Study.....28
Table 3.1: The main field inspection findings are summarized..... 34
Table 3.2: Snow loads based on elevation above sea level 47
Table 3.3: Determination of velocity pressure exposure coefficient based on ASCE 7-16 51
Table 3.4: Wind directionality factor specified by ASCE 7-16 for structural design 52
Table 3.5: Interpolated external roof pressure coefficients 53
Table 3.6: Wind pressure equation and internal pressure coefficient (GCpi) selection.....55
Table 3.7: External wind pressure coefficients (GCpf) for Load Cases A and B 55
Table 3.8: Linear interpolation of external pressure coefficients for Load Case A 56
Table 3.9: External and internal pressure coefficients for the transverse wind direction. 56
Table 3.10: Design wind pressures for the transverse direction under Load Case 1 57
Table 3.11: Design wind pressures for the transverse direction under Load Case 2 57
Table 3.12: External and internal pressure coefficients for the longitudinal wind direction....57
Table 3.13: Design wind pressures for the longitudinal direction under internal pressure Case 1 57
Table 3.14: Design wind pressures for the longitudinal direction under internal pressure Case 2 58
Table 3.15: ASCE 7 tabulated importance factors based on the building risk category 59
Table 3.16: Determination of the short-period and long-period seismic site coefficients based on ASCE 7 provisions 60
Table 3.17: Seismic Design Category determination tables 61
Table 3.18: Approximate fundamental period parameters 62
Table 4.1: Summary of the assigned structural steel profiles, including European designations, physical dimensions, and cross-sectional properties 67
Table 4.2: Adopted section loss scenarios 70
Table 4.3: Adopted column inclination scenarios 72
Table 4.4: Applied load cases and load combinations 76
Table 5.1: CBFEM Verification Summary for Truss Apex Splice..... 103
Table 5.2: Comparison of structural condition before and after rehabilitation 105
Table 5.3: LCCA cost symbols 109
Table 5.4: Preliminary cost estimate for full structural replacement 110
Table 5.5: Replacement cost variables 111
Table 5.6: Rehabilitation cost variables 112
Table 5.7: Life-cycle cost comparison between replacement and rehabilitation 112
Table 5.8: Adopted service life for LCCA comparison 114
Table 5.9: Technical and economic evaluation of structural alternatives 114

Chapter 1: Introduction

1.1 Background

In modern structural engineering, **Forensic Engineering** has evolved into a crucial investigative discipline aimed at diagnosing structural deficiencies, uncovering the root causes of material performance failures, and evaluating the ultimate limit states of built infrastructure under extreme environmental conditions. Unlike traditional forward-design paradigms that rely heavily on ideal predictive models, forensic engineering operates on a diagnostic, reverse-engineering framework. It reconstructs structural failure paths and identifies systemic vulnerabilities to prevent future structural collapses. This diagnostic approach is particularly essential when auditing light-gauge and steel truss industrial assets—commonly termed hangars or workshops—which constitute a vast portion of the economic infrastructure in developing and rapidly expanding regions.

The construction of steel truss industrial facilities experienced a major increase during the last few decades because regional industrial development brought new construction projects to different areas. The industrial facilities which used this construction method became the most common building type because its design enabled quick construction and provided large functional work areas through its lightweight structural system. The construction industry built most of this building stock when municipal zoning regulations were not enforced and building projects lacked proper engineering supervision. The majority of these facilities were built through empirical methods while local fabricators constructed them without following international and local building codes.

This research examines regional vulnerability through a case study which uses a specific 25-year-old industrial hangar as its main research object . The building serves as a common example which represents the entire undocumented infrastructure that exists from that time period.

The selected structure was completely built by a local blacksmith who performed all traditional metal fabrication tasks without using any formal engineering design or structural calculation sheets or professional supervision. The audit process evaluates unengineered assets through their raw state which creates a true baseline assessment that identifies all hidden risks present in operating workshops.

Extreme weather conditions which occurred recently in the eastern Mediterranean region exposed all major design weaknesses that exist in unengineered steel structures that were built using empirical methods. The historic December 2013 snowstorm which became known as Storm "Alexa" marked a crucial point in history. The unprecedented meteorological event was caused by an intense polar air mass which originated from Siberia.

1) **Exceedance of Nominal Design Thresholds:** The absolute depth of the snow accumulation far surpassed the historical baseline values traditionally embedded in regional codes, which typically accounted for moderate design snow loads ranging from (0.5 - 1.5) KN/m^2

2) **Wet Snow Density Saturation:** The precipitation was characterized by a high moisture content and intermittent freezing rain, which sharply elevated the volumetric mass density of the snow blanket, thereby compounding the gravity load exerted on roof systems.

3) **Aerodynamic Snow Drifting:** High-velocity winds drove massive volumes of snow into highly asymmetric configurations, particularly at roof steps, valleys, and adjacent structural canopies.

This non-uniform accumulation generated severe eccentric loading, unexpected structural torsion, and stress concentrations that local framing components were never designed to redistribute.

The 2013 disaster led to complete operational collapse of multiple facilities which resulted in substantial financial losses and major interruptions of essential industrial supply networks. The Palestinian Central Bureau of Statistics (PCBS) and the Palestinian Economic Policy Research Institute (MAS) released post-disaster economic impact assessments which showed that agricultural and industrial infrastructure across the territory sustained direct financial losses exceeding 35 million USD.

Forensic engineering functions as an active disaster mitigation system after climate-driven hazards because its responsibilities extend beyond post-collapse analysis work. The evaluation process of this specific 25-year-old asset is uniquely complex because the building experienced disaster when Storm Alexa struck and brought about localized failure and partial structural collapse, which local authorities fixed through emergency unengineered reconstruction work by a blacksmith. Structural engineers need to evaluate how original structural weaknesses and undocumented post-failure improvements including extra columns and non-standard bracing elements work together. The forensic diagnostic method determines total plastic deformation and atmospheric corrosion environmental damage and residual stresses which developed from extreme loading experiences. Forensic retrofitting helps protect structural assets which improves economic resilience of regions through affordable solutions that substitute complete building demolition and reconstruction.

1.2 Problem Statement

A significant portion of the active regional infrastructure consists of industrial steel truss buildings which have existed for two and a half decades and remain operational despite severe structural jeopardy. The buildings present systemic vulnerabilities because their construction omitted essential professional engineering analysis together with strict material testing and quality control procedures required for safety compliance with current gravity wind and seismic standards.

The specific focus of this investigation is an existing, single-story industrial steel truss hangar estimated to be approximately 25 years old (erected circa the late 1990s or early 2000s). The building exists as the actual structural design which local fabricators made through their artisanal methods without any official engineering supervision and without any architectural blueprints or approved calculation documents. The facility's preliminary forensic field inspections together with its geometric mapping process have uncovered multiple structural deficiencies which develop into a complete system of critical structural failures.

Geometric Out-of-Plumbness: Minor to moderate misalignment within the main truss-supporting columns, contrasted by severe, high-degree out-of-plumbness (structural tilting) observed in the vertical columns of the independent rear frame extension.

- **Deficient Frame Extension & Non-Engineered Splicing:** The added rear section operates on an independent rigid frame system, where critical columns exhibit dangerous mid-height field-welded splices, representing a severe execution defect highly vulnerable to localized buckling under heavy snow drift accumulation.

- **Absence of Lateral Bracing:** A total lack of a defined vertical or horizontal lateral load-resisting system (sway or cross-bracing) across both the original truss and the added frame extension.

- **Deficient Foundation Anchorage:** Missing or structurally inadequate anchor bolts at the column-to-footing connections, severely limiting base boundary rigidity.

- **Substandard Execution:** Partial, discontinuous, and uncertified structural welds across major load-bearing nodes and connection gusset plates.

- **Atmospheric Degradation:** Advanced local corrosion resulting in critical cross-sectional loss (*section loss*) in members exposed to industrial moisture and poor ventilation.

Because this structure experienced partial collapse during Storm Alexa in 2013 and was subsequently reconstructed and modified using empirical, non-engineered methods, it currently poses a highly complex forensic puzzle. The post-failure modifications—characterized by randomly added columns, arbitrary steel bracing, and the structural patching done entirely by a local blacksmith—likely introduced unrecorded eccentricities, residual installation stresses, and unpredictable load distribution paths. Under modern operational demands, compounded by heavy suspended utilities and the ongoing threat of future climate-induced weather anomalies, these accumulated geometric imperfections and execution flaws severely impair the structure's limit state capacity. Without a systematic forensic evaluation and the implementation of targeted, code-compliant rehabilitation schemes, the facility poses an immediate risk of localized component failure, which could trigger a catastrophic progressive global collapse.

1.3 Research Objectives and Methodology

1.3.1 Research Objectives

The researcher used a forensic engineering framework to assess the structural safety and integrity of the industrial steel truss building which has stood for 25 years. The specific sub-objectives are to:

1.Conduct a forensic diagnostic assessment to quantify structural defects, geometric misalignments, and corrosion-induced section loss.

2.Investigate the structure's baseline capacity under extreme loading conditions, explicitly simulating its vulnerability to snow loads reminiscent of the 2013 storm, alongside modern ASCE 7 gravity, wind, and seismic combinations.

3.Identify the critical failure modes and bottleneck structural components that dictate the system's susceptibility to progressive collapse.

4. Develop engineered, cost-effective, and code-compliant (AISC 360) rehabilitation and retrofitting strategies to restore the asset's structural integrity.

1.3.2 Research Methodology

To achieve these objectives, the study implements a multi-phased forensic methodology:

- **Forensic Field Mapping:** Executing a comprehensive site survey to reconstruct the as-built geometry, map structural anomalies, and measure member cross-sections and connection configurations.
- **Degradation & Stress Analysis:** Quantifying material degradation (corrosion) and examining the historical impact of extreme loading environments on the surviving frame.
- **Advanced As-Built Numerical Modeling:** Generating a high-fidelity 3D structural model that accurately embeds the discovered field flaws (misalignments, missing braces, section loss).
- **Code-Based Demand Evaluation:** Executing structural analysis under **ASCE 7** and **AISC 360** criteria, with a dedicated parametric focus on extreme snow-load scenarios.
- **Retrofit Design & Validation:** Designing targeted structural interventions (e.g., member sleeving, connection upgrades, bracing integration) and validating their efficiency via post-rehabilitation modeling.

1.4 Scope of the Research

This research focuses on forensic structural assessment and rehabilitation design of an existing, single-story industrial steel truss hangar and its independent rear frame extension under gravity and lateral loading. The scope is limited to numerical simulation and deterministic structural analysis, and does not include destructive laboratory material testing.

The analysis considers modern ASCE 7 gravity, wind, and seismic combinations for the global as-built model, along with a dedicated parametric focus on extreme snow-load drifting scenarios reminiscent of Storm Alexa. Geometric misalignments, secondary stresses from suspended utilities, and non-engineered field-welded column splices are included in the models, while architectural, thermodynamic, and dynamic mechanical behaviors are excluded.

The study aims to evaluate the structural limit state response and validate code-compliant (AISC 360) retrofit interventions within these defined boundaries.

1.5 Significance and Impact of the Research

The research demonstrates important scientific value for both regional area and practical applications. The study moves from its first theoretical structural assessment phase into its second stage that deals with disaster mitigation and infrastructure resilience. The research uses a 2013 snowstorm vulnerability assessment to create a protective evaluation system that saves industrial assets throughout the entire region. The study uses forensic rehabilitation methods to create a framework that supports both economic development and environmental protection. The engineered methodology provides a safe building upgrading solution which helps industrial operators solve their financial problems through building rehabilitation instead of complete demolition. The process reduces environmental impact because it cuts down both carbon emissions and waste production which would occur during building demolition and new steel production while it supports engineering methods that help with climate adaptation.

1.6 Research Contributions

The thesis makes academic and practical contributions through its primary research findings which demonstrate two main results.

• **Forensic Case Study Integration:** The research provides a documented forensic engineering case study which shows how a 25-year-old steel asset without engineering design proves that construction errors lead to numerical code compliance problems.

• **Extreme Load Vulnerability Analysis:** The study measures how truss structures lose their failure point when they experience extreme weather conditions because of two factors which include column misalignment and material degradation.

• **Targeted Retrofitting Library:** The study developed multiple retrofitting solutions which require minimal operational disruption to solve problems at unengineered joints and missing anchorages and insufficient braces while meeting AISC 360 standards.

• **Resilience Framework:** The framework provides municipal authorities and consulting engineers with a standardized process which they can use to perform forensic assessments and create rehabilitation plans that protect industrial sectors from future climate dangers.

Chapter 2: Advanced Literature Review

Forensic Engineering, Stability Theory, and Assessment of Non-Engineered Steel Trusses

2.1 Introduction: The Forensic Engineering Paradigm

The evaluation of the structural integrity of legacy industrial steel truss buildings requires a fundamental shift toward comprehensive forensic diagnostic techniques and advanced stability assessment methods which move away from established design-based assessment approaches (Ratay, 2010). As emphasized in seminal forensic literature (Carper, 2001; Noon, 2000), the forensic engineering paradigm evaluates the actual performance of an existing structure through its in-situ state, its actual construction defects, and accumulated environmental damage according to current building codes. Conversely, prospective engineering design methods focus primarily on forward-looking predictions under idealized material and geometric configurations. This diagnostic framework becomes highly critical when evaluating industrial facilities that feature non-engineered extensions or components executed without formal technical documentation, professional engineering supervision, or material certification protocols—a scenario frequently highlighted in structural failure investigations (Ellingwood, 2005).

The research demonstrates a systematic forensic method which investigates second-order stability in aging steel infrastructures although standard prospective calculations can still be performed. In contrast to conventional design methods that assume material homogeneity and geometric perfection, the investigative framework gathers empirical field information about how geometric boundary changes and material degradation progress, while modern wind and seismic codes impose strict demand requirements on the surviving frame (Biediger, 2002). The analytical approach maintains structural responsibility by following both the American Society of Civil Engineers (ASCE 7-16) and American Institute of Steel Construction (AISC 360-16) regulatory requirements. As validated by modern stability assessment studies (Surovek & Ziemian, 2005), these standards govern the implementation of stability verification methods which specifically apply to non-standard boundary configurations that use the Effective Length Method (ELM) as their foundational structural assessment technique.

2.2 Stability Methodologies: The Forensic Application of ELM in Non-Engineered Contexts

The structural literature demonstrates a fundamental divergence regarding stability requirements and their analytical determination. The research employs the Effective Length Method (ELM) according to AISC 360-16 Appendix 7 because modern standards increasingly favor the Direct Analysis Method (DAM) for the economic optimization and streamlined design of new steel frames (Deierlein et al., 2002). The selection of ELM is not merely a methodological preference but a forensic necessity dictated by the specific requirements of assessing legacy industrial assets characterized by highly unpredictable execution configurations and geometric boundaries (Maleck, 2006).

2.2.1 Traditional Literature (The Idealized Approach)

- **Emphasis on Perfection**: Seminal **structural stability** works, such as those by **Ziemian (2010)** and **White & Griffith (2007)**, heavily emphasize stability in "perfect" frames where initial imperfections are modeled as minor theoretical perturbations, typically limited to standard code-allowable thresholds of L/500.
- **Standardized Assumptions**: Research focusing on modern **Pre-Engineered Buildings (PEBs)** often relies on rigid or idealized pinned connection assumptions, which may not reflect the highly complex semi-rigid behavior of hand-welded joints found in legacy structures.
- **Methodological Limitations**: Conventional literature often focuses on the **Direct Analysis Method (DAM)** for new design efficiency. However, in a forensic context DAM may obscure member-level vulnerabilities in existing structures by utilizing automated stiffness reductions that do not account for localized forensic defects.

2.2.2 Comparative Analysis of Stability Frameworks

To contextualize the methodological choice of this study, the following table compares the current approach with prevailing trends in structural research:

Table 2.1: Comparison of Stability Methodologies and Structural Contexts in Industrial Steel Research.

Feature	Modern Warehouse Research	Legacy Asset Assessment	Current Study (Al-Omari Building)
Primary Methodology	**Direct Analysis Method (DAM)**	**Effective Length Method (ELM)**	**ELM (AISC 360-16, App. 7)**
Structure Type	**Pre-engineered Buildings (PEB)**	**Historic Steel Bridges/Trusses**	**Non-engineered Industrial Trusses**
Connection Assumptions	**Rigid or Idealized Pinned**	**Riveted or Aged Joints**	**Hand-welded Semi-rigid Joints**
Stability Focus	**Global Frame Sensitivity (P-Δ)**	**Member-level Buckling**	**Forensic Member Capacity & K-factor Sensitivity**
Justification	**Optimized for new design economy**	**Suited for historic verification**	**Reflects in-situ connection vulnerabilities**

2.2.3 Discussion of Methodological Divergence

The majority of contemporary literature utilizes the Direct Analysis Method (DAM) to handle modern PEB design configurations because it requires less computational effort than determining member-specific K-factor values for typical redundant building systems. The studies usually depend on "idealized" conditions which assume that the entire structure maintains a fixed and uniform stiffness level.

The Al-Omari building's steel trusses present major challenges because they lack an official engineering design which makes joint stiffness measurement impossible. The ELM framework provides this research with a distinct forensic advantage: it allows for the manual modification of K-factors to effectively "penalize" specific members that exhibit dangerous unbraced lengths or compromised boundary conditions which automated stiffness reductions in DAM might otherwise obscure. Consequently, the ELM framework establishes a transparent reference baseline to evaluate how individual truss members perform during high lateral surge loads, seamlessly combining both seismic and wind assessments for a comprehensive structural evaluation.

2.3 Research Gaps and Scientific Novelty

The existing peer-reviewed studies primarily concentrate on designing better future systems while this research investigates the proper process to evaluate and reclaim steel industrial buildings which lack official engineering design status.

The scientific novelty of this work lies in the implementation of " As-Built Structural Modeling". The research establishes a connection between theoretical shop drawings and actual built structures through its use of in-situ geometric deviations and actual corrosion section loss and site-specific environmental data. The methodology creates an impartial foundation to confirm system stability which especially applies to systems that have reached their critical point of structural failure. The study used the mirroring method to discover that the critical canopy stress ratio reached 2.71 with primary column overstressing at 1.51, which traditional idealized models would predict lower than actual values.

2.3.1 Comparative Matrix of Research Dimensions

The following matrix highlights the scientific novelty of this work by bridging the gap between "Shop Drawing Design" and "As-Built Reality" in complex environments.

Table 2.2: Research Gaps and Scientific Novelty of the Current Study.

Research Dimension	Conventional Literature (Engineered Systems)	Current Study (Al-Omari Building - Ramallah)	Scientific Novelty
Geometry Assumption	Idealized, perfectly straight members with standard tolerances.	Structural Mirroring: Incorporating real-world out-of-plumbness (L/500).	Accounts for "Initial Imperfections" in non-engineered frames that exceed code limits.
Material Integrity	Assumptions based on nominal catalog properties and pristine steel.	Degradation Modeling: Incorporating actual section loss and corrosion effects.	Bridges the gap between "As-Designed" and the "As-Is" residual strength.
Stability Method	Predominantly DAM (Direct Analysis) for efficiency in new builds.	Forensic ELM: Manual derivation of K-factors for semi-rigid connectivity.	Provides a baseline for stability in structures with high connection uncertainty.
Load Path Analysis	Clearly defined and redundant Lateral Load Resisting Systems (LLRS).	Analysis of "Informal Load Paths" in systems lacking formal bracing.	Evaluates the "Hidden Resilience" or extreme vulnerability of modified trusses.
Environmental Context	Standard terrain assumptions (Exposure C) and low-altitude data.	Complex Topography (833m elevation): High Kzt and internal pressure dynamics.	Redefines "Governing Loads" for industrial structures in mountainous regions.

2.3.2 Synthesizing the Forensic Approach

The research presents scientific innovation through its development from theoretical idealization to the implementation of " As-Built Structural Modeling" method. The majority of research studies which focus on steel trusses through standard PEB warehouse analysis make structural perfection assumptions that do not reflect real-world conditions of historical industrial resources.

The study develops a local assessment framework through its use of in-situ geometric deviations material section loss and topographic wind amplification factors that are specific to the Ramallah highlands. The methodology develops a scientific foundation which enables future recovery plan implementation while assessing infrastructure rehabilitation strategies for "non-engineered" industrial sites based on technical requirements and economic viability.

2.4 The Methodology of Structural Mirroring in As-Built Reconstruction

The concept of "Structural Mirroring" represents a paradigm shift from idealized modeling to the creation of a High-Fidelity Digital Twin. The study uses isomorphic mapping to convert the actual building defects of Al-Omari building into the analytical space whereas traditional engineering methods depend on standard architectural drawings.

2.4.1 Comparison with Conventional Modeling Approaches

To validate the necessity of this approach, it is essential to contrast the "Mirroring" methodology with traditional simplifications found in structural literature:

1) Idealized vs. Real Geometry: Traditional studies, such as the seminal work by Ziemian (2010) and White & Griffith (2007), emphasize stability in "perfect" frames where initial imperfections are modeled as small, theoretical perturbations (typically L/500). Our study, however, aligns with "Forensic Reconstruction" frameworks (e.g., Biediger, 2002), which argue that in non-engineered assets, actual deviations often exceed code-allowable limits, making idealized models non-conservative.

2) The "Scan-to-FEM" Workflow: Recent research into the digital preservation of legacy structures (e.g., Wang et al., 2015) advocates for the Scan-to-BIM-to-FEM workflow. Our research advances this by integrating LiDAR point clouds and Trimble geospatial data directly into the ELM framework. This ensures that the "Problem Space"-including misalignments, missing anchor bolts, and hand-welded joint deficiencies-is not just "estimated" but explicitly modeled.

2.4.2 Comparative Advantages of the Mirroring Approach

The following table summarizes how the "Mirroring" methodology in this study provides a more robust analysis compared to standard peer-reviewed practices:

Table 2.3: Comparative Advantages of Structural Mirroring vs. Idealized Modeling.

Feature	Standard Literature (Idealized)	Current Research (Mirroring)	Scientific Advantage
Geometric Fidelity	**Assumes nominal "as-designed" dimensions.**	**Captures "as-built" deformations via LiDAR.**	**Accounts for real-world P-Δ effects accurately.**
Joint Connectivity	**Rigid or Pinned (0% or 100% stiffness).**	**Semi-rigid (Hand-welded) calibration.**	**Reflects actual load distribution in informal frames.**
Imperfection Modeling	**Theoretical Notional Loads.**	**Direct Displacement Mapping.**	**Eliminates guesswork in stability verification.**
Section Properties	**Catalog/Nominal values.**	**Corrosion-adjusted (Section Loss).**	**Evaluates residual capacity, not theoretical capacity.**

2.4.3 Supporting the Recovery Plan

The main advantage of this approach lies in its ability to make accurate predictions. The second-order effects (P-Δ and P-Δ are calculated through actual geometric representation because the method replicates the out-of-plumbness condition and connection vulnerabilities. The scientific "baseline" establishes support for the Recovery Plan which enables specific retrofitting to occur at its most critical locations instead of performing expensive system-wide upgrades.

2.5 Impact of Atmospheric Corrosion on Residual Structural Capacity

The process of steel truss degradation through atmospheric corrosion develops in a non-linear manner, which significantly compounds the challenges of industrial asset assessment. Based on qualitative findings from forensic field inspections, a 10% cross-sectional section loss was established as a critical baseline benchmark to determine residual structural stability. Kayser and Nowak (1989) demonstrated that corrosion causes a direct decrease in cross-sectional area, which simultaneously triggers a disproportionate degradation in the moment of inertia (I) and radius of gyration (r) values.

The Al-Omari building presents a more complicated situation governed by severe localized "pitting" and hidden internal corrosion propagating within its circular hollow sections (CHS)—an structural anomaly which conventional numerical models fail to detect. The following table demonstrates that a 10% reduction in gross cross-sectional area induces highly non-linear changes to the mechanical characteristics of a typical section, exponentially accelerating the risk of premature member buckling.

Table 2.4: Impact of Localized 10% Section Loss on Mechanical Properties (Sample CHS 114.3 × 4.0 mm Section)

Structural Property	Pristine Section Value	Corroded Section Value (10% Loss)	Percentage Change (%)	Forensic Implication on Stability
Cross-Sectional Area (A)	13.86 cm^2	12.47 cm^2	-10.0	Direct reduction in pure axial tensile and compressive capacity.
Moment of Inertia (I)	211.30 cm^4	185.94 cm^4	-12.0	Loss in flexural rigidity (EI); exacerbates second-order deflections.
Radius of Gyration (r)	3.90 cm	3.86 cm	1.03	Increases the member slenderness ratio λ= KL/r).
Section Modulus (S)	36.97 cm^3	32.53 cm^3	-12.0	Reduces local moment resistance, hastening plastic hinge formation.
Critical Buckling Load (Pcr)	120.5 KN	103.6 KN	-14.0	Non-linear compound drop; triggers premature stability failure.

2.6 Wind Topographic Amplification and Internal Pressure Dynamics in Mountainous Regions

The structural vulnerability of non-engineered legacy assets is severely increased through the combined effects of site-specific microclimates and the complex macro-topography at each site. Traditional prospective design methods calculate wind loading parameters through the assumption that all areas share the same wind conditions which exist at low-altitude locations. Simiu and Wright (2006) established that industrial facilities located at high elevations need to follow specific wind velocity patterns which become stronger in areas with abrupt topographic changes that exist at the Ramallah highlands which reach 833 meters above sea level.

ASCE 7-16 (Chapter 26) regulatory framework establishes a mathematical method to calculate the velocity speed-up effect through the topographic factor (Kzt) which derives from its defined formula.

$$\boldsymbol{k_{zt} = (1 + k_1 + k_2 + k_3)^2}$$

The three variables which track specific ridge geometry and upstream fetch distance and of crest proximity to the ridge crest need to multiply by their respective values. Non-engineered industrial buildings without localized wind-bracing systems experience unexpected structural demands because their amplification effect produces concentrated structural loads.Furthermore, Holmes (2015) highlights that environmental degradation or informal modifications often compromise the building envelope (cladding and doors).

The sudden opening of a building envelope which engineers did not assess creates strong internal pressure forces which lead to the building becoming between fully enclosed and completely open. Existing truss top chords experience extreme uplift demands which cause their remaining structural integrity to deteriorate while they suffer from early member buckling.

2.7 Structural Mechanics of Non-Standard Hand-Welded and Semi-Rigid Connections

The common practice in steel research requires researchers to study beam-to-column and member-to-chord connections through two different methods which include testing their materials until complete failure occurs. The research for forensic failure investigations (Bjorhovde 2006 Astaneh-Asl 2008) shows that actual informal structures which exist in the real world display semi-rigid structural behavior. The field-executed hand-welded connections which lack adequate welding procedure specifications (WPS) and non-destructive material certification protocols create unpredictable boundary conditions. The non-standard joints operate according to their moment-rotation relationship which controls their fundamental behavior through their non-linear(M - θ) relationship between rotational stiffness ($\mathbf{k_s}$) and internal load distribution.

$$\mathbf{M = k_s * \theta}$$

The informal hand-welded setups operate without AISC 360-16 requirements which demand specific geometric designs and material ductility thus making them vulnerable to localized stress points and weld throat failure and excessive rotational movement. Nethercot (2000) demonstrates that using idealized pins for joint analysis leads to non-conservative results because uncalculated partial restraint will create unexpected secondary bending moments which affect slender truss members. The application of rigid frame analysis results in an excessive estimation of global frame stability.

Table 2.5: Comparison of Boundary Condition Idealizations and Forensic Risks

Boundary Idealization	Rotational Stiffness (ks)	Secondary Moments in Truss Members	Forensic Risk in Legacy Assets
Perfectly Pinned	0%	Completely ignored	Non-conservative: Underestimates localized structural demands and localized stresses.
Perfectly Rigid	100%	Fully transferred	Unsafe: Overestimates global frame stability and structural safety margins.
Semi-Rigid (Real-world)	Non-linear ($M = k_s * \theta$	Partially transferred (Unpredictable)	Accurate Representation: Captures true boundary configurations and weld throat vulnerabilities.

Therefore, a forensic literature framework must account for connection semi-rigidity to accurately simulate the cascading structural vulnerabilities of existing, unbraced industrial infrastructure. This rotational flexibility directly impacts global stability parameters; in a forensic verification context utilizing the Effective Length Method (ELM), the degradation of connection stiffness yields an escalation in the effective length factor (K) of adjacent compression members, severely compromising the baseline buckling resistance of the asset.

2.8 Structural Mechanics and Capacity Enhancement of Built-up Laced Columns

In the domain of forensic engineering and infrastructure rehabilitation, the structural performance optimization of deficient or highly slender compression members is widely achieved through the implementation of built-up laced configurations. As strictly regulated by Section E6 of AISC 360-16, converting independent structural profiles into a unified lattice or trussed column mechanism significantly alters the governing failure modes.

Seminal stability literature, including the definitive criteria by Ziemian (2010), demonstrates that the addition of continuous diagonal and vertical web ties onto existing structural boundaries introduces a high shear stiffness mechanism. This structural intervention drastically amplifies the global radius of gyration (r) and the cross-sectional moment of inertia (I) without substantially increasing the net steel tonnage.

Consequently, the modified or effective slenderness ratio(λ_m) of the composite assembly drops below critical design thresholds, effectively shifting the member limit-state from premature elastic buckling into predictable post-yield capacity ranges. This engineered practice is highly effective for retrofitting unengineered legacy assets that exhibit structural tilting, material degradation, or lack dedicated lateral load-resisting frameworks.

2.9 Comparative Review of Previous Studies

A considerable body of research has been conducted on the behavior, assessment, and rehabilitation of steel structures. Most published studies have focused on individual deterioration mechanisms, connection behavior, corrosion effects, structural stability, or the performance of newly designed industrial steel systems. However, limited attention has been given to existing non-engineered industrial buildings that suffer from multiple concurrent deficiencies, including geometric imperfections, inadequate connections, corrosion damage, missing bracing systems, and uncertain load paths.

To better position the current research within the existing body of knowledge, Table 2.5 presents a comparative review of selected studies relevant to steel structural assessment and rehabilitation.

Table 2.6: Comparative Summary of Previous Studies and Research Gaps

Author(s)	Research Focus	Methodology	Main Findings	Research Gap
Kayser & Nowak (1989)	Effect of corrosion on steel members	Analytical and experimental investigation	Corrosion significantly reduces cross-sectional area, stiffness, and buckling resistance.	Did not investigate complete industrial structural systems or rehabilitation strategies.
Nethercot (2000)	Semi-rigid steel connections	Theoretical and behavioral analysis	Connection stiffness significantly influences force distribution and global stability.	Focused primarily on connection behavior without evaluating existing deteriorated structures.
Biediger (2002)	Forensic structural investigations	Field assessment and failure analysis	Accurate diagnosis requires incorporation of actual construction deficiencies.	Limited integration with advanced finite element modeling.
Wang et al. (2015)	Digital reconstruction of existing structures	Scan-to-BIM-to-FEM workflow	High-fidelity geometric models improve structural assessment accuracy.	Did not address non-engineered industrial facilities with severe deterioration.
Recent studies on PEB systems	Industrial steel buildings	Numerical modeling and code-based design	Modern steel systems exhibit efficient structural performance under design loads.	Assumed ideal construction quality and code-compliant detailing.
Current Study	Existing industrial steel truss building in Ramallah	Field investigation, forensic assessment, STAAD.Pro analysis, and rehabilitation design	Evaluates real-world structural deficiencies, environmental effects, connection irregularities, and rehabilitation alternatives.	Bridges the gap between idealized design assumptions and actual as-built structural conditions.

The reviewed literature confirms that most previous investigations concentrated on isolated structural phenomena or newly engineered systems designed according to modern codes. In contrast, the assessment of aging industrial steel buildings constructed without formal engineering design remains insufficiently addressed.

Therefore, the current study contributes to the existing body of knowledge by integrating forensic field investigation, as-built structural reconstruction, advanced finite element analysis, and rehabilitation planning into a unified framework for assessing and recovering deteriorated non-engineered industrial steel structures.

2.10 Literature on In-Situ Structural Retrofitting, Analytical Formulations, and Strengthening Techniques

For non-engineered and degraded steel structures, the structural rehabilitation is demanding and requires in-situ rehabilitation methods that can strengthen the capacity of the members, reduce the structural geometric instability and retain the continuity of the load path without involving the complete demolition of the structure (AISC Design Guide 15, 2002; Formisano et al., 2022). This is an analytical and experimental survey of the retrofitting mechanics, mathematical models, and schematic relationships used for structural rehabilitation studies.

2.10.1 Built-up and Laced Column Upgrading

Isolated compression columns are often very weak-axis slenderness in legacy industrial steel frames. The method of converting independent structural profiles into a unified "built-up laced assembly" to prevent buckling early in the elastic range is a mature retrofitting technique that is well known and often practiced (Ziemian, 2010; Galambos & Surovek, 2008). The parallel-axis theorem (also known as Steiner's Theorem) predicts that the composite column's moment of inertia I_{comp} and the composite radius of gyration r_{comp} will be significantly increased when the primary column (cross-sectional area A_1) and the secondary profile (cross-sectional area A_2) are coupled together, laced continuously with diagonals and horizontally, by a centroidal distance of d.

$$I_{comp} = I_1 + I_2 + A_1 d_1^2 + A_2 d_2^2$$

$$r_{comp} = \sqrt{\frac{I_{comp}}{A_1 + A_2}}$$

However, unlike solid-webbed sections, built-up laced columns experience additional lateral deflection due to shear deformation within the diagonal lacing network. In accordance with **AISC 360-16 (Section E6)** and classic stability formulations by Timoshenko and Gere (1961), the governing compressive capacity is controlled by the **modified slenderness ratio** ($\left(\frac{KL}{r}\right)_m$):

- **For snug-tight bolted or welded interconnected built-up members:**

$$\left(\frac{KL}{r}\right)_m = \sqrt{\left(\frac{KL}{r}\right)_o^2 + \left(\frac{a}{r_i}\right)^2}$$

where $\left(\frac{KL}{r}\right)_o$ is the global column slenderness acting as a unified unit, a is the longitudinal spacing between intermediate lacing nodes (panel increment), and r_i is the minimum radius of gyration of an individual chord component. To prevent local chord buckling between panel nodes prior to global column buckling, AISC 360-16 enforces the criterion:

$$\frac{a}{r_i} \leq 0.75 \left(\frac{KL}{r}\right)_m$$

Experimental and numerical investigations by **Dar et al. (2018)** and **Talebi et al. (2016)** demonstrated that optimizing lacing inclination angles between 45° and 60° prevents local chord distortion and enhances lateral energy dissipation by over 65%. These formulations provide the direct mechanical basis for the engineered column-trussing scheme implemented for the CHS 250×5.0 mm columns

in the Al-Omari building (Chapter 5).

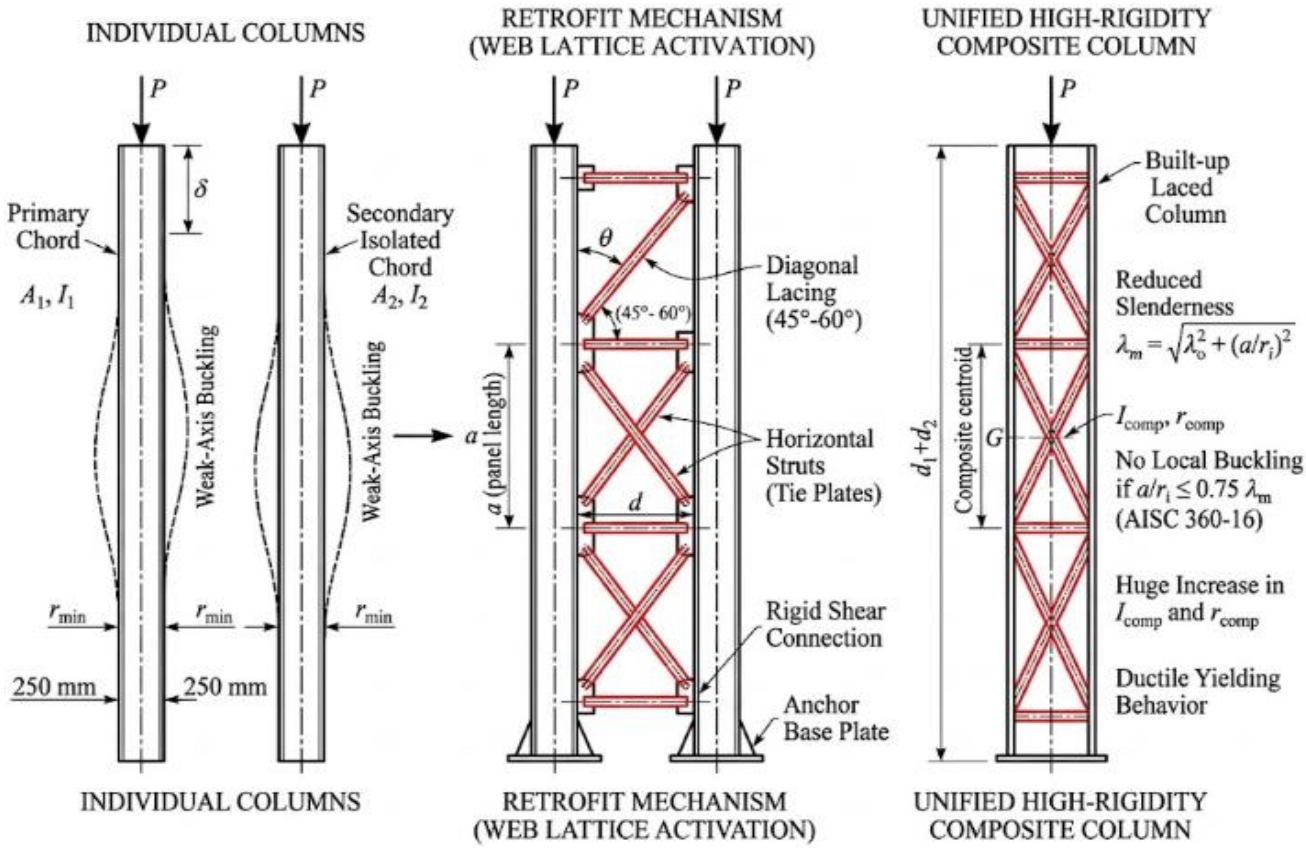


Figure 2.1: Mechanical transformation, web lattice activation, and geometric parameters of the engineered built-up laced column retrofitting scheme for legacy CHS members (Adapted from Ziemian, 2010; AISC 360-16; Dar et al., 2018).

2.10.2 Strengthening and Steel Sleeving (Jacketing) of Deteriorated Tubular (CHS) Members

Circular Hollow Sections (CHS) subjected to atmospheric corrosion and mechanical impact indentations suffer from localized wall thinning ($t_{corr} < t_o$), which induces a disproportionate, non-linear drop in Euler elastic buckling resistance (P_e) and local shell buckling stress (Kayser & Nowak, 1989):

$$P_e = \frac{\pi^2 E I_{corr}}{(KL)^2}$$

In-situ Steel Sleeving (or Grouted/Welded Steel Jacketing) is widely proven to be a no-dig rehabilitation method to achieve the return of axial and flexural capacity without having to dismantle

the existing roof trusses.

Experimental tests conducted by Ahn et al. (2018), Toledo et al. (2020) and finite element parametric studies performed by Wang et al. (2017) demonstrated that an external steel sleeve (split pipe) welded around the corroded or dented area of a CHS member joins the defective area and helps to prevent the wall from local plastification. The axial compressive capacity ($\phi_c P_n$) and flexural capacity ($\phi_b M_n$) of the sleeved composite tubular section is determined by:

$$A_{eff} = A_{existing,corr} + A_{sleeve} = \frac{\pi}{4}\left[\left(D_o^2 - D_{i,corr}^2\right) + \left(D_{s,o}^2 - D_{s,i}^2\right)\right]$$

$$(EI)_{eff} = E_s I_{existing,corr} + E_s I_{sleeve}$$

$$\phi_c P_n = 0.90\, F_{cr}\, A_{eff}$$

where F_{cr} is the flexural buckling stress calculated using AISC 360-16 (Chapter E) with the composite slenderness parameter $KL/\pi r_{eff}\sqrt{\left(F_y/E\right)}$ where K is the buckling coefficient, L is the length of the member, r_{eff} is the radius of gyration of the composite member, F_y is the yield stress, and E is the elastic modulus. Ahn et al. (2018) found that the capacity of the original member is restored to more than 95% to 105% of the original capacity when the sleeve length (L_s) is at least $1.5D_o$ on each side longer than the damaged zone.

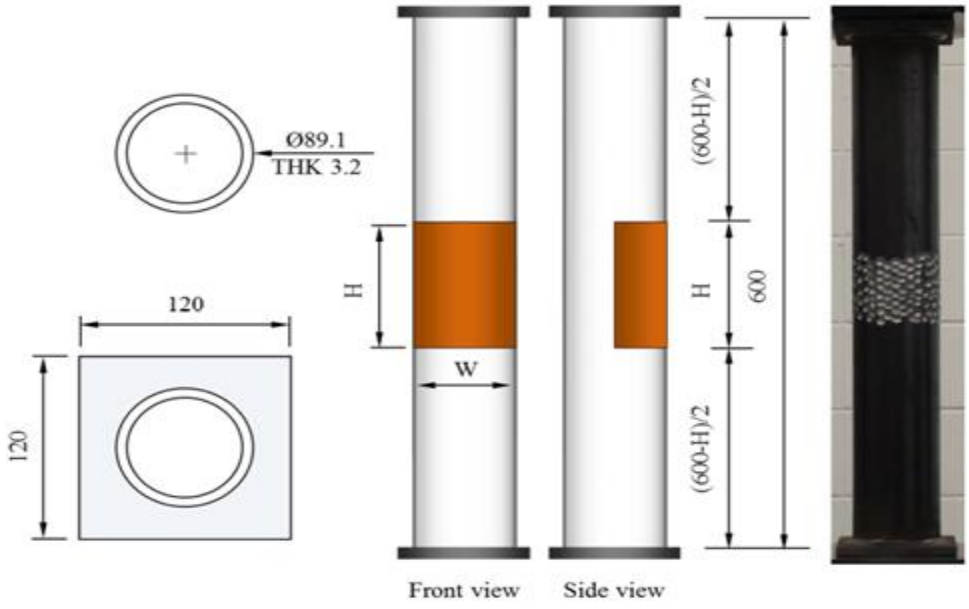


Figure 2.2: *Geometric configuration, dimensions (*Ø89.1 × 3.2 mm*), and artificial pitting corrosion damage parameters*

$(H \times W)$ on circular hollow steel (CHS) tubular test specimens (Source: Ahn et al., 2018).

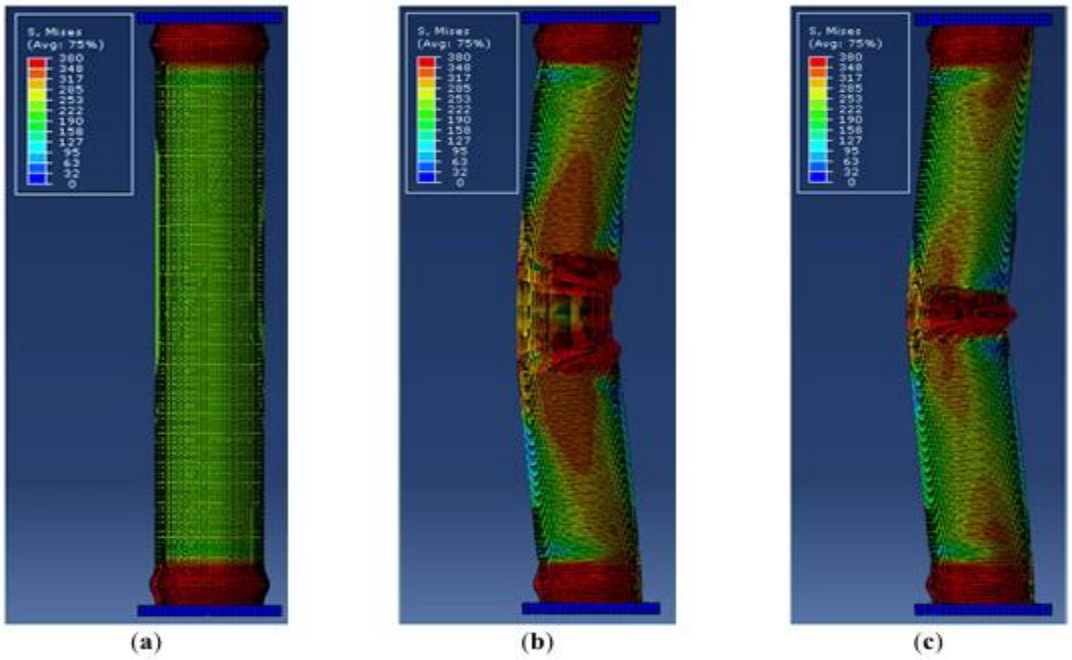


Figure 2.3: *Experimental configuration versus Finite Element Analysis (FEA) Von Mises stress distributions and progressive local/lateral buckling failure modes of locally corroded CHS tubular columns: (a) initial elastic state, (b) intermediate localized yielding, and (c) ultimate failure under axial compression (Source: Ahn et al., 2018).*

2.10.3 Integration of Lateral Bracing Systems and Stiffness Demand

When there is no continuous Lateral Force-Resisting System (LFRS), slender gravity columns must carry wind and seismic base shear with weak-axis cantilever bending which increases second-order $P-\Delta$ moments. AISC Design Guide 28 (Carter and Geschwindner, 2008) and Yura (2001) have shown that it is necessary for an effective nodal bracing system to meet both strength and stiffness requirements in order to stabilize compression frames.

AISC 360-16 (Appendix 6) specifies the minimum design strength (P_{br}) and minimum design stiffness (β_{br}) of bracing for a relative lateral bracing system for a column load P_r are:

$$\beta_{br} = \frac{1}{\phi}\left(\frac{2P_r}{L_b}\right) \quad (\text{with } \phi = 0.75)$$

$$P_{br} = 0.01\,P_r \text{ to } 0.02\,P_r$$

Furthermore, the axial tensile/compressive stiffness (K_{brace}) contributed by an added diagonal X-bracing member of cross-sectional area A_b, length L_d, and inclination angle θ relative to the horizontal plane is given by:

$$K_{brace} = \frac{EA_b}{L_d}\cos^2\theta$$

Numerical studies by **Chen et al. (2012)** and **Formisano et al. (2022)** demonstrated that integrating continuous diagonal roof and wall X-bracing reduces roof lateral drift and secondary P-Δ column moments by up to **75%**, directly justifying the longitudinal bracing network introduced in Chapter 4 (Figure 4.1).

2.10.4 Purlin System Rectification and Combined Axial-Flexural Interaction

In non-engineered steel trusses, placing roof purlins between panel points (non-nodal eccentric loading) subjects the top chord to simultaneous axial compression (P_u) and localized transverse bending (M_u). Instead of behaving as a pure pin-ended axial member, the chord is governed by the **AISC 360-16 (Section H1.1)** beam-column interaction equations:

- **For** $\frac{P_r}{P_c} \geq 0.2$**:**

$$\frac{P_r}{P_c} + \frac{8}{9}\left(\frac{M_{rx}}{M_{cx}} + \frac{M_{ry}}{M_{cy}}\right) \leq 1.0$$

- **For** $\frac{P_r}{P_c} < 0.2$**:**

$$\frac{P_r}{2P_c} + \left(\frac{M_{rx}}{M_{cx}} + \frac{M_{ry}}{M_{cy}}\right) \leq 1.0$$

As highlighted by **Fisher and Tartaglia (2009)** and **Packer et al. (2010, CIDECT Design Guide 3)**, rectifying this deficiency requires relocating purlins strictly to panel nodes using custom welded bracket adapters ($M_{rx} \to 0$) and upgrading ad-hoc pipes to continuous lap-spliced cold-formed **Z-purlins** (Yu & LaBoube, 2010; AISI S100-16), which eliminate local chord plastification and reduce the interaction ratio below 1.0.

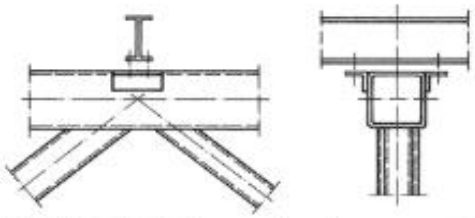
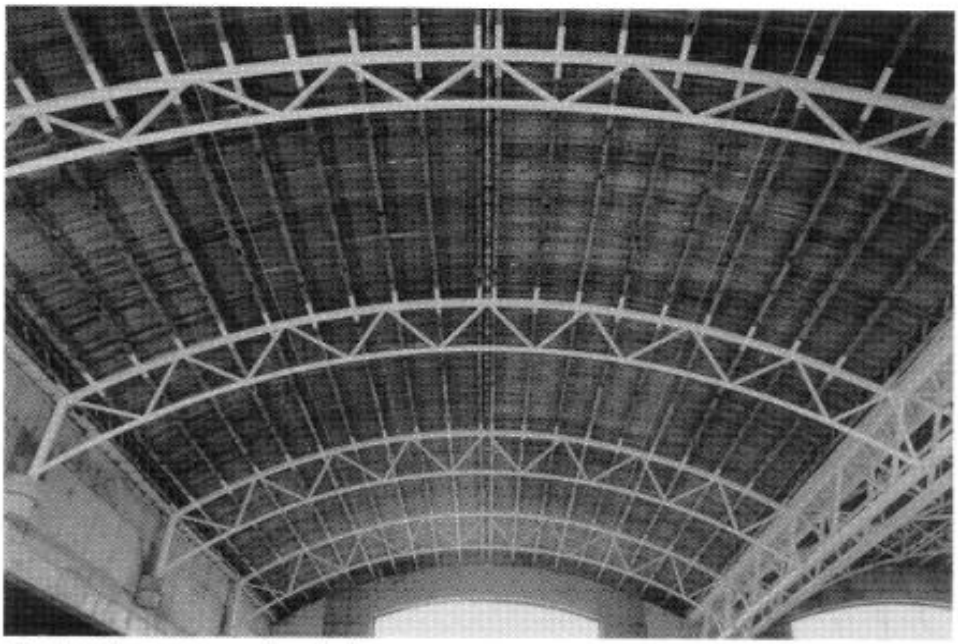


Fig. 30 – Possible purlin cleat connection at truss connection no. 2



Arched roof trusses for a multi-use hall

Figure 2.4: Typical engineered purlin cleat connection detail and arched truss configuration demonstrating nodal load transfer mechanisms to eliminate secondary bending moments.

2.10.5 Substructure Anchorage and Post-Installed Chemical Anchor Mechanics

Restoring deficient column bases without demolishing existing concrete pedestals relies on post-installed chemical adhesive anchors and stiffened hollow base plates (**Fisher & Kloiber, 2006 - AISC Design Guide 1**; **ACI 318-19 Chapter 17**).

Under combined wind uplift (tension N_{ua}) and lateral base shear (V_{ua}), **Gomez et al. (2010)** demonstrated that post-installed adhesive anchors must be verified against steel rupture, concrete breakout, and chemical bond pullout, governed by the **ACI 318-19** elliptical tension-shear interaction equation:

$$\left(\frac{N_{ua}}{\phi N_n}\right)^{5/3} + \left(\frac{V_{ua}}{\phi V_n}\right)^{5/3} \leq 1.0 \quad \text{(or simplified linear interaction } \frac{N_{ua}}{\phi N_n} + \frac{V_{ua}}{\phi V_n} \leq 1.2\text{)}$$

where the nominal bond strength (N_{ba}) of a single chemical anchor of diameter d_a and effective embedment depth h_{ef} is expressed as:

$$N_{ba} = \lambda_a \, \tau_{cr} \, \pi \, d_a \, h_{ef}$$

Additionally, per **AISC Design Guide 1**, the required base plate thickness (t_{pl}) to resist upward bearing pressure or anchor bolt tension bending (M_{pl}) without prying failure is determined by:

$$t_{pl(\text{req})} = \sqrt{\frac{4M_{pl}}{\phi_b F_y}}$$

Table 2.7: Summary of Literature-Based Retrofitting Techniques, Governing Equations, and Application to the Case Study.

Retrofitting Technique	Key Literature References	Governing Design Code & Mathematical Criterion	Forensic Problem Addressed in Al-Omari Building
Built-up Laced Columns	Ziemian (2010); Dar et al. (2018); Talebi et al. (2016)	**AISC 360-16 (Sec. E6):** $\left(\frac{KL}{r}\right)_m = \sqrt{\left(\frac{KL}{r}\right)_o^2 + \left(\frac{a}{r_i}\right)^2}$	Suppresses weak-axis buckling in slender CHS 250×5 columns (D/C reduced from 1.51 to $<$ 0.52).
CHS Steel Sleeving (Jacketing)	Kayser & Nowak (1989); Ahn et al. (2018); Toledo et al. (2020)	**AISC 360-16 (Ch. E) & AWS D1.1:** $A_{eff} = A_{corr} + A_{sleeve}$, $\phi_c P_n = 0.9 F_{cr} A_{eff}$	Restores >95% axial/flexural capacity in corroded (10% loss) and dented tubular web/column members.
Continuous X-Bracing Integration	Carter & Geschwindner (2008); Chen et al. (2012); Formisano et al. (2022)	**AISC 360-16 (App. 6):** $\beta_{br} = \frac{2P_r}{\phi L_b}$, $K_{brace} = \frac{EA_b}{L_d}\cos^2\theta$	Eliminates longitudinal sway and establishes a complete load path for the 188.13 kN wind base shear.
Nodal Z-Purlin Rectification	Fisher & Tartaglia (2009); Yu & LaBoube (2010); Packer et al. (2010)	**AISC 360-16 (Sec. H1.1) & AISI S100:** $\frac{P_r}{P_c} + \frac{8}{9}\frac{M_r}{M_c} \leq 1.0$	Eliminates eccentric non-nodal bending in CHS 155 mm top chords (D/C reduced from 2.16 to 0.88).
Post-Installed Chemical Anchors	Fisher & Kloiber (2006); Gomez et al. (2010)	**ACI 318-19 (Ch. 17) & AISC DG1:** $\left(\frac{N_{ua}}{\phi N_n}\right)^{5/3} + \left(\frac{V_{ua}}{\phi V_n}\right)^{5/3} \leq 1.0$	Restores base rotational fixity, grout consolidation, and wind uplift resistance without footing demolition

Chapter 3: Field Investigation, Structural Assessment, and Loading Analysis

This chapter establishes the technical and analytical framework necessary to evaluate the existing structural conditions of the selected asset, detect inherent structural deficiencies, and specify the loading parameters required for forensic structural analysis and subsequent rehabilitation design.

3.1. Description of the Studied Industrial Steel Building

The industrial steel truss building which was the subject of the study is the property of Mr. As'ad Al-Omari and is situated in Ramallah, Palestine, at a height of around 832.8 m above sea level. The building has existed for more than 25 years as a factory site because it maintains its original industrial function which makes it an established industrial facility in the city. The structure has experienced continuous operational loads together with machinery vibrations while outdoor weather conditions have affected it throughout its operational period which led to its current performance issues.

The site survey team conducted complete site evaluation together with field assessment to document the building's actual dimensions and structural framework and element dimensions and connection details and complete building condition assessment. The data collected were used to depict the structure as it is in reality by means of an accurate as-built structural model.

This chapter establishes all analytical and technical requirements which need to evaluate the current state of the structure and find its faults and determine all structural analysis and rehabilitation study loading requirements.

.



Figure 3.1 Field inspection and site survey conducted to document the as-built geometry of the existing industrial building.

3.2 Structural Assessment and Causes of Deterioration in Steel Structures

The evaluation and strengthening of steel structures are major parts of structural engineering practices, and this is especially true for old industrial buildings which have experienced a variety of environmental and operational conditions throughout their long service lives. The decay of such constructions is generally the result of a mixture of causes, such as the harshness of the environment, the manner in which the structures were used, flaws in the manufacturing process, and construction techniques, as well as the gradual reduction of the material properties that eventually comes with time.

This part intends to scientifically and systematically lay the foundation for the assessment and reinvention of steel structures with the help of accepted American codes and norms. Among such codes and standards are AISC 360 that participated in the design and the appraisal of steel structures, ASCE 7-16 for load calculations, and AWS D1.1 for welding standards and inspection of quality. These standards are regarded as the peak references for the inspection, analysis, strengthening, and rehabilitation of steel structures in the U.S. code configuration.

3.2.1 Causes of Deterioration in Steel Structures

There are a number of mechanisms by which steel structures could deteriorate, and those mechanisms can have a direct impact on the performance and safety of the structures in the long term. Below are the most important ones:

Corrosion:

The corrosion process is triggered by the presence of moisture, condensation, industrial pollutants or chemicals, and it results in the loss of material along with the corresponding reduction in the load-bearing capacity of the structural members.

Fatigue:

The fatigue process is a result of the cyclical or dynamic loadings which alternately happen and are due to the operation of the industrial equipment or the continuous vibrations, and this process may cause the development of cracks or even the complete failure of the structural elements over time.

Overloading:

Overloading happens when the applied loads go beyond the original design expectations, either because of changes in use or new equipment being added.

Fabrication and Construction Defects:

These defects embrace incomplete welds, misalignment of members, and dimensional inaccuracies, and all these can negatively influence the load transfer efficiency.

Connection Failure:

Connection failure may occur due to inadequate bolting, low-quality welding, or high stresses that are concentrated in the connection zones.

Fire Exposure:

The strength and stiffness of the steel get reduced in case of fire events, and this could lead to a significant loss of the structural capacity.

Buckling Instability:

The slender columns or bracing members without sufficient lateral support, especially under compressive loading, are the most common ones that experience buckling instability.

Impact Damage:

The impact damage results from vehicle accidents or dropping heavy objects and can cause localized deformation or even destruction of the structural members.

Aging Effect:

The aging effect is the gradual decay of the structure over decades because of no regular inspections and maintenance.

3.2.2 Steel Structure Assessment Procedure

The rehabilitation process starts with a thorough examination of the structure to evaluate its condition and recognize all the existing weaknesses and problems.

1- Visual Inspection

The examination that is done initially by the inspectors is the one that yields the following findings:

• Cracks in welds

• Rusted and corroded areas

• Areas of local buckling or deformations

• Unsecured or missing connections

• Distorted members and misalignment

2- Non-Destructive Testing (NDT)

Non-destructive tests that are advanced methods are applying include the following:

• **UT (Ultrasonic Testing)** – it finds flaws inside the material

• **MT (Magnetic Particle Testing)** – it finds cracks on the surface

• **PT (Dye Penetrant Testing)** – it is for very small surface discontinuities

• **RT (Radiographic Testing)** – it finds imperfections within the structure and weld defects

3- Structural Analysis

Structural Analysis:

Creating a finite element model that shows the actual condition of the structure has been done to determine the internal forces, stresses, and deformations, and also to study the overall performance of the structure under the applied loads

3.3 Existing Structural Deficiencies and Performance Issues

The case of the industrial building in question dates back **approximately 25 years** , when a local steel fabricator with no formal engineering knowledge built the structure without relying on official engineering drawings or standard codes of practice. The building is a living example of the type of unengineered legacy infrastructure that completely lacked professional design validation and rigorous site supervision during its construction process.

1) Misalignment of the columns which means that there are unbalanced stresses and the behavior of the steel trusses is affected.

2) Members and connections built in an irregular way, with varying dimensions and use of assembly practices that result in a reduction of the overall structural performance.

3) The building has no structural system that can withstand the wind and lateral loads, and hence the building is left exposed to strong winds and vibrations from industrial machines.

4) At the column bases, anchor bolts are missing which causes the main structural elements to have weak connections and hence the building has reduced overall stability under loads.

5) Non-engineered methods of connecting members sometimes use ad-hoc welding or partial fastening and this makes it difficult for trusses to resist tension, compression, and buckling.

6) Some members have corroded and lost their sections due to moisture and bad weather conditions over a long period of time, thus making the structure less resilient.

7)There has been no documented periodic maintenance, so the building has accumulated operational and mechanical deficiencies for decades.

All the above issues together are a **serious threat to the structural performance of the building** which means that the risk of local failure or partial collapse under service and environmental loads has increased. **Thus, a thorough assessment of the current condition**, detailed load analysis, and the development of an **effective rehabilitation plan are needed**.

3.4 Field Inspection Results

The field inspection was done to check the actual as-built condition of the existing industrial steel truss building, and to pick out the main structural deficiencies that are affecting its current safety and performance. The inspection itself involved a sort of visual assessment, geometric verification, member identification, connection observation, plus the documentation of deterioration signs, all in a real on site context. The information gathered was then used as the backbone for building the structural model and also for laying out the rehabilitation measures that would actually be needed.

From the site visit it was noticed that the building was erected without formal engineering drawings, or documented structural calculations. The overall structural system is mainly made of steel trusses that are supported by circular hollow section columns, while roof purlins, transfer gravity and environmental loads to the main truss members. During the walk through, several structural irregularities were spotted. These issues suggest that the existing system does not really satisfy today's structural design expectations, like not fully, or not in a consistent way with current requirements.

Table 3.1 The main field inspection findings are summarized as follows:

No.	Observed Condition	Structural Significance
1	Column misalignment and out-of-plumbness were observed in several locations.	This may increase secondary bending moments and reduce the effective axial capacity of the columns.
2	The truss configuration was irregular and did not form a fully consistent triangulated load-transfer system.	This reduces truss efficiency and causes additional bending and shear forces in members that are ideally expected to carry axial forces only.
3	Roof purlins were not always positioned directly at truss panel points.	Non-nodal loading introduces local bending moments in the truss chords and increases stress concentrations.
4	The building lacks a continuous lateral bracing system in the longitudinal direction.	This creates an incomplete lateral load path and reduces the ability of the structure to resist wind and seismic forces.
5	Some wall bracing elements were observed, but they were discontinuous and not properly connected to the foundation level.	Discontinuous bracing limits the ability of the system to transfer lateral forces safely to the supports.
6	Anchor bolts at some column bases were missing,	This weakens the column-base connection and reduces

	insufficient, or poorly detailed.	the reliability of the assumed support conditions.
7	Several welded connections appeared to be non-standard, discontinuous, or executed without proper quality control.	Poor welding quality may lead to local connection failure, stress concentration, and unpredictable semi-rigid behavior.
8	Local corrosion and surface deterioration were observed in some exposed steel members.	Corrosion may reduce the effective cross-sectional area and decrease member strength and stiffness.
9	A large main door/opening exists in one façade of the building.	This affects the wind classification of the building and increases the importance of internal pressure effects.
10	Previous repair or modification works appeared to have been executed using empirical methods.	Such modifications may introduce uncertain load paths, eccentricities, and residual stresses.
11	A non-engineered mid-height welded splice was observed in one of the circular hollow steel columns, accompanied by local deformation, surface indentation, and coating damage.	This may create a weak zone at the splice location, increase stress concentration, reduce the effective capacity of the column, and increase the risk of local or global buckling under axial and lateral loads.
12	Poor column-base connection detailing was observed, including inadequate anchor bolt arrangement, insufficient base plate detailing, and lack of proper grout finishing.	This may reduce the ability of the base connection to transfer axial forces, shear forces, and lateral moments to the foundation, increasing the risk of base rotation, uplift, or sliding under wind and seismic loads.
13	Local impact damage and surface indentation were observed on one of the circular hollow steel columns, accompanied by coating deterioration.	This may create localized stress concentration, introduce geometric imperfections, reduce the column's resistance to axial compression and bending, and increase the risk of local buckling.
14	Discontinuous X-bracing was observed in the background of the building, where the bracing members do not form a complete lateral load-resisting path.	This reduces the global lateral stability of the building and may force columns and truss members to resist wind and seismic loads through bending instead of an efficient axial bracing mechanism.
15	A non-standard welded tie plate was observed connecting two adjacent circular hollow steel columns.	This may introduce uncertain force transfer, local stress concentrations, and unreliable lateral restraint if the connection is not properly designed and detailed.

So based on the field inspection results, the existing building, can be classified as a structurally vulnerable steel system, with several deficiencies tied to geometry, load path continuity, connection reliability and also member deterioration. The lack of a fully complete lateral bracing system is, in my view, one of the most critical findings, because it directly affects the overall stability of the building during wind and seismic actions.

Also, the observed non-nodal loading of the truss members and the irregular truss configuration suggest that the structure does not actually behave like an ideal pin-jointed truss. Rather than that, some members are expected to carry a mix of axial forces , shear forces and bending moments. Because of this, that combined behavior was taken into account in the structural analysis model, to get a more realistic representation of the as-built system.

Overall, the field inspection results really confirm the need for a detailed structural assessment, and they also support the justification for creating rehabilitation alternatives. These findings additionally align with the modeling assumptions used in the analytical phase, such as imperfect load paths, deficient lateral bracing ,and uncertain connection behavior.



Figure 3.2: Non-engineered mid-height welded splice in a circular hollow steel column, showing local deformation, surface indentation, and coating damage.

Figure 3.2 shows a circular hollow steel column in which a mid-height field-welded splice was observed. The column appears to have been previously cut and reconnected by site welding without clear evidence of an engineered splice detail. Local deformation and surface indentation can also be

seen near the welded region, in addition to damage to the protective coating and exposure of the steel surface.

This condition is considered structurally critical because a welded splice located within the height of a compression member may create a weak zone and cause stress concentration, especially when the welding quality and splice detailing are not verified. The observed local deformation may also affect the straightness of the column and increase the possibility of local or global buckling under axial compression and lateral wind-induced bending moments. Therefore, this defect was documented as one of the major field inspection findings and should be considered in the structural assessment and rehabilitation design.



Figure 3.3: Deficient column-base connection showing inadequate anchor bolt arrangement, poor base plate detailing, and lack of proper grout finishing.

Figure 3.3 shows the base connection of one of the circular hollow steel columns. The observed condition indicates poor base plate detailing, inadequate anchorage arrangement, and the absence of proper grout or finishing around the column base. The anchor bolts appear insufficient and not properly detailed to ensure reliable transfer of forces between the steel column and the concrete foundation.

This condition is structurally significant because the column-base connection plays a critical role in transferring axial forces, shear forces, and wind-induced moments to the foundation. Inadequate anchorage may reduce the base restraint capacity and may lead to excessive rotation, uplift, or sliding under lateral loads. Therefore, the observed base connection deficiency was documented as a major field inspection finding and should be considered in the structural assessment and rehabilitation design.



Figure 3.4: Local coating damage and surface corrosion observed on a circular hollow steel column.

Figure 3.4 shows local damage to the protective coating of one of the circular hollow steel columns, with visible exposure of the steel surface and signs of surface corrosion. The deterioration appears to be localized; however, it indicates that the steel member has been exposed to environmental effects such as moisture, abrasion, or inadequate maintenance during its service life.

This condition is important because damage to the protective coating may accelerate corrosion and gradually reduce the effective cross-sectional area of the steel member if not treated. Although the observed corrosion appears local at the inspection stage, it should be considered in the structural assessment, especially for compression members where section loss may reduce axial capacity,



stiffness, and buckling resistance. Therefore, cleaning, corrosion treatment, and protective repainting are recommended as part of the rehabilitation works.

Figure 3.5: Local impact damage and surface indentation observed on a circular hollow steel column, accompanied by coating deterioration.

Figure 3.5 shows a circular hollow steel column with visible local impact damage, surface indentation, and coating deterioration. The observed deformation indicates that the column may have been subjected to accidental mechanical impact during service, possibly due to equipment movement or repeated operational contact within the industrial facility. In addition to the local dent, scratches and coating loss can be observed, which may expose the steel surface to environmental deterioration.

This condition is structurally significant because local impact damage may introduce geometric imperfections and localized stress concentrations in the column wall. These imperfections can reduce the structural efficiency of the member, especially under axial compression and bending moments, and may increase the possibility of local buckling in the affected region. Therefore, this defect was documented as one of the field inspection findings and should be considered in the structural assessment and rehabilitation process.



Figure 3.6: Field survey process showing discontinuous X-bracing in the background of the industrial steel building.

Figure 3.6 shows the field survey process conducted inside the industrial steel building. The image also clearly illustrates the presence of discontinuous X-bracing in the background, where the bracing system does not form a complete and continuous lateral load path. Although diagonal bracing elements are present in some locations, they are not properly extended or connected to create an effective bracing system capable of transferring lateral forces from the roof and wall levels down to the foundation.

This observation is structurally significant because an incomplete X-bracing system reduces the global lateral stability of the building, especially in the longitudinal direction. Under wind or seismic actions, the absence of a continuous bracing path may force the columns and truss members to resist lateral loads through bending rather than through an efficient axial bracing mechanism. Therefore, the discontinuity of the X-bracing system was documented as a major field inspection finding and was considered in the structural assessment and rehabilitation recommendations.

Summary of Field Inspection Findings

The field inspection results indicate that the existing steel structure suffers from several interrelated deficiencies affecting geometry, member condition, connection reliability, and lateral load resistance. The most critical issues include discontinuous bracing, deficient column-base connections, non-engineered welded splices, local impact damage, coating deterioration, and uncertain load-transfer mechanisms. These observations confirm that the structure should not be evaluated as an ideal engineered steel system, but rather as an as-built structure with imperfections and irregularities that must be reflected in the structural assessment and rehabilitation design.

3.5 Structural System Idealization and Modeling Assumptions

The industrial steel building that was the subject of the study was quite old and the structural system it depended on was not designed using modern engineering principles. Hence, creating an accurate representation of the existing structure was a prerequisite for load determination and structural analysis. Aiming at this, a detailed site survey and thorough field inspection led to the creation of an as-built structural model that encompassed the entire geometry, structural configuration, member dimensions, column layout, and connection details of the building.

The model took into consideration the existing structural condition, especially the deterioration effects like corrosion and loss of section. The recommended modeling assumptions that were in line with the situation on site were used for connections and column bases, while non-structural elements were not taken into account.

This idealized model is the starting point from which load cases are applied and the structural response is evaluated according to the applicable code provisions.

This idealized model serves as the computational platform upon which standard and extreme hazard loads are applied. Crucially, the mathematical idealization of boundary configurations and frame connectivity is strictly tailored to align with the **Effective Length Method (ELM)** framework established in Appendix 7 of AISC 360-16. By opting for the ELM framework over automated global stiffness reduction methods, the finite element modeling environment preserves member-specific boundary constraints. This choice enables the manual calibration and penalization of effective length factors (K) to reflect the true, in-situ semi-rigid actions of the hand-welded joints and missing foundation anchorages observed during the forensic field mapping.

3.6 Load Calculation

- Structural loads computations are among the preliminary and most important activities in structural design. Hence, the loads will be identified for conducting a good analysis and checking the safety and stability of the structure. Given that the building is already there, the load calculations will reflect the real situation of the structure as it is today.

3.6.1 Dead Loads (DL):

Self-weight of members: automatically computed by the structural analysis software

- **Electrical + Mechanical installations:** 10 kg/m² (≈ **0.10 kN/m²)**
- **Roof cladding (roof sheets**): 5.2 kg/m² (≈ **0.05 kN/m²)**
- **Collateral Loads :** 10 kg/m² (≈ **0.10 kN/m²)**

Total additional dead load (excluding self-weight): 0.25 kN/m²

3.6.2 Live Loads

Roof Live Load Due to Maintenance Activities

Among the roof live load are the temporary loads resulting from maintenance activities on the roof, for instance, the presence of maintenance personnel as well as the tools, equipment, and materials used during these activities. In this project, a roof live load of **0.96 kN/m²** is selected which is the recommended value for maintenance loading. Although these loads are not permanent, they have to be taken into account during structural design so that roof safety and serviceability are assured.

Partial Live Load Application (ASCE 7 – Section 4.3.3)

ASCE 7 states that the full intensity of the live load—after the proper live load reduction is applied—will be taken into account on a part of the structural element only if this situation leads to a more critical load effect than applying the same load uniformly over the whole element.

This requirement makes sure that the structure is tested under the most severe and realistic loading conditions.

Also, the roof live load distribution shall comply with the specifications in Table 4.3-1 of the standard.

Reduction of Uniform Live Loads (ASCE 7-16) The live loads Lo for structural members (excluding roof live loads) may be decreased according to ASCE 7-16 with the help of the following formula:

Method 1 – KLL × AT (Equation 4.7-1):

This method employs KLL (element live load factor) and tributary area AT for the computation of lowered live load.

This method is utilized for structural elements such as interior and edge columns.

where:

- **L = design live load after reduction (kN/m²)**
- **Lo = unreduced design live load from Table 4.3-1**
- **KLL = live load factor for the element (from Table 4.7-1)**
- **AT = tributary area supported by the element (m² or ft²)**

Minimum limits for reduction:

- **Elements supporting one floor: L ≥ 0.50 Lo**
- **Elements supporting two or more floors: L ≥ 0.40 Lo**

This reduction applies only when KLL × AT ≥ 37.16 m² (400 ft²) and allows the design to account for realistic load conditions while maintaining safety.

Revised Reduced Live Load Calculation (KLL × AT Method)

Unreduced Live Load:

$$L_o = 0.96 \text{ kN/m}^2$$

KLL Values:

- **Interior Columns = 4**
- **Edge Columns = 2**

Design Equation (Metric Units):

$$L = L_o(0.25 + \frac{4.57}{\sqrt{K_{LL} \cdot A_T}})$$

1) Interior Columns (KLL = 4, AT = 112.5 m²)

$$\sqrt{K_{LL} \cdot A_T} = \sqrt{4 \cdot 112.5} = \sqrt{450} \approx 21.21$$

$$L = 0.96(0.25 + \frac{4.57}{21.21}) = 0.96(0.25 + 0.2155) = 0.96 \times 0.4655$$

$$\approx 0.447 \text{ kN/m}^2$$

2) Edge Columns (KLL = 2, AT = 56.25 m²)

$$\sqrt{K_{LL} \cdot A_T} = \sqrt{2 \cdot 56.25} = \sqrt{112.5} \approx 10.61$$

$$L = 0.96(0.25 + \frac{4.57}{10.61}) = 0.96(0.25 + 0.4308) = 0.96 \times 0.6808$$

$$\approx 0.653 \text{ kN/m}^2$$

Updated Table – KLL × AT Method

Column Type	KLL	AT (m^2)	Reduced Live Load L (kN/m^2)
Interior Columns	4	112.5	0.447
Edge Columns	2	56.25	0.653

Method 2 – R1 × R2 (Roof Live Load Reduction, ASCE 7-16):

This method employs R1 (assessed using tributary area) and R2 (assessed using roof slope or rise-to-span ratio).

Flat or slightly sloped roofs will especially benefit from this method, as it provides a more uniform approach for roof live loads.

Reduced Live Load on Columns Using R1 and R2 (ASCE 7-16)

Given Data:

- **Unreduced live load: $L_o = 0.96$ kN/m²**
- **Tributary area per column: $A_T = 112.5$ m²**
- **Column heights: 8.6 m**
- **Span of roof/truss: 22.50 m**
- **Maximum height of truss above column: 3.5 m**

1) Determination of Reduction Factors

R1 – Based on Tributary Area (AT):

$$R_1 = \begin{cases} 1 & A_T \le 18.58 \text{ m}^2 \\ 1.2 - 0.011A_T & 18.58 < A_T < 55.74 \text{ m}^2 \\ 0.6 & A_T \ge 55.74 \text{ m}^2 \end{cases}$$

For $A_T = 58.62$ m² ≥ 55.74, we get:

$$R_1 = 0.6$$

R2 – Based on Roof Slope (F):

$$F = 0.12 \times \text{slope (\%)}$$

Roof rise = 3.5 m, span = 22.50 m

$$\text{slope} = 17.28\%$$

$$F = 0.12 \times 12.5 = 1.5$$

$$R_2 = \begin{cases} 1 & F \leq 4 \\ 1.2 - 0.05F & 4 < F < 12 \\ 0.6 & F \geq 12 \end{cases}$$

Here, $F = 1.5 < 4 \rightarrow R_2 = 1$

2) Reduced Live Load

$$L_{\text{reduced}} = L_o \cdot R_1 \cdot R_2 = 0.96 \times 0.6 \times 1 = 0.576 \text{ kN/m}^2$$

3) Summary Table

Column Type	Tributary Area AT (m²)	R1	R2	Reduced Live Load L (kN/m²)
Interior & Edge Columns	112.5	0.6	1	0.576

Notes:

• The tributary area (R1) is the main controlling factor of the reduction, as the slope factor R2 = 1 due to the negligible roof pitch.

Live Load Reduction Methods for Columns

Two different approaches were employed to calculate the diminished live loads for the interior and edge columns: the **KLL × AT method** and the **R1 × R2** method prescribed by **ASCE 7-16**. The KLL × AT approach employs the live load factor of the structural element along with the tributary area to determine the reduced live load, while the R1 × R2 approach entails considering the tributary area (R1) along with the slope of the roof or the ratio of rise to span (R2), thereby giving one a more balmy approach for roof live loads. For the internal columns (AT = 112.5 m²), the reduced load was 0.447 kN/m² using the KLL × AT method and **0.576 kN/m²** using R1 × R2. For the corner columns (AT = 56.25 m²), the reduced load was **0.653 kN/m²** with KLL × AT and **0.576 kN/m²** with R1 × R2. To maintain uniformity and at the **same time comply with the code, the R1 × R2 method values were used for both interior and edge columns.**

3.6.3 Rain Load

Rain Load is the load resulting from the accumulation of rainfall on roofs and surfaces, and it is considered a temporary load that must be taken into account in structural design. The magnitude of this load depends on rainfall intensity, roof slope, drainage capacity, and local code requirements. In this project, the building is equipped with an efficient water drainage system to prevent water ponding on the roof, **taking into account that the roof slope is 12.5°.** Rain load is typically combined with other loads such as dead load, live load, and snow load to ensure structural safety and prevent excessive deflection or structural failure.

3.6.4 Snow Load

Snow loads depend on the elevation of the site above sea level and the roof design. These loads are determined using building codes that provide tables based on the building's elevation and the roof slope angle. The following table, extracted from the Jordanian Code, specifies snow loads based on elevation:

Table 3.2 : Snow loads based on elevation above sea level

Elevation Above Sea Level (m)	Snow Load (KN/m^2)
h<250	0
500>h>250	(h−250)/1000
1500>h>500	(h−400)/400
2500>h>1500	(h−812.5)/250

Based on Table (3.1) and after determining the building's elevation above sea level (832.8 m), the snow loads were calculated accordingly.

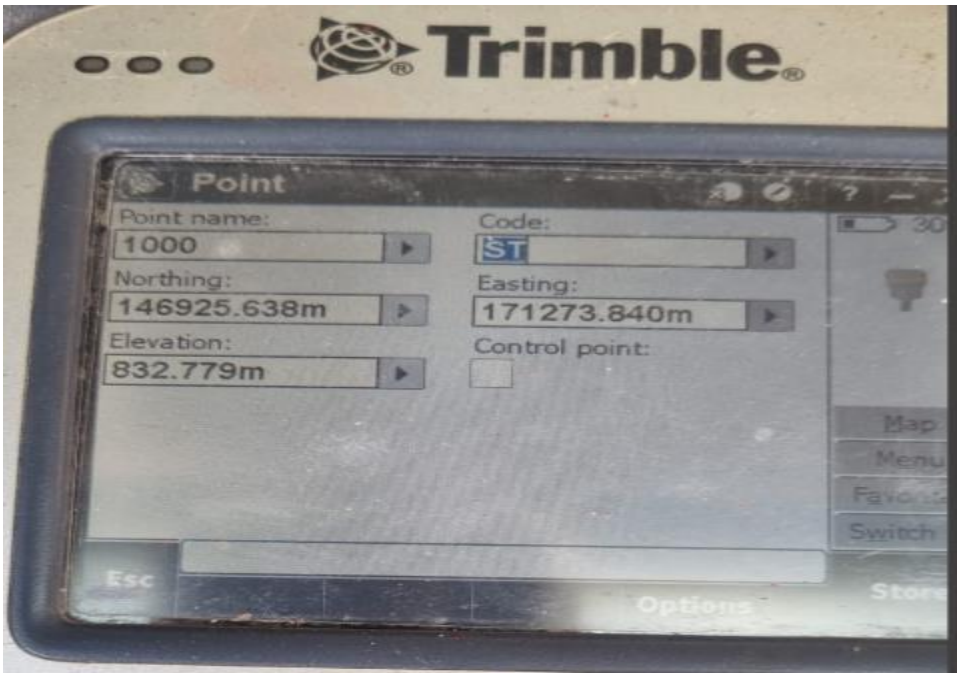


Figure 3.7 Determination of site elevation using a surveying instrument (Trimble) for the calculation of the basic ground snow load (pg).

1.

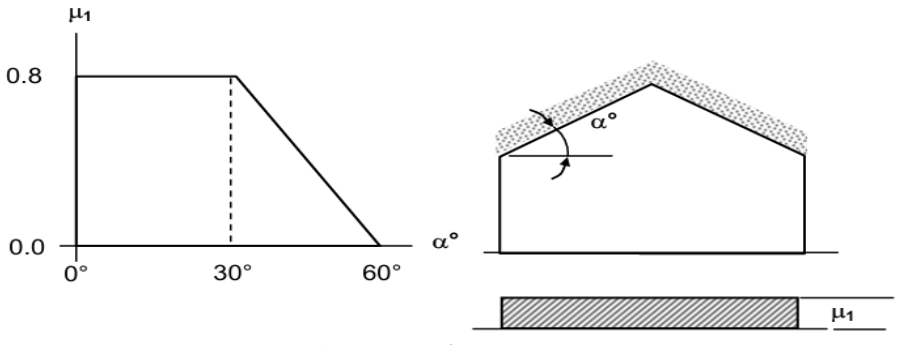
H=832.779 m

Ground snow load p_g

$$p_g = \frac{832.8 - 400}{400} = \frac{432.8}{400} = 1.082 \text{ kN/m}^2$$

2. **Sloped (balanced) roof snow load**

$60° \le \alpha°$	$30° < \alpha° < 60°$	$0° \le \alpha° \le 30$	زاوية ميل السقف $\alpha°$
$\mu_1 = 0$	$\mu_1 = 0.8\left[\frac{60-\alpha}{30}\right]$	$\mu_1 = 0.8$	معامل الشكل μ_1



الشكل (٣-٢-أ)

معاملات الشكل لحمل الثلج للسقوف المائلة في حالة الحمل المتماثل (منتظم التوزيع).

Figure 3. 8 Ground snow load calculation and sloped roof shape coefficients.

3.

$$Sd = \mu i \, So$$

$$\boldsymbol{Sd = \mu i \, So = 0.80 \times 1.082 = 0.865 \ kN/m^2}$$

3.6.5 Wind Loads (ASCE 7 – Low-Rise Method)

3.6.5.1 Introduction

In this chapter, the wind loads calculated using the **Low-Rise Buildings Method** as per the **American standard ASCE 7** – Minimum Design Loads for Buildings and Other Structures are discussed. This method can be applied to steel buildings with a simple roof shape and relatively low height. The procedure **calculates the wind pressure on the main wind-force resisting system (MWFRS)**, taking into account the external and internal pressure coefficients, building exposure, and site wind speed.

3.6.5.2 Design Wind Speed

The ASCE 7-16 requirements define basic design wind speed V as 3-second gust wind speed measured at 10 meters above ground level in Exposure Category C. The project site required wind speed assessment through local meteorological data and regional building code standards because it lies outside ASCE 7 mapped areas. The basic design wind speed used to calculate wind pressure on the Main Wind-Force Resisting System (MWFRS) requires the following information:

V=44 m/s.

3.6.5.3 Exposure Category

The exposure classification of the structure is established according to the attributes of the project location, which is mainly residential and is also close to buildings with moderate height and density.

The aforementioned obstructions lead to a decrease in the wind speed at the ground level and also change the wind pressure that acts on the building.

Hence, the decision to use the Exposure **Category B is made**.

This category of exposure is typical for urban and sub-urban regions where residential buildings are the primary types of obstructions, and they are closely spaced. As a result, the building experiences wind pressures that are significantly less than those in open terrain conditions.

3.6.5.4 Building Height and Elevation-Dependent Factors

(a) Building Heights

- Eave height:

$$h_{\text{eave}} = 8.6 \text{ m}$$

Ridge height:

$$h_{\text{ridge}} = 11.1 \text{ m}$$

The mean roof height, used in the Low-Rise method, is:

$$h_{\text{mean}} = \frac{8.6 + 11.1}{2} = 9.85 \text{ m}$$

Table 26.10-1 Velocity Pressure Exposure Coefficients, K_h and K_z

Height above Ground Level, z		Exposure		
ft	m	B	C	D
0–15	0–4.6	0.57 (0.70)[a]	0.85	1.03
20	6.1	0.62 (0.70)[a]	0.90	1.08
25	7.6	0.66 (0.70)[a]	0.94	1.12
30	9.1	0.70	0.98	1.16
40	12.2	0.76	1.04	1.22
50	15.2	0.81	1.09	1.27
60	18.0	0.85	1.13	1.31
70	21.3	0.89	1.17	1.34
80	24.4	0.93	1.21	1.38
90	27.4	0.96	1.24	1.40
100	30.5	0.99	1.26	1.43
120	36.6	1.04	1.31	1.48
140	42.7	1.09	1.36	1.52
160	48.8	1.13	1.39	1.55
180	54.9	1.17	1.43	1.58
200	61.0	1.20	1.46	1.61
250	76.2	1.28	1.53	1.68
300	91.4	1.35	1.59	1.73
350	106.7	1.41	1.64	1.78
400	121.9	1.47	1.69	1.82
450	137.2	1.52	1.73	1.86
500	152.4	1.56	1.77	1.89

Table 3.*3* Determination of velocity pressure exposure coefficient (Kz) based on ASCE 7-16.

Using linear interpolation from ASCE 7 Table 26.10-1 for Exposure Category B:

- **At z = 9.1 m (30 ft) → $K = 0.70$**
- **At z = 12.2 m (40 ft) → $K = 0.76$**

For z = 9.85 m, the velocity pressure exposure coefficient is obtained as:

$$Kz = 0.70 + \frac{9.85 - 9.1}{12.2 - 9.1} \times (0.76 - 0.70) = 0.715$$

Therefore, the adopted value is:

$$\boxed{Kz = 0.715}$$

(b) Elevation and Terrain Coefficients

According to the Low-Rise analytical procedure prescribed by ASCE 7-16:

$$K_z = 0.715, K_{zt} = 1, K_h = 1.0, K_e = 1.0$$

For the global wind force computations, the topographic factor is taken as **Kzt = 1.0**. While Chapter 2 highlights the long-term forensic risks associated with wind velocity speed-up effects in mountainous microclimates like the Ramallah highlands , a baseline value of Kzt = 1.0 is adopted herein as a conservative design benchmark.

This assumption presumes that the surrounding urban obstructions and suburban density layout (Exposure Category B) provide a stabilizing shielding mechanism that partially counteracts macro-topographic wind amplifications at the specific localized asset crest.

(c) Wind Directionality Factor

For MWFRS wind load calculations:

$$K_d = 0.85$$

Structure Type	Directionality Factor K_d
Buildings	
Main Wind Force Resisting System	0.85
Components and Cladding	0.85
Arched Roofs	0.85
Circular Domes	1.0[a]
Chimneys, Tanks, and Similar Structures	
Square	0.90
Hexagonal	0.95
Octagonal	1.0[a]
Round	1.0[a]
Solid Freestanding Walls, Roof Top Equipment, and Solid Freestanding and Attached Signs	0.85
Open Signs and Single-Plane Open Frames	0.85
Trussed Towers	
Triangular, square, or rectangular	0.85
All other cross sections	0.95

[a]Directionality factor $K_d = 0.95$ shall be permitted for round or octagonal structures with nonaxisymmetric structural systems.

Table 3.*4* Wind directionality factor (Kd) specified by ASCE 7-16 for structural design.

3.6.5.5 Velocity Pressure Calculation

The velocity pressure at the mean roof height is calculated using:

$$\boldsymbol{q_z = 0.613\, K_z\, K_{zt}\, K_d\, K_e\, V^2 (\mathrm{N/m^2})}$$

where *V* is the basic wind speed in meters per second (m/s).

Substituting the adopted values:

$$q_z = 0.613 \times 0.715 \times 1.0 \times 1.0 \times 0.85 \times 44^2$$

$$q_z = 0.7213 \text{ kN/m}^2$$

Thus, the **design velocity pressure** used in subsequent calculations is:

$$\boxed{q_z = 0.72 \text{ kN/m}^2}$$

3.6.5.6 External Pressure Coefficients for the Roof (Cp)

The roof has a slope angle:

$$\theta = 12.5^\circ$$

External pressures were determined using ASCE 7 Low-Rise roof pressure coefficients. Since 12.5° lies between the tabulated values for 5° and 20°, linear interpolation was performed. The resulting coefficients are:

Roof Zone	C_p
Zone 1	**0.50**4
Zone 2	**–0.69**
Zone 3	**–0.458**
Zone 4	**–0.40**2

Table 3.5 Interpolated external roof pressure coefficients

These coefficients are applied to the corresponding roof areas according to the wind direction.

3.6.5.7 Internal Pressure Coefficient (GCpi)

One of the main factors affecting the internal pressure in the building is the existence of a large main door in one of its façades. Therefore, according to **ASCE 7**, the building is categorized as a Partially Enclosed Building.

For the windward wall:

- Gross wall area:

$$A_g = 221 \text{ m}^2$$

- Main door opening area:

$$A_o = 5.08 \times 14.22 = 72.24\ \text{m}^2$$

- Opening ratio:

$$\frac{A_o}{A_g} = \frac{72.24}{221} = 0.33\ (33\%)$$

Since the opening area on the windward wall significantly exceeds both **1% of the wall area (2.21 m²)** and **0.37 m²**, and no openings are present in the remaining façades ($A_{oi} = 0$), the criteria for a **Partially Enclosed Building** are satisfied.

Accordingly, ASCE 7 prescribes the internal pressure coefficient as:

$$(\boldsymbol{GC_{pi}}) = \pm \mathbf{0.55}$$

Both positive and negative internal pressure cases shall be considered in the design and the applicable condition for each structural surface shall prevail.

3.6.5.8 Wind Pressure Coefficients and Roof Angle Interpolation

The net design wind pressure on each building surface is calculated using:

$$p = q_z \cdot GC_p \pm q_z \cdot GC_{pi}$$

Table 26.13-1 Main Wind Force Resisting System and Components and Cladding (All Heights): Internal Pressure Coefficient, (GC_{pi}), for Enclosed, Partially Enclosed, Partially Open, and Open Buildings (Walls and Roof)

Enclosure Classification	Criteria for Enclosure Classification	Internal Pressure	Internal Pressure Coefficient, (GC_{pi})
Enclosed buildings	A_o is less than the smaller of $0.01A_g$ or 4 sq ft (0.37 m) and $A_{oi}/A_{gi} \le 0.2$	Moderate	+0.18 −0.18
Partially enclosed buildings	$A_o > 1.1A_{oi}$ and $A_o >$ the lesser of $0.01A_g$ or 4 sq ft (0.37 m) and $A_{oi}/A_{gi} \le 0.2$	High	+0.55 −0.55
Partially open buildings	A building that does not comply with Enclosed, Partially Enclosed, or Open classifications	Moderate	+0.18 −0.18
Open buildings	Each wall is at least 80% open	Negligible	0.00

Notes
1. Plus and minus signs signify pressures acting toward and away from the internal surfaces, respectively.
2. Values of (GC_{pi}) shall be used with q_z or q_h as specified.
3. Two cases shall be considered to determine the critical load requirements for the appropriate condition:
   a. A positive value of (GC_{pi}) applied to all internal surfaces, or
   b. A negative value of (GC_{pi}) applied to all internal surfaces.

Table 3.6 Wind pressure equation and internal pressure coefficient (GCpi) selection.

where:

- $q_z = 0.72\ \text{kN/m}^2$

- GC_p: external pressure coefficient (roof and walls)
- $GC_{pi} = \pm 0.55$

This formula is applied to compute pressures on:

- Roof zones (1, 2, 3, 4)
- Windward wall
- Leeward wall
- Side walls
- The large entrance door

The resulting pressures are subsequently applied to the main steel frames in the structural analysis model.

Load Case A

	Building Surface							
Roof Angle θ (degrees)	1	2	3	4	1E	2E	3E	4E
0–5	0.40	−0.69	−0.37	−0.29	0.61	−1.07	−0.53	−0.43
20	0.53	−0.69	−0.48	−0.43	0.80	−1.07	−0.69	−0.64
30–45	0.56	0.21	−0.43	−0.37	0.69	0.27	−0.53	−0.48
90	0.56	0.56	−0.37	−0.37	0.69	0.69	−0.48	−0.48

Load Case B

	Building Surface											
Roof Angle θ (degrees)	1	2	3	4	5	6	1E	2E	3E	4E	5E	6E
0–90	−0.45	−0.69	−0.37	−0.45	0.40	−0.29	−0.48	−1.07	−0.53	−0.48	0.61	−0.43

Table 1.7 External wind pressure coefficients (GCpf) for Load Cases A and B

interpolation only with Load Case A

	degrees	1	2	3	4	5	6
Roof Angle 1	5	0.400	-0.69	-0.37	-0.29	0	0
Roof Angle 2	20	0.530	-0.69	-0.48	-0.43	0	0
Actual Roof Angle	12.5	0.465	-0.69	-0.425	-0.360	0.000	0.000

Table 3.8 Linear interpolation of external pressure coefficients for Load Case A

3.6.5.9 Design Wind Pressure Evaluation

Wind pressures responsible for the design were calculated for all surfaces of the building based on the guidelines of ASCE 7. The following equation was employed to determine the wind pressure for each surface:

$$\boldsymbol{p = q_h\left[(GC_{pf}) - (GC_{pi})\right]}$$

where $q_h$is the velocity pressure evaluated at the mean roof height, $GC_{pf}$is the external pressure coefficient, and $GC_{pi}$is the internal pressure coefficient.
Due to the presence of a large main door in one façade, the building is classified as a Partially Enclosed Building. Therefore, the internal pressure coefficient was taken as:

$$\boldsymbol{(GC_{pi}) = \pm 0.55}$$

Both positive and negative internal pressure cases were considered. For each wind direction, two load cases were analyzed, and the governing pressure (pressure or suction) was selected for design.

External and Internal Pressure Coefficients – Transverse Wind Direction

Table 3.9 External and internal pressure coefficients (GCpf and GCpi) for the transverse wind direction.

Surface	$\boldsymbol{GC_{pf}}$	$\boldsymbol{GC_{pi}(+)}$	$\boldsymbol{GC_{pi}(-)}$
1	0.465	+0.55	−0.55
2	−0.69	+0.55	−0.55
3	−0.425	+0.55	−0.55
4	−0.36	+0.55	−0.55

.

Design Wind Pressures – Transverse Wind Direction
Case 1: $GC_{pi} = +0.55$

Table 3.10 Design wind pressures for the transverse direction under Load Case 1 (GCpi = +0.55).

Surface	$\boldsymbol{GC_{pf} - GC_{pi}}$	**Wind Pressure (kN/m²)**
1	−0.085	-0.061
2	−1.24	-0.894
3	−0.975	-0.703
4	−0.91	-0.656

Case 2: $GC_{pi} = -0.55$

Surface	$GC_{pf} - GC_{pi}$	Wind Pressure (kN/m²)
1	1.015	0.732
2	−0.14	-0.101
3	0.125	0.090
4	0.19	0.137

Table 3.11 Design wind pressures for the transverse direction under Load Case 2 (GCpi = -0.55).

External and Internal Pressure Coefficients – Longitudinal Wind Direction

Table 3.12 External and internal pressure coefficients (GCpf} and GCpi) for the longitudinal wind direction.

Surface	GC_{pf}	$GC_{pi}(+)$	$GC_{pi}(-)$
1	−0.45	+0.55	−0.55
2	−0.69	+0.55	−0.55
3	−0.37	+0.55	−0.55
4	−0.45	+0.55	−0.55
5	0.40	+0.55	−0.55
6	−0.29	+0.55	−0.55

Design Wind Pressures – Longitudinal Wind Direction

Case 1: $GC_{pi} = +0.55$

Table 3.13 Design wind pressures for the longitudinal direction under both internal pressure cases.

Surface	$GC_{pf} - GC_{pi}$	Wind Pressure (kN/m²)
1	−1.00	-0.721
2	−1.24	-0.894
3	−0.92	-0.664
4	−1.00	-0.721
5	−0.15	-0.108
6	−0.84	-0.606

Case 2: $GC_{pi} = -0.55$

Table 3.14 Design wind pressures for the longitudinal direction under internal pressure Case 2.

Surface	$GC_{pf} - GC_{pi}$	Wind Pressure (kN/m²)
1	0.10	0.072
2	−0.14	-0.101
3	0.18	0.130
4	0.10	0.072
5	0.95	0.685
6	0.26	0.188

Design Note
The evaluation of pressure and suction for all surfaces was carried out, respectively, and the maximum wind pressure was selected for the structural design in order to meet **ASCE 7** standards.

1. Wind Base Shear in X-Direction
(Walls: Surface 1 and Surface 4)
Case 1 $(GC_{pi} = +0.55)$

$$V_{X,1} = 146.48 \text{ kN}$$

Case 2 $(GC_{pi} = -0.55)$

$$V_{X,2} = 188.13 \text{ kN}$$

Governing Wind Base Shear – X Direction

$$\boxed{V_X = 188.13 \text{ kN(Case 2)}}$$

The wind base shear of **188.13 kN** was distributed among five frames using the tributary width concept, so that each interior frame had **47.03 kN**, while each edge frame had **23.51 kN**.

2. Wind Base Shear in Y-Direction
(Walls: Surface 5 and Surface 6)
Case 1 $(GC_{pi} = +0.55)$

$$V_{Y,1} = 158.16 \text{ kN}$$

Case 2 $(GC_{pi} = -0.55)$

$$V_{Y,2} = 193.11 \text{ kN}$$

Governing Wind Base Shear – Y Direction

$$\boxed{V_Y = 193.11 \text{ kN(Case 2)}}$$

3.6.6 SEISMIC ANALYSIS

Prepared for Steel Truss Building – **Height = 11.1 m**

This chapter explains the seismically designed parameters and methods that were used to carry out the analysis of the proposed steel truss structure. The seismic design is in harmony with the stipulations of ASCE 7-16 and the Equivalent Lateral Force (ELF) Procedure is used for the analysis of the regular and low-rise buildings as per the provisions.

The total seismic height of the single-story steel truss hall is: ht = 11.1m

The structure is taken to be **Risk Category II** while the Importance Factor is:

Ie=1.0

Table 1.5-2 Importance Factors by Risk Category of Buildings and Other Structures for Snow, Ice, and Earthquake Loads

Risk Category from Table 1.5-1	Snow Importance Factor, I_s	Ice Importance Factor—Thickness, I_i	Ice Importance Factor—Wind, I_w	Seismic Importance Factor, I_e
I	0.80	0.80	1.00	1.00
II	1.00	1.00	1.00	1.00
III	1.10	1.15	1.00	1.25
IV	1.20	1.25	1.00	1.50

Note: The component importance factor, I_p, applicable to earthquake loads, is not included in this table because it depends on the importance of the individual component rather than that of the building as a whole, or its occupancy. Refer to Section 13.1.3.

Table 3.15 ASCE 7 tabulated importance factors based on the building's risk category.

3.6.6.2 Seismic Hazard Parameters

The site has the following mapped spectral accelerations:

Ss=0.56g

Sl=0.28g

And it is placed in **Site Class B** according to the geotechnical conditions that are supposed.

3.6.6.3. Site Coefficients and Design Spectrum

According to ASCE 7-16 Tables 11.4-1 and 11.4-2:

$$F_a = 0.9$$

$$F_v = 0.8$$

Table 11.4-1 Short-Period Site Coefficient, F_a

Site Class	Mapped Risk-Targeted Maximum Considered Earthquake (MCE_R) Spectral Response Acceleration Parameter at Short Period					
	$S_S \le 0.25$	$S_S = 0.5$	$S_S = 0.75$	$S_S = 1.0$	$S_S = 1.25$	$S_S \ge 1.5$
A	0.8	0.8	0.8	0.8	0.8	0.8
B	0.9	0.9	0.9	0.9	0.9	0.9
C	1.3	1.3	1.2	1.2	1.2	1.2
D	1.6	1.4	1.2	1.1	1.0	1.0
E	2.4	1.7	1.3	See Section 11.4.8	See Section 11.4.8	See Section 11.4.8
F	See Section 11.4.8	See Section 11.4.8	See Section 11.4.8	See Section 11.4.8	See Section 11.4.8	See Section 11.4.8

Note: Use straight-line interpolation for intermediate values of S_s.

Table 11.4-2 Long-Period Site Coefficient, F_v

Site Class	Mapped Risk-Targeted Maximum Considered Earthquake (MCE_R) Spectral Response Acceleration Parameter at 1-s Period					
	$S_1 \le 0.1$	$S_1 = 0.2$	$S_1 = 0.3$	$S_1 = 0.4$	$S_1 = 0.5$	$S_1 \ge 0.6$
A	0.8	0.8	0.8	0.8	0.8	0.8
B	0.8	0.8	0.8	0.8	0.8	0.8
C	1.5	1.5	1.5	1.5	1.5	1.4
D	2.4	2.2[a]	2.0[a]	1.9[a]	1.8[a]	1.7[a]
E	4.2	See Section 11.4.8	See Section 11.4.8	See Section 11.4.8	See Section 11.4.8	See Section 11.4.8
F	See Section 11.4.8	See Section 11.4.8	See Section 11.4.8	See Section 11.4.8	See Section 11.4.8	See Section 11.4.8

Note: Use straight-line interpolation for intermediate values of S_1.
[a]Also, see requirements for site-specific ground motions in Section 11.4.8.

Table 3.16 Determination of the short-period (Fa) and long-period (Fv) seismic site coefficients based on ASCE 7 provisions, highlighting the values corresponding to Site Class B.

MCER Spectral Response Accelerations

$$S_{MS} = F_a S_s = 0.9 \times 0.56 = 0.504$$

$$S_{M1} = F_v S_1 = 0.8 \times 0.28 = 0.224$$

Design Spectral Response Accelerations

$$S_{DS} = \frac{2}{3} S_{MS} = \frac{2}{3} \times 0.504 = 0.336$$

$$S_{D1} = \frac{2}{3} S_{M1} = \frac{2}{3} \times 0.224 = 0.149$$

Seismic Design Category

TABLE 11.6-1 Seismic Design Category Based on Short-Period Response Acceleration Parameter

Value of S_{DS}	Risk Category: I or II or III	Risk Category: IV
$S_{DS} < 0.167$	A	A
$0.167 \le S_{DS} < 0.33$	B	C
$0.33 \le S_{DS} < 0.50$	C	D
$0.50 \le S_{DS}$	D	D

TABLE 11.6-2 Seismic Design Category Based on 1-s Period Response Acceleration Parameter

Value of S_{D1}	Risk Category: I or II or III	Risk Category: IV
$S_{D1} < 0.067$	A	A
$0.067 \le S_{D1} < 0.133$	B	C
$0.133 \le S_{D1} < 0.20$	C	D
$0.20 \le S_{D1}$	D	D

Table 3.17 Seismic Design Category (SDC) determination tables

$$\text{Seismic Design Category} = C$$

3.6.6.4. Seismic Force Resisting System

The structure lacks ductile seismic systems because it does not possess seismic detailing and ductile connections together with its Moment-Resisting Frames and specially detailed Braced Frames.

The structure receives strict classification as a "Steel System Not Specifically Detailed for Seismic Resistance" according to ASCE 7 provisions which use Table 12.2-1 for this purpose. The assigned seismic parameters for this classification are:

Response Modification Coefficient (R): 3

Overstrength Factor (Ω_o): 3

Deflection Amplification Factor (Cd): 3

Justification: The as-built condition requires R-value 3 as a sustainable yet precise measurement. The analysis produces higher elastic design seismic forces because of the absence of proper structural ductility and detailing.

3.6.6.5. Fundamental Period Calculation (Using Meters)

The approximate fundamental period is calculated using:

$$T = C_t h_t^x$$

Values are converted to operate directly with meters.

Table 12.8-2 Values of Approximate Period Parameters C_t and x

Structure Type	C_t	x
Moment-resisting frame systems in which the frames resist 100% of the required seismic force and are not enclosed or adjoined by components that are more rigid and will prevent the frames from deflecting where subjected to seismic forces:		
Steel moment-resisting frames	0.028 (0.0724)[a]	0.8
Concrete moment-resisting frames	0.016 (0.0466)[a]	0.9
Steel eccentrically braced frames in accordance with Table 12.2-1 lines B1 or D1	0.03 (0.0731)[a]	0.75
Steel buckling-restrained braced frames	0.03 (0.0731)[a]	0.75
All other structural systems	0.02 (0.0488)[a]	0.75

[a]Metric equivalents are shown in parentheses.

Table 3.18 Approximate fundamental period parameters (Ct and x)

3.6.6.5.1 Steel System Not Specifically Detailed for Seismic Resistance

Given:

- $C_t = 0.0488$
- $x = 0.75$

Convert Ct:

$$T = 0.0488 \times (11.1)^{0.75} = 0.297 \text{ s}$$

3.6.6.6. Seismic Response Coefficient C_s

According to ASCE 7-16 12.8.1:

$$C_s = \frac{S_{DS}}{R/I_e}$$

$$C_s \leq \frac{S_{D1}}{T(R/I_e)}$$

$$C_s \geq 0.044 S_{DS} \frac{I_e}{R}, C_s \geq 0.01$$

3.6.6.6.1 For Moment-Resisting Frame (R = 3 , T = 0.297 s)

$$C_{s,eq} = \frac{S_{DS}}{\frac{R}{I_e}} = \frac{0.336}{3.5} = 0.112 \ \ldots\ldots\ldots\ldots\ldots \textbf{control}$$

$$C_{s,max} = \frac{S_{D1}}{T\left(\frac{R}{I_e}\right)} = \frac{0.149}{0.497 \times 3.5} = 0.167$$

$$C_{s,mim} = 0.015$$

Weight Calculation

The effective seismic weight of the building was determined ASCE 7 by including the self-weight of the structure, the additional roof dead loads. The self-weight of the structure was determined to be 112.57 kN, and the additional dead load contribution was 132.25 kN. The total effective seismic weight of the building is thus:

$$\boxed{\boldsymbol{W = 244.82 \text{ kN}}}$$

3.6.6.7. Base Shear Calculation

$$\boldsymbol{V = C_s W}$$

Where W is the seismic weight of the structure.

Final Expressions

$$\boldsymbol{V = 0.112 \ * 244.82 = 27.41} \text{ KN}$$

3.6.7 Wind–Seismic Load Comparison and Governing Load Case

- A comparison of the lateral demands caused by wind and seismic was done by aligning the base shear in the different principal directions. The winning wind base shear values were:

  (Wind): $V_{\text{wind},X} = 148.02$ kN

The seismic base shear was calculated using $V = C_s W$ with $W = 321.00$ kN, resulting in:

- (Seismic): $V_{\text{EQ},X} = 27.41$ kN

Accordingly, wind governs in both directions:

$$V_{\text{wind},X} = 188.13 \text{ kN} \;>>>>\; V_{\text{EQ},X} = 27.41 \text{ kN}$$

Therefore, the wind load case controls the global lateral shear demand of the studied building in both the X- and Y-directions.

CHAPTER4: Structural Assessment and Design Verification.

4.1 Introduction

The chapter displays the structural analysis together with the design assessment of the current industrial steel truss building that uses STAAD.Pro software for its evaluation. The applied loads which were established in Chapter 3 exist as a result of calculations that follow ASCE 7-16 standards for structural loading and AISC 360-16 requirements for steel design.

The main purpose of this chapter requires assessment of current structural condition of the building together with its critical weaknesses and assessment of proposed strengthening methods. The complete structural study required model stability to be established before its execution could begin.

The analytical model needed redesign because it had to include a complete longitudinal bracing system and all height extensions needed for end-wall column support. The design changes create a permanent structural pathway which enables safe movement of wind and seismic loads from the building to its foundation. The analysis tests a stabilized structural system which uses main trusses to handle transverse loads and newly installed bracing to manage longitudinal forces.

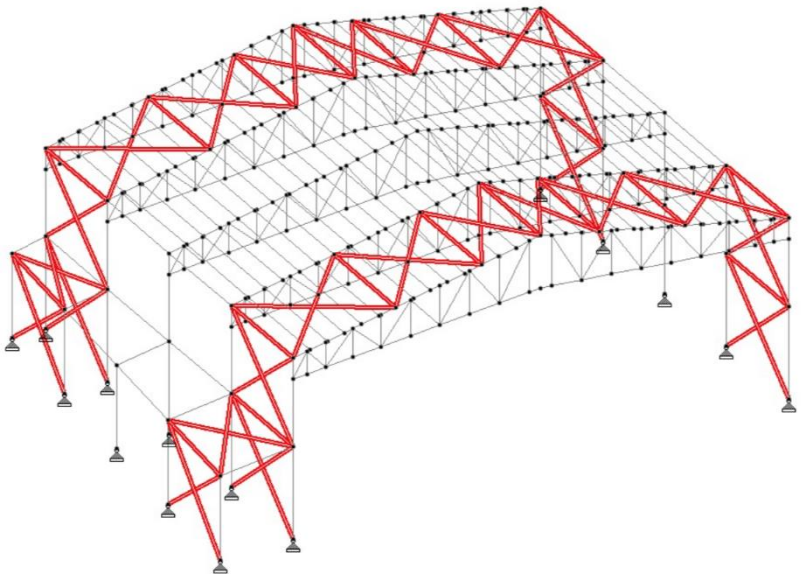


Figure 4.1 : 3D analytical model of the industrial building generated in STAAD.Pro, highlighting the proposed longitudinal bracing system and end-wall column extensions (in red) required for global stability.

4.2 Development of the Structural Model

The development of a three-dimensional building model used STAAD.Pro to create an accurate representation of the building's real structural performance. The model geometry was constructed based on precise field measurements obtained during the site inspection, encompassing member dimensions, structural layout, and as-built connection details.

The model included all structural components which were designed to match their actual field conditions. The truss members were modeled in accordance with their existing physical configuration, while the tubular purlins were modeled as secondary beams responsible for transferring roof loads to the main frames. Structural loads from distributed gravity roof loads and lateral wind forces were applied to the structure to create actual loading conditions. The software generated a complete three-dimensional analytical model which is shown in Figure 4.2.

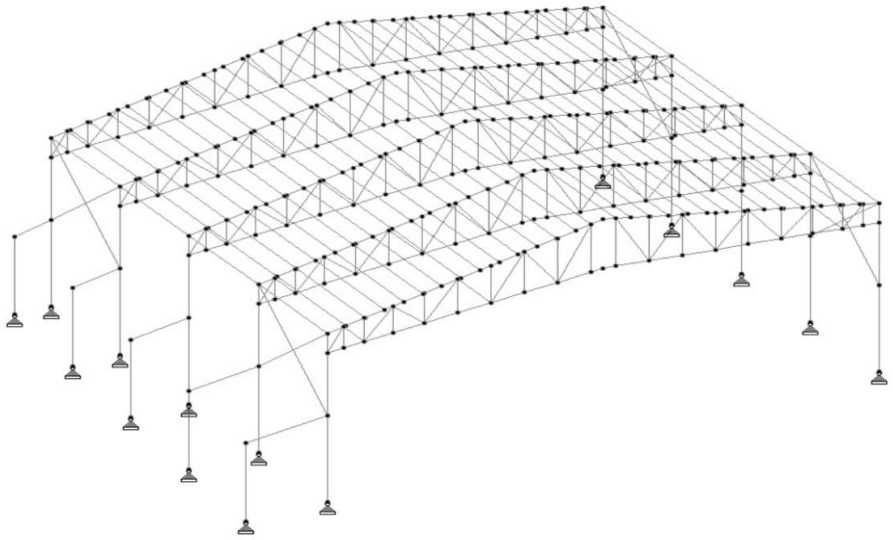


Figure 4.2 : Three-dimensional analytical wireframe model of the existing steel truss building developed in STAAD.Pro based on field measurements.

4.2.1 Structural Sections and Profile Assignments

The STAAD.Pro model required each member to receive actual as-built section properties which engineers found through field surveys. Figure 4.2 shows the structural layout together with the distribution of profiles across the truss and main frame

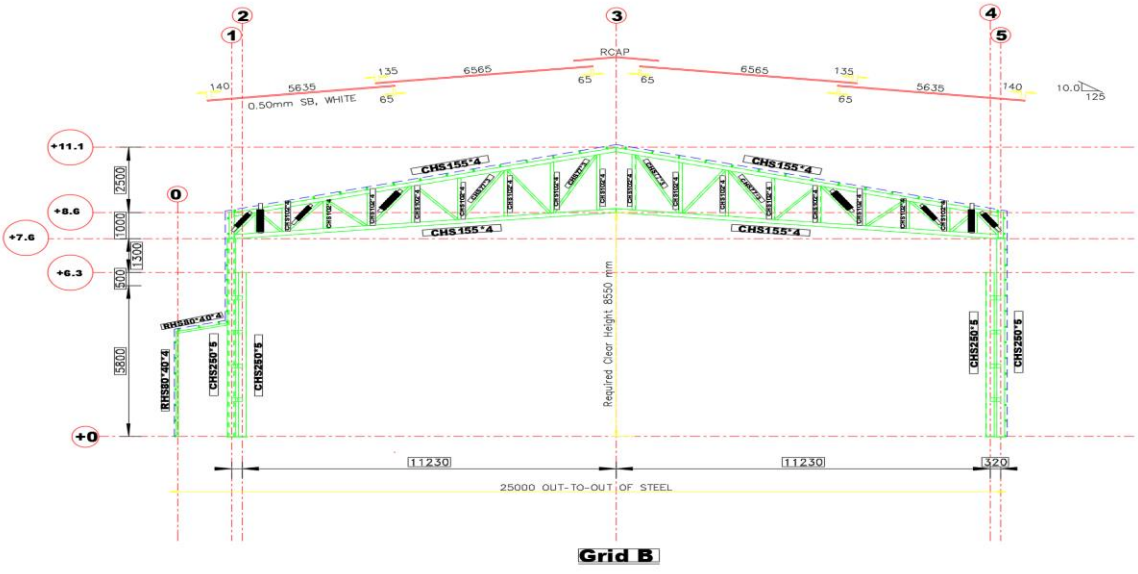


Figure 4.3 Transverse cross-section of the existing steel warehouse (Grid B) showing overall geometry and structural member sizes.

The technical specifications for these sections, including their European standard designations (EN 10210) and the specific geometric properties (Area and Moments of Inertia) utilized during the computational analysis, are summarized in Table 4.1.

Table 4.1 Summary of the assigned structural steel profiles, including European designations, physical dimensions, and cross-sectional properties for the main frame elements.

Prop	European Designation	Structural Component	OD / Dimensions (mm)	Thick. (mm)	Area (in2)	Inertia Iyy /Izz (in4)
1	**CHS 155.0 x 4.0**	Top and Bottom Chords (6")	155.0	4.0	2.941	13.002
2	**RHS 80 x 40 x 4.0**	Side Canopy & Purlins	80 x 40	4.0	1.376	0.543 / 1.672
3	**CHS 250.0 x 5.0**	Main Support Columns	250.0	5.0	5.965	69.402
4	**CHS 102.0 x 4.0**	Truss Vertical Members (4")	102.0	4.0	1.910	2.285
5	**CHS 77.0 x 3.0**	Truss Diagonal Members (3")	77.0	3.0	1.081	1.149

4.3 Modeling Assumptions and Simplifications

To ensure the accuracy and reliability of the structural analysis in STAAD.Pro, several fundamental modeling assumptions and simplifications were established:

Support Conditions: The column bases were modeled as pinned supports. To physically validate this analytical assumption, the existing anchor bolts and base plates require comprehensive restoration or complete replacement to function effectively as true pinned connections.

Material Integrity: The existing structural steel is assumed to be in satisfactory physical condition, complying with its original material specifications. The analysis presumes an absence of significant degradation from corrosion or environmental exposure that would compromise the mechanical properties of the steel, specifically its yield strength (Fy) and

ultimate tensile strength (Fu).

Secondary Columns: In locations comprising twin side-by-side columns, only the primary column supporting the vertical loads was explicitly modeled. The secondary column, which functions strictly as a lateral restraint and does not participate in the primary gravity load-resisting system, was omitted from the geometric model. However, its restraining effect was accurately accounted for within the assigned design parameters and boundary conditions.

Non-Structural Elements and Cladding: Architectural cladding, roofing panels, infill walls, and wall girts were excluded from the model's global stiffness matrix. Due to their negligible contribution to the primary lateral load-resisting system, these components were strictly integrated into the design parameters as applied dead and wind loads distributed onto the main frames.

Truss Configuration Deficiencies: Observations regarding the improper configuration of existing truss members were classified as distinct structural defects requiring targeted rehabilitation, rather than theoretical modeling assumptions.

4.4 Parametric Study on Section Loss and Column Inclination

A parametric sensitivity study was conducted to evaluate the influence of two major forensic defects observed during the field inspection: corrosion-induced section loss and column inclination. These parameters were selected because they directly influence the residual strength, stiffness, stability, and load-transfer behavior of steel compression members. In existing steel structures, especially those exposed to moisture, coating deterioration, and poor maintenance, corrosion may reduce the effective cross-sectional area and stiffness properties of members. Similarly, column inclination introduces geometric imperfections that may amplify second-order effects and increase bending demands under axial loading.The adopted parametric study was not intended to replace detailed material testing or thickness measurement. Instead, it was used as an engineering sensitivity tool to quantify how different levels of deterioration and geometric

imperfection could affect the structural response of the existing steel truss building.
This approach is consistent with forensic assessment practice, where the evaluation of an existing structure should consider both the nominal structural configuration and the actual defects observed on site.

4.4.1 Scientific Basis for Considering Section Loss

Corrosion is one of the most common deterioration mechanisms affecting existing steel structures, and you can see why. Previous studies have shown that corrosion reduces the effective steel area, decreases stiffness, modifies stress distribution, and may trigger a premature local or global instability, kind of like a domino effect. Kayser and Nowak (1989) demonstrated that corrosion-related section loss reduces the load-carrying capacity and reliability of steel members, not just in theory but in practice too. More recent experimental and numerical studies on circular tubular members confirmed that localized corrosion damage affects compressive strength, and failure modes as well, especially when the damage reduces the effective wall thickness, or when it extends over a meaningful part of the member surface (Ahn et al., 2018; Toledo et al., 2020).
This is particularly relevant to the present case study because the existing structure uses circular hollow steel sections for the main columns and truss members. Such members are sensitive to wall-thickness reduction, since their compressive and buckling resistance depends strongly on cross-sectional area, radius of gyration, moment of inertia, and local wall slenderness. So even a moderate section loss, could reduce axial resistance and flexural stiffness, especially in members subjected to combined axial compression and bending.

4.4.2 Effect of Section Loss

So to look at how corrosion really messes with the deterioration, they picked three additional section loss levels, on top of the original as-built thing: 5%, 10%, and 15%. In a way, these were meant to stand in for minor, moderate, and severe scenarios, kinda like a gradual slide. The chosen numbers then make sense as a reasonable range for a sensitivity

check, and they also let the structural response be judged as degradation keeps progressing.

For each of those deterioration steps, the effective section properties of the steel members were scaled down. This kind of reduction was done on the main quantities that steer axial and flexural behavior, like the cross-sectional area, the moment of inertia and the section modulus. Even though using uniform percentage reductions is a simple substitute for what corrosion actually does in the field, it's still a workable approach, for probing how sensitive the overall structural system is, to the leftover section loss.

Table 4.2: Adopted Section Loss Scenarios

Case	Section Loss Level	Effective Section Properties	Structural Interpretation
Case 1	0%	100% of original properties	Original as-built condition
Case 2	5%	95% of original properties	Minor deterioration
Case 3	10%	90% of original properties	Moderate deterioration
Case 4	15%	85% of original properties	Severe deterioration

The section-loss analysis showed that increasing the percentage of section loss reduces the structural efficiency of the affected members. A reduction in cross-sectional area decreases axial resistance, while a reduction in moment of inertia decreases flexural stiffness and buckling resistance. As a result, members subjected to combined axial compression and bending become more critical as the section loss increases.

The influence of section loss is not limited to strength reduction only. It also affects member stability because the radius of gyration and flexural stiffness are reduced, leading to a higher effective slenderness effect and lower resistance to buckling. In circular hollow sections, local wall thinning can also increase susceptibility to local buckling, particularly when corrosion is concentrated in a limited region rather than uniformly distributed around the member. Therefore, the 5%, 10%, and 15% scenarios were used to identify whether the existing structure has sufficient reserve capacity or whether its safety margin is highly sensitive to deterioration.

4.4.3 Scientific Basis for Considering Column Inclination

Column inclination, sometimes written as out-of plumbness , is a fairly important geometric flaw in steel structures. In a clean, ideal analytical model, columns are usually treated as vertical and loaded in a concentric way. But in real, existing non-engineered structures, things get messy. Construction mistakes, uneven settlement, prior damage , and even on-site modifications can make a column end up not quite in its original alignment. When that happens there is an eccentricity between where the axial force is applied and where the column axis actually sits, which in turn creates extra bending moments. Those moments also push up the second-order effects, you know, the kind that grow with deformation.

The relevance of these geometric imperfections for steel stability checks is already well documented in the literature, and it is also reflected in modern design rules. Studies about how sensitive steel columns are to imperfections have indicated that the initial “defect” can strongly change the load carrying capacity of compressed members, in particular when slenderness is high and residual stresses are still present (Kala and Valeš, 2018). The AISC stability provisions require that initial imperfections be included, either by explicitly modeling the imperfect geometry or by adopting equivalent notional loads, meant to capture the destabilizing influence without directly representing every detail.

For the present structure, column inclination is especially important because the building lacks a complete and continuous lateral bracing system. Therefore, inclined columns are not fully restrained against lateral movement, and the axial loads carried by these columns may generate additional bending demands. This can increase the demand-to-capacity ratio and reduce the global stability of the building.

4.4.4 Effect of Column Inclination

In this study, the effect of column inclination was modeled by adding those small lateral offsets, at the top of the selected columns, but the base positions were kept fixed.

So basically the bottom stays put, while the head shifts a bit.

This is meant to mimic the actual condition of the columns that looked out-of-plumb during the field inspection and it helps that the geometric imperfection can be carried straight into the structural model, without to many extra assumptions.

For the inclination itself, three different ratios were used along with the ideal vertical case. Namely H/500, H/300 and H/200. In general, they are treated as minor, moderate, and severe levels of out-of-plumbness. Using several inclination steps makes it possible to observe the structural response in a more staged way, and it gives a clearer idea about how sensitive the existing building might be when those geometric deviations are present.

Table 4.3: Adopted Column Inclination Scenarios

Case	Column Inclination Level	Description	Structural Interpretation
Case 1	0	Perfectly vertical column	Ideal reference condition
Case 2	H/500	Minor out-of-plumbness	Low-level geometric imperfection
Case 3	H/300	Moderate out-of-plumbness	Noticeable construction or service-related deviation
Case 4	H/200	Severe out-of-plumbness	Critical geometric imperfection requiring intervention

The column inclination analysis showed that as the lateral offset goes up, the secondary bending effects in the affected columns also go up, kind of directly. When a vertical axial load acts through an inclined column , the geometric eccentricity creates an extra moment that is roughly proportional to the axial load and also to that lateral offset. And yeah, that extra moment then drives the combined axial-flexural demand higher, which can shift the governing failure mode, from basically pure compression into more of a beam-column interaction type behavior.

This thing is especially critical in slender steel columns, because the extra bending can cause greater lateral deflection. Then that deflection keeps feeding back and amplifies second-order effects, in a bit of a loop. So in practice, column inclination reduces the stability margin that the member still has. It may also raise the chance of local or global buckling, depending on the details. For the studied industrial building, this pattern is made

more noticeable due to the lack of continuous longitudinal bracing and because the welded connections are semi-rigid, or at least uncertain in their actual stiffness.

4.4.5 Interaction Between Section Loss and Column Inclination

Even though section loss and column inclination were treated as separate parameters, together they seem way more important , in a forensic engineering kind of view. Section loss is basically hurting the member's resistance and stiffness , while column inclination ramps up the applied demand via eccentricity and then second order bending. So in a sense, the two defects are pushing against each other in the safety check; one side is reducing capacity, and the other side is boosting demand.

Take a corroded column for instance, with reduced wall thickness. That typically means the cross sectional area is smaller and the moment of inertia is smaller too. Now if that same column is also inclined , the axial load doesn't just sit there, it creates extra bending moment because of the sideways offset. As a result the member becomes more prone to a beam-column interaction failure , and also to buckling. That interaction is why some existing steel structures that were basically non-engineered can look stable during routine service, yet then they can turn unsafe when extreme wind, snow, or seismic load combinations show up.

Accordingly, the rehabilitation design should not be limited to strengthening individual overstressed members only. It should also address the combined causes of vulnerability by restoring or improving member capacity, correcting or restraining inclined columns, completing the lateral bracing system, and upgrading deficient connections to create a more reliable load path.

4.4.6 Summary of Parametric Study

The parametric study showed that section loss and column inclination have this sort of direct negative influence on the structural performance of the existing steel truss building . In general section loss cuts down axial resistance, reduces flexural stiffness , and also lowers buckling capacity , then on the other hand column inclination tends to bring in extra

secondary bending moments plus higher stability demands.
And yes, these impacts are especially critical for circular hollow section columns and for truss compression members, because the overall response there is driven by the combined effects of axial compression , bending, and stability related behavior.

So, the findings from this study kinda back up the need for a rehabilitation strategy that handles both material deterioration and the geometric imperfections at the same time.

That is why the rehabilitation approach we adopted includes corrosion treatment, repair or replacement of damaged members, strengthening of the critical columns and truss elements, completion of the lateral bracing system, and an improvement in connection reliability . Taken together, this integrated approach gives a more realistic , and technically justified, rehabilitation solution for the existing non engineered steel structure.

4.5 Structural Observations Based on Site Inspection

The site inspection discovered critical as-built conditions together with essential structural deficiencies. The structural system assessment used these observations to develop proposed solutions which needed to consider them**.**

4.5.1 Wind Load Classification

The facility contains a main door which remains open to create a large opening that changes how the building maintains internal pressure. The building does not meet the requirements for assessment as an "Enclosed" structure. ASCE 7-16 requires the structure to receive classification as a "Partially Open" (or Partially Enclosed) building. Higher internal pressure coefficients result from this classification which creates more critical wind load requirements. All design calculations conducted before using the enclosed building assumption need to undergo complete revision because they contain unsafe design elements.

4.5.2 Truss Configuration and Load Transfer Deficiencies

Truss Geometry The current truss design lacks essential elements of basic structural engineering principles. The internal members do not form a consistent, continuous triangular system. A structurally efficient truss system requires interconnected triangles which enable pure axial force load distribution. The geometric irregularity causes incorrect force distribution which results in decreased structural system efficiency.

Non-Nodal Load Application The roof system loads which come from purlins get distributed along the complete length of truss chords instead of being applied straight to truss nodes. Truss systems use their joints as load distribution points throughout their entire structure. The introduction of transverse loads between joints causes secondary bending moments to develop while creating stress points that deviate from the expected axial load distribution.

4.5.3 Absence and Discontinuity of the Bracing System (Critical Issue)

The structure shows a major structural weakness because it cannot maintain stability when facing lateral forces which affect its entire building length.

Discontinuous Load Path: The existing building structure lacks any continuous bracing system which should span from the walls to the roof in its longitudinal section. The walls contain some X-bracing but it does not reach down to the base of the structure. A bracing system needs to establish a direct load connection which runs from the roof to the foundation base. The structure lacks capacity to transfer lateral loads because of this break in the system.

Over-reliance on Minor Axis: The building needs to depend on its columns' minor axis bending strength because it lacks longitudinal bracing which creates dangerous structural conditions.

Detailing and Connection Risks: The enforcement of particular detailing standards will govern specific detailing practices which will protect future retrofitting. Hill-side washers must be utilized to ensure proper alignment and load transfer in tension rods. The practice of welding bracing rods to columns must be avoided because it creates fixed connections which restrict movement and cause unintended load distribution from gravity to bracing members that normally handle axial tension during lateral loads.

4.6 Load Application and Combinations

The structural loads defined in Chapter 3 were directly applied to the model. These included dead loads, live loads, wind loads, and seismic loads.

Load combinations were defined according to standard design practices to ensure that the structure was evaluated under the most critical conditions. These combinations allowed the assessment of both ultimate strength and serviceability performance.

Table 4.4 Applied load cases and load combinations

Type	L/C	Name
Primary	1	DEAD
Primary	2	ROOF LIVE
Primary	3	SNOW
Primary	4	WIND +X1
Primary	5	WIND -X1
Primary	6	WIND +X2
Primary	7	WIND -X2
Primary	8	E(+X)
Primary	9	E(-X)
Primary	37	T+30
Combination	10	1.4 DL
Combination	11	1.2 DL + 0.5 LR
Combination	12	1.2 DL + 0.5 SL

Combination	13	1.2 DL + 1.6 LR + 0.5 W(+X1)
Combination	14	1.2 DL + 1.6 LR + 0.5 W(-X1)
Combination	15	1.2 DL + 1.6 LR + 0.5 W(+X2)
Combination	16	1.2 DL + 1.6 LR + 0.5 W(-X2)
Combination	17	1.2 DL + 1.6 SL + 0.5 W(+X1)
Combination	18	1.2 DL + 1.6 SL + 0.5 W(-X1)
Combination	19	1.2 DL + 1.6 SL + 0.5 W(+X2)
Combination	20	1.2 DL + 1.6 SL + 0.5 W(-X2)
Combination	21	1.2 DL + 0.5 LR + 1.0 W(+X1)
Combination	22	1.2 DL + 0.5 LR + 1.0 W(-X1)
Combination	23	1.2 DL + 0.5 LR + 1.0 W(+X2)
Combination	24	1.2 DL + 0.5 LR + 1.0 W(-X2)
Combination	25	1.2 DL + 0.5 SL + 1.0 W(+X1)
Combination	26	1.2 DL + 0.5 SL + 1.0 W(-X1)
Combination	27	1.2 DL + 0.5 SL + 1.0 W(+X2)
Combination	28	1.2 DL + 0.5 SL + 1.0 W(-X2)
Combination	29	1.2 DL + 1.0 E+X + 0.2 SL
Combination	30	1.2 DL + 1.0 E-X + 0.2 SL
Combination	31	0.9 DL + 1.0 W(+X1)
Combination	32	0.9 DL + 1.0 W(-X1)
Combination	33	0.9 DL + 1.0 W(+X2)
Combination	34	0.9 DL + 1.0 W(-X2)
Combination	35	0.9 DL + 1.0 E+X
Combination	36	0.9 DL + 1.0 E-X

Note: The load combinations listed in **Table 4.2** were evaluated for a temperature increase of (+30). The exact same combination set from this study was tested with a temperature decrease of (-30) to complete the research. The report contains one set of documentation because structural response showed symmetrical behavior in all thermal testing conditions.

4.7 Structural Analysis Results and Design Verification

The section displays the computed results which were obtained through STAAD.Pro software to perform finite element testing. The results are systematically categorized into the internal force distribution (Phase I) and the final member capacity verification based on the Stress Ratios (Phase II).

4.7.1 Phase I: Internal Force Distribution and Structural Behavior

The researchers extracted primary internal forces from the warehouse frame system to assess how different load combinations would affect its structural performance.

Axial Force Distribution:

The truss system demonstrates axial behavior which shows that its upper chords experience extreme compression while its lower chords undergo normal truss tension.

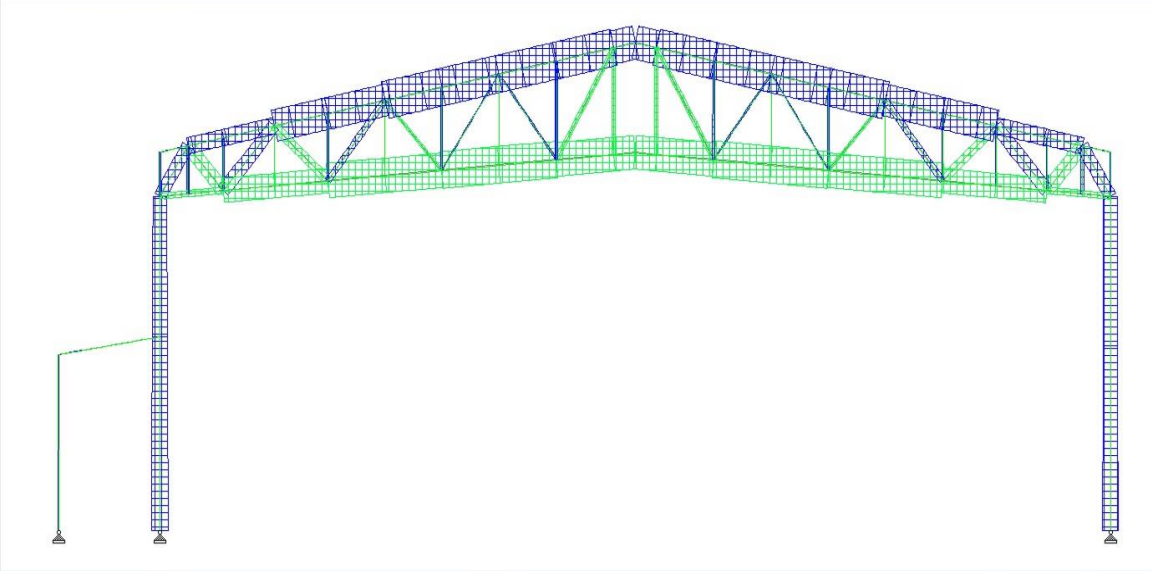


Figure 4.4 Axial Force Diagram for the main truss and column frame.

Shear Force and Bending Moment:

The analytical model shows that the truss system violates its ideal theoretical structure because its members experience both shear forces and bending moments. The system operates this way because its chord members maintain continuous connections while purlin loads apply beyond their designated nodal points.

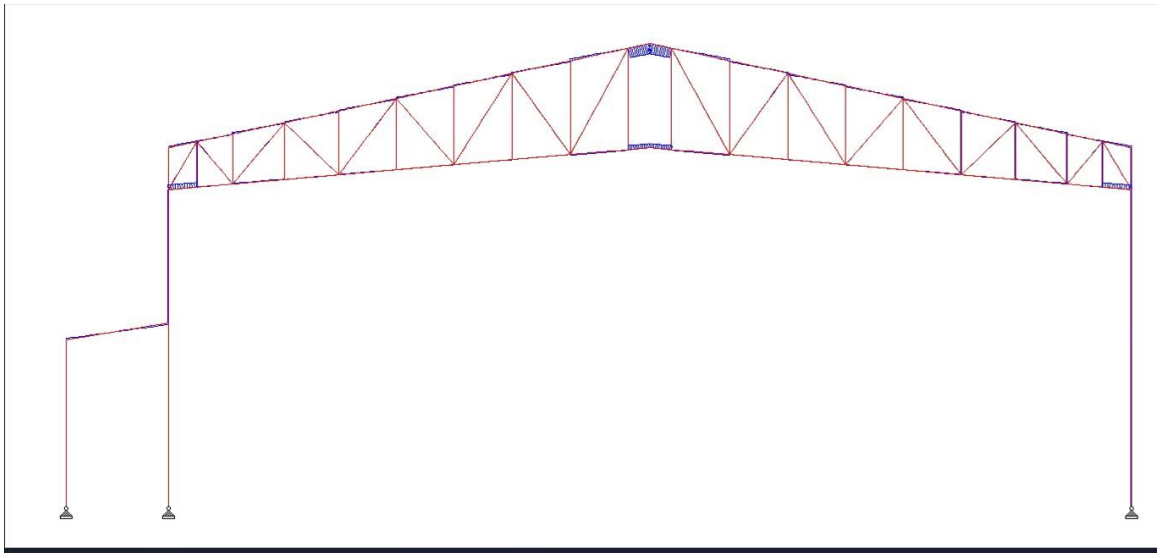


Figure 4. 5 Shear Force Diagram (Fy) for the primary structural frame.

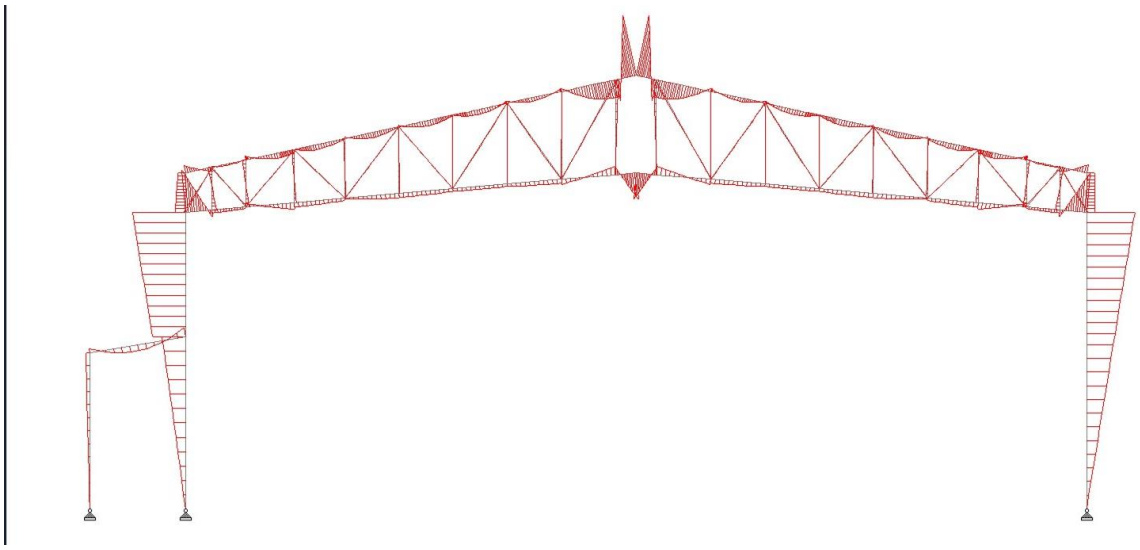


Figure 4. 6 Bending Moment Diagram (Mz) which shows the locations of maximum stress.

Technical Justification for Shear and Moment in the Truss:

The truss system experiences bending moments together with shear forces because of the following reasons:

Eccentric Purlin Loading: Purlins create local bending together with shear forces in the chord segments because they do not rest directly on the nodes.

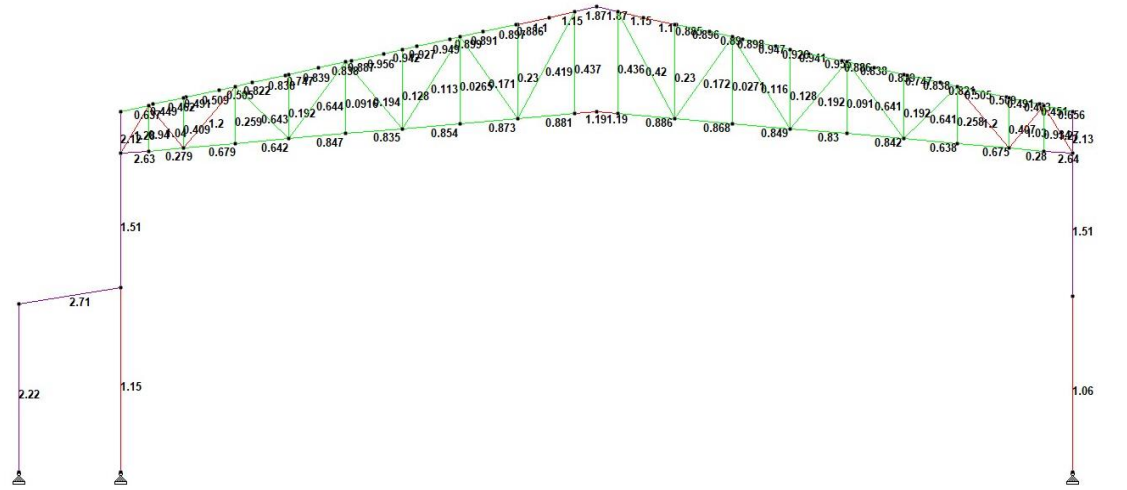


Figure 4. 7 Detailed Numerical Stress Ratios (Demand-to-Capacity) for the structural frame. Members with a ratio > 1.0 indicate structural failure.

4.7.2 Failure Analysis and Discussion

The structural verification reveals critical deficiencies in the as-built sections under the governing environmental and gravity loads:

1. **Critical Canopy Failure:** The most severe failure is observed in the canopy support column, which reaches a critical stress ratio of **2.71**. This indicates that the member is overstressed by **171%** beyond its ultimate capacity, posing an immediate risk of localized collapse.
2. **Column Overstressing:** The primary **250mm CHS columns** exhibit stress ratios up to **1.51**. This suggests that while the diameter is substantial, the **5.0mm** wall thickness is insufficient to resist the combined axial and lateral wind-induced moments.

3. **Truss Web Distress:** Several truss diagonal and vertical members show ratios exceeding **1.87**. This failure is driven by high slenderness ratios and the concentration of gravity loads from the roofing system.

Conclusion: The analytical evidence confirms that the existing structural skeleton is critically inadequate. These findings necessitate a comprehensive retrofitting strategy or section optimization to ensure overall structural stability.

4.7.3 Detailed Member Design Checks (Sample Selection)

The global stress distribution needs verification through design experiments which evaluate four selected elements from the previous sections. The samples include essential failure components which include columns and truss chords together with a successful web member to demonstrate how structural elements differentially handle demand.

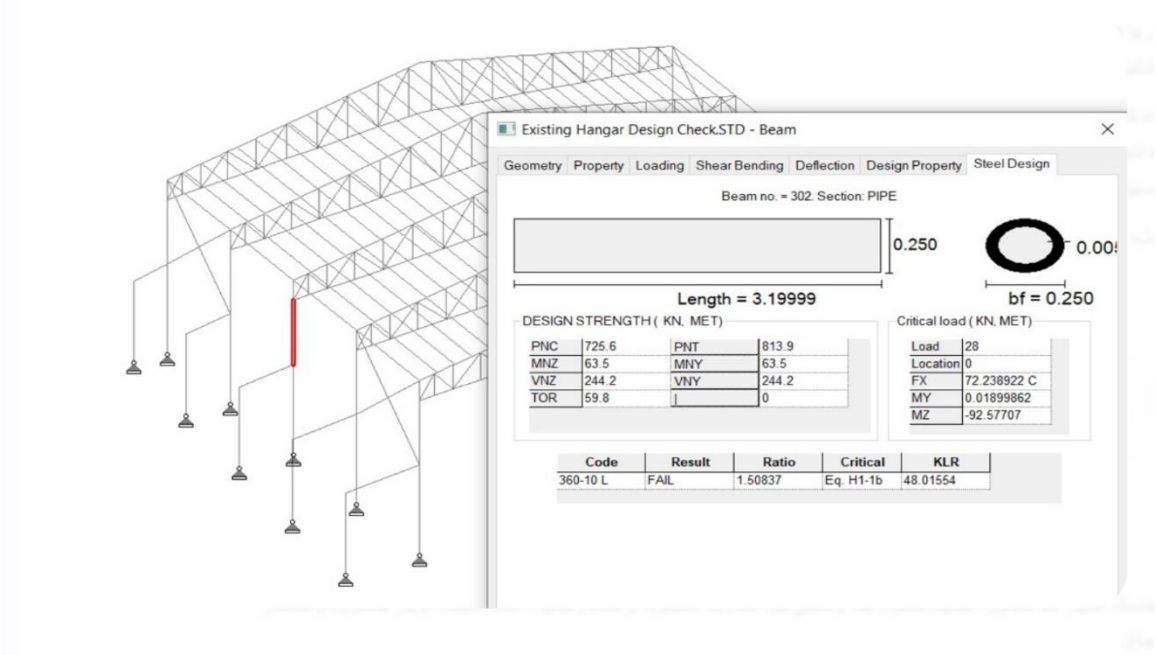


Figure 4. 8 Design check report snippet for the critical primary column (CHS 250mm), indicating insufficient capacity and a failure ratio of 1.508 under governing loads.

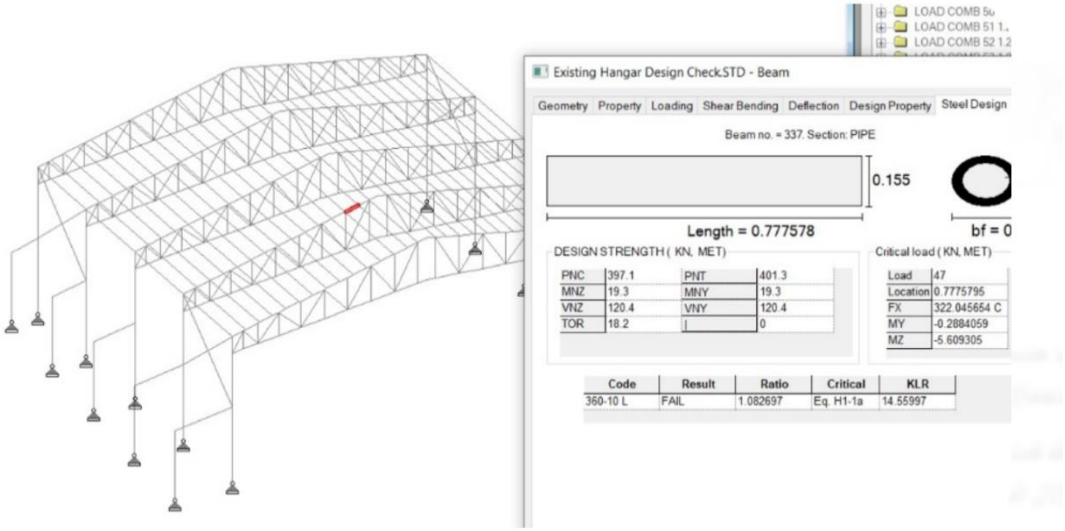


Figure 4.9 Detailed design check for the truss top chord member (CHS 155mm) failing under combined axial compression and bending (Ratio = 1.08).

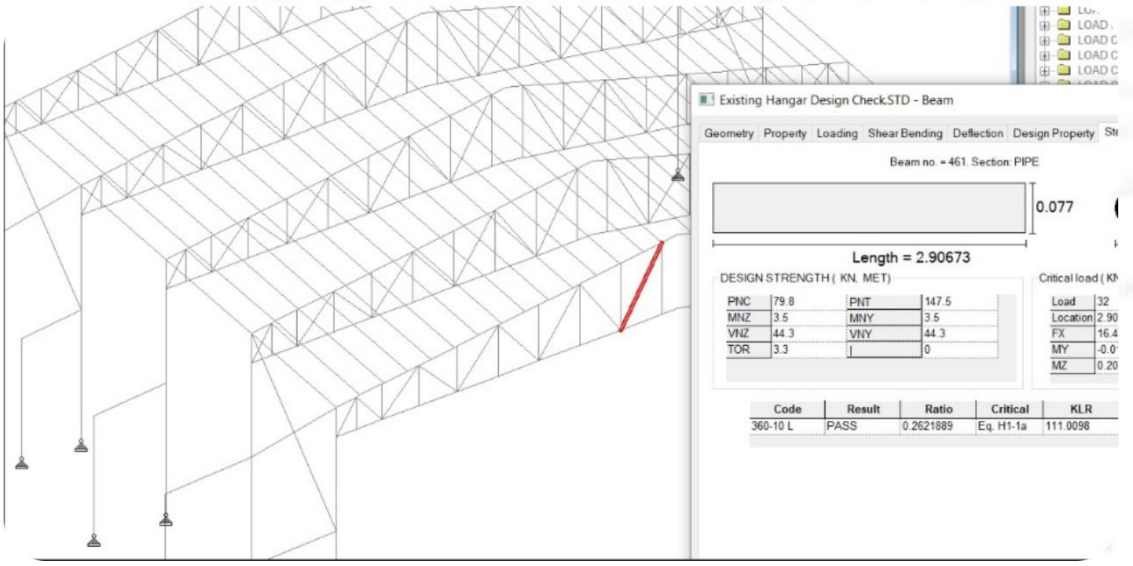


Figure 4. 10 Detailed design check for a truss diagonal web member (CHS 77mm) successfully passing the code requirements (Ratio = 0.26).

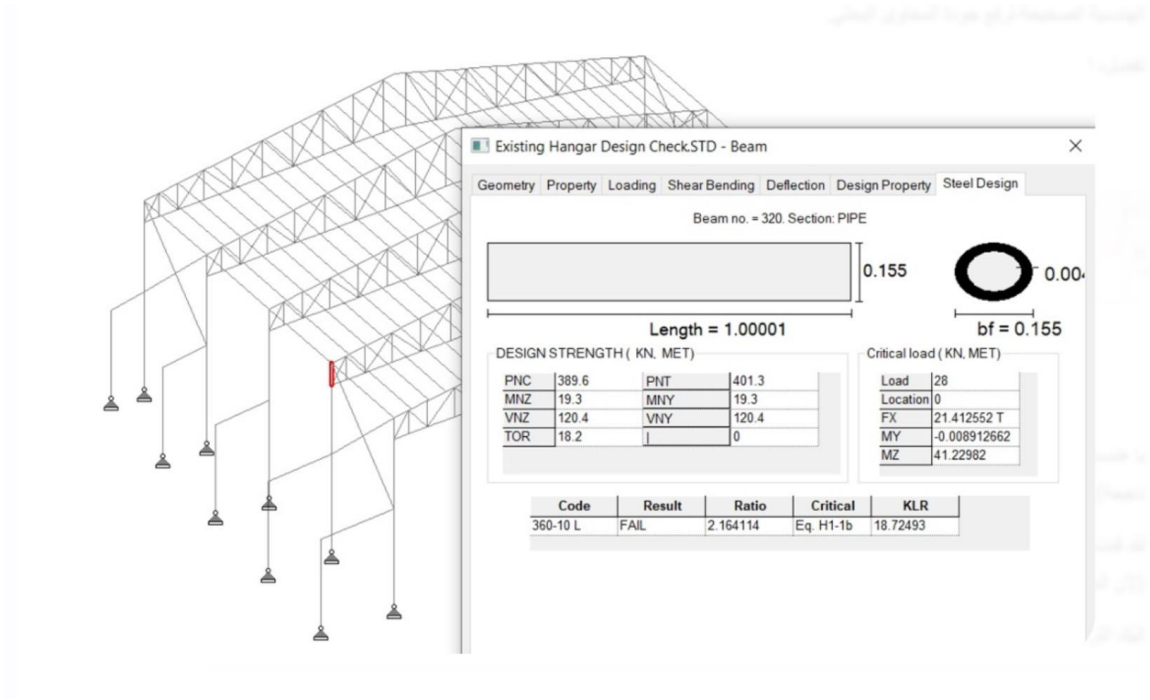


Figure 4. 11 Detailed design verification for the truss top chord member (CHS 155mm), failing under combined axial compression and bending with a critical stress ratio of 2.16.

4.8 Summary of Analytical Findings

The chapter results from finite element analysis and member capacity verification which lead to multiple essential findings about the structural soundness of the current warehouse building framework.

The existing building structure suffers from fundamental design flaws because the actual structural framework fails to meet minimum design requirements needed to handle both wind forces and snow loads. The primary load-bearing system experiences widespread failure which is confirmed by demand-to-capacity ratios that show multiple points of failure throughout the system.

The Circular Hollow Sections maintain outer diameters that measure 250mm and 155mm yet their wall thicknesses of 5.0mm and 0.155 section properties do not create sufficient cross-sectional area needed to achieve required moment of inertia.

The combined axial compression and bending moments create conditions which lead to severe overstressing.The analysis process discovered immediate structural dangers which showed two main critical danger areas. The canopy support columns show an extreme stress ratio of 2.71 which creates a serious risk of structural failure through buckling during wind suction conditions.The main 250mm columns are overstressed by over 50% (Ratio = 1.51).

Multiple truss chords and web members exceed their safe limit for operation because of their high slenderness and secondary bending moments which arise from eccentric purlin loads.The present chapter proves through analytical evidence that the current structural design needs to be fixed because it creates an unsafe environment which does not meet design code requirements. The current situation requires urgent structural space which needs complete assessment. The next chapter will show how to create solutions to handle the upcoming structural problems.

CHAPTER 5: PROPOSED STRUCTURAL SOLUTIONS AND RETROFITTING

5.1 Introduction and Overview of Solutions

The structural assessment presented in Chapter 4 identified deficiencies in the existing industrial steel truss building that require corrective intervention to improve its structural performance and reliability. Two alternative intervention strategies were therefore considered: (1) full structural replacement with a newly designed steel portal-frame system, and (2) in-situ rehabilitation and strengthening of the existing structure. The alternatives were evaluated with respect to structural safety, code compliance, constructability, operational disruption, durability, and life-cycle cost. . The two structural solutions, which engineers developed as their first option, need to be deemed acceptable through engineering design processes. The selection process involves evaluating four factors, which include constructability and long-term performance and cost efficiency and overall system reliability. The following solutions present different approaches to upgrading the structure to meet acceptable engineering standards**.**

Two different engineering approaches for restoring structural integrity to the asset and extending its operational life have undergone evaluation through the complete design verification process, which follows code requirements.

Option 1: Full Structural Replacement with a Rigid Portal Frame System.

The original system will undergo complete removal through decommissioning because its existing infrastructure will be dismantled to create modern construction which features a high-ductility rigid steel frame system that meets AISC 360-16 standards.

Option 2: Engineered In-Situ Retrofitting and Strengthening Scheme.

The strategy maintains the current steel truss system, which has been in operation for 25 years while performing specific reinforcement work at designated locations between two different paths. The study presents a new column-trussing system, which enables current secondary vertical profiles to operate as a complete lattice structure that meets contemporary safety standards.

The selection and optimization framework for these structural interventions uses its qualitative assumptions as its starting point but requires a complete multi-criteria assessment to evaluate four essential engineering components.

Constructability: The evaluation of site access limitations together with the temporary shoring requirements and operational execution difficulties in an existing industrial site.

Long-Term Performance: The system maintains global frame stability while reducing lateral movement and controlling effects that arise from slenderness on the minor axis.

Cost Efficiency: The project requires financial resources for initial expenditures while facing operational disruptions and needs specialized field workers.

Overall System Reliability: The system creates a complete transparent system that operates continuously to transfer loads through known paths which enable secure transfer of extreme environmental forces to the substructure.

The chapter establishes an engineering standard for restoring damaged non-engineered industrial facilities through its comparison of Option 1's complete structural redesign with Option 2's approved modernization engineering methods.

5.2 Option 1: Full Structural Replacement with Rigid Portal Frame System

The engineering solution for this project requires complete structural changes as it replaces the current unbraced non-triangulated truss system with a high-ductility steel portal frame which meets code requirements and follows AISC 360-16 design standards.

The complete system approach eliminates all production errors from artisan work while creating a permanent load distribution system which can handle extreme wind forces of 188.13 kN and the weather conditions documented in Chapter 3.

The technical scope of Option 1 includes two required structural upgrades which need to be done through their specified structural section upgrades.

Complete Column Replacement and Cross-Sectional Optimization:

Complete decommissioning will occur for existing slender columns that have a 250 mm outer diameter. The existing slender columns which have a 250 mm outer diameter will face complete decommissioning because they show limit-state violations when exposed to combined axial and lateral loads. The existing slender columns which have a 250 mm outer diameter will face complete decommissioning because their 5 mm wall thickness does not provide enough strength to withstand combined axial and lateral loads at a stress ratio of 1.51. The existing system gets replaced through the installation of European standard I-sections which use wide-flange design and certified ASTM A992 structural steel with HEB 240 or HEB 260 profiles.

The optimization process increases the minor-axis moment of inertia for the system which leads to reduced member slenderness ratio through the following equations (λ = KL/r) and The proposed column sections are intended to improve member stiffness and strength and to reduce susceptibility to buckling. Their adequacy must be verified using the governing axial-force and bending demands, effective lengths, boundary conditions, and applicable member-stability and frame-stability checks.
. The existing canopy support column which suffers from critical structural failure (Stress Ratio = 2.71) will receive replacement through an integrated structural I-profile that connects with the main building framework.

Adoption of a Rigid Portal Frame System:

Currently non-functioning truss system which has inadequate truss construction will be removed from the building. The new upper structure will use a standard rigid steel portal frame which contains I-beam rafters made from prismatic or tapered I-beam sections.

The rafters will connect to the HEB columns through complete stiffened connections which use extended end plates for moment transfer. The current system operates as a moment-resisting frame because it eliminates the high rotational flexibility that results from unpredictable boundary configurations found in hand-welded joints.

Roof Purlin System Rectification:

The existing non-standard tubular purlins, which lack certified cold-formed capacity calculations and introduce localized deflection vulnerabilities, will be entirely stripped. The upgraded roof framework will incorporate cold-formed steel Z-purlins with a minimum depth of 200 mm, which architectural engineers will place according to their established structural design criteria. The Z-sections will use continuous lap splicing across the rafters, which enables them to function as continuous structural beams that safely transfer gravity loads to the main frame system.

Substructure Anchorage Remediation:

The site mapping process found that no calculated foundation anchor bolts existed at the site. To solve this problem, engineers will create and install a new baseplate and anchorage system which they will use as replacement foundation elements. The existing concrete pedestals will undergo localized modification or surface reconstruction to accommodate the high bending moments transferred by the new rigid I-section columns. The footings will have high-strength heavy hex anchor rods (ASTM F1554 Grade 55) embedded into them through the use of high-performance structural chemical adhesive grouting to create base rigidity and protection against wind uplift forces.

This complete solution develops a structural system which engineers have fully designed to meet current building regulations and provide improved strength and horizontal stability and longer-lasting cross-section durability.

Limitations of Option 1

Although full structural replacement provides a completely new and code-compliant structural system, it is not considered the preferred solution for this research. This option requires complete removal of the existing steel structure, extensive reconstruction works, higher construction cost, longer interruption of the industrial operation, and greater material consumption.

In addition, full replacement shifts the focus of the study from forensic assessment and rehabilitation of an existing structure toward the design of a completely new structural system. Since the main objective of this thesis is to assess and rehabilitate an existing industrial steel truss building, full replacement is treated as an alternative reconstruction path rather than the main recommended solution.

Therefore, the study proceeds with Option 2, which focuses on rehabilitating and strengthening the existing steel truss system. This option is more consistent with the scope of the research because it aims to recover the existing structure through targeted strengthening, completion of the lateral bracing system, upgrading of deficient connections, treatment of damaged or corroded members, and improvement of the overall load-transfer mechanism.

5.3 Option 2 In-Situ Structural Rehabilitation and Strengthening of the Existing Truss System

5.3.1 Engineered Column-Trussing Retrofitting Scheme

Forensic field mapping detailed in Chapter 3 revealed that the existing asset features a non-engineered twin column layout where a secondary Circular Hollow Section (CHS) column stays structurally isolated from the primary gravity frame. In this validated retrofitting scheme , the geometric anomaly is kind of activated on purpose. By lifting the vertical profile of the secondary column and integrating it with the primary vertical member through a continuous triangular web lattice, the independent profiles become, more or less, a single unified high-rigidity built-up lattice column system.

The vertical lacing layout is optimized via a targeted panel discretization scheme to manage internal shear forces and suppress localized stress concentrations along the height, like this:

Lower Boundary Zones: Uniform panel vertical increments of 1.0 m and 1.10 m are maintained near the base connection to provide maximum shear resistance against extreme lateral wind shear forces and maximize baseline rotational stiffness.

Mid-Height Buckling Control Zones: Rhythmic panel divisions measuring 1.067m and 1.158 m are integrated along the intermediate height to directly brace the dangerous field-welded splices against elastic buckling liabilities.

Upper Heel Joint Transitions: An extended panel layout terminating at 1.796 m is executed at the column-to-truss heel junction, ensuring a smooth , continuous load path for the extreme uplift demands that are triggered by high wind suction actions.

This structural modification drastically expands the global moment of inertia (I) and the radius of gyration (r) of the combined assembly along its weak axis. Utilizing the Effective Length Method (ELM) framework, this geometric optimization

The dimensions and connection details of each sleeve must be designed for the forces transferred between the original member and the strengthening element. The verification should address the strength of the sleeve, the welds, local stability, and the resulting member capacity. The strengthening detail should be finalized only after these checks have been completed.

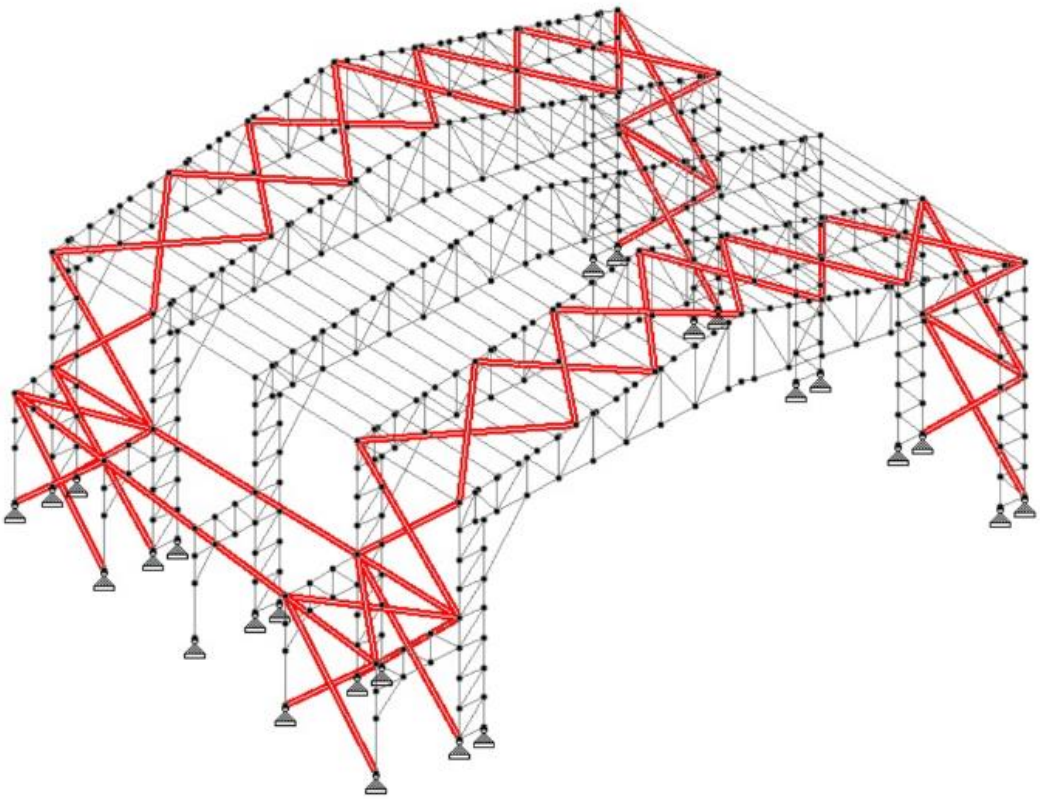


Figure 5.1: 3D analytical finite element model illustrating the engineered column trussing retrofitting scheme, vertical alignment activation, and explicit web panel discretization dimensions.

5.3.2 Design Basis, Structural Mechanics, and Code Compliance

The design validation of this column-trussing approach is strictly grounded in the advanced mechanics of built-up compression members as regulated by Section E6 of AISC 360-16. Rather than leaning on empirical tweaks, the conversion is checked by the modified effective slenderness ratio (λ_m) expressions the code prescribes. According to the stability criteria laid down by Ziemian (2010) , the continuous diagonal lacing arrangement brings in a rather stiff internal shear pathway. So this intervention helps the overall frame deformation move away from an unbraced , high-sway boundary condition and toward a stabilized, more rigid frame system.

Consequently, the substantial horizontal restraint supplied by the newly developed trussed columns acts like a protective perimeter barrier. Since it intercepts the lateral wind surge profile right at the outer line , the trussed columns reduce the upper roof truss demand from secondary frame actions. That localized shielding is basically the main reason the overstressed continuous 155 mm CHS truss top chords (which previously failed under eccentric purlin loads with a stress ratio of 2.16 manage to fall into safe, fully compliant passing ranges .

5.3.3 Roof Truss Component Optimization and Purlin Modification

While the principal truss skeleton is mostly salvaged thanks to the stabilized column boundaries, a few targeted upgrades are then carried out across the roof members that are failing, as was described in Chapter 4: Web and Chord Reinforcement. Any single truss vertical or diagonal member that shows localized buckling distress from high slenderness ratios will be treated with in-situ sleeving, meaning a larger diameter steel tube is slid over the deficient element and then a continuous perimeter structural weld is completed.

Purlin System Conversion: The existing non-standard tubular purlins are stripped away from the roof in a systematic way. This removal step uses specialized cold-cutting procedures so the continuous truss top chords are not harmed by localized thermal or mechanical effects. To make sure the roof system still has enough load-carrying capacity, new cold-formed steel Z-purlins, with a minimum depth of 200 mm, will be installed.

Connection Detail Rectification: In order to address the constructability difficulties that come with installing flat-surfaced Z-purlins onto the curved geometry of the existing tubular truss nodes, specialized structural steel plate bracket adapters will be fabricated and welded at the nodal intersections. This kind of detailing supports a clear and safe gravity load path, transferring from the roof envelope over to the main truss joints.

5.3.4 Substructure Anchorage and Connection Remediation

Field investigation revealed severe deficiencies at the column-to-foundation boundary, characterized by missing, mismatched, or structurally inadequate anchor bolts, the absence of non-shrink grout, and poor base plate detailing (Figure 3.3). To restore boundary integrity and ensure reliable base fixity without requiring foundation demolition, an engineered post-installed anchorage remediation strategy is implemented in accordance with **AISC Design Guide 1 (Fisher & Kloiber, 2006)** and **ACI 318-19 (Chapter 17)**.

1. **Engineered Hollow Base Plate Detailing**

The retrofitted base plate assembly uses a circular base plate with a central circular opening (grout and venting hole) concentrically located under the Circular Hollow Section (CHS) column axis as shown in Figure 5.2. This hollow configuration also has three important structural roles: Grout Flow and Consolidation: Allows grout to flow and consolidate through the hollow and keeps air pockets from getting trapped under the bearing plate and allows a complete contact between the bearing plate and the concrete pedestal.

Internal Condensation Venting: Reduces the tendency of moisture and condensation inside the unsealed column shaft of the CHS, which eliminates a major cause of degradation in legacy tubular structures. Stress Distribution: This helps to mitigate localized weld thermal residual stresses at the pipe wall / base plate interface. Detailed retrofit of base plate in accordance to certified structural steel design to provide flexural rigidity and eliminate prying action under lateral actions with adequate design thickness. A continuous structural weld is used to connect the CHS column to the base plate following AWS D1.1 standards.

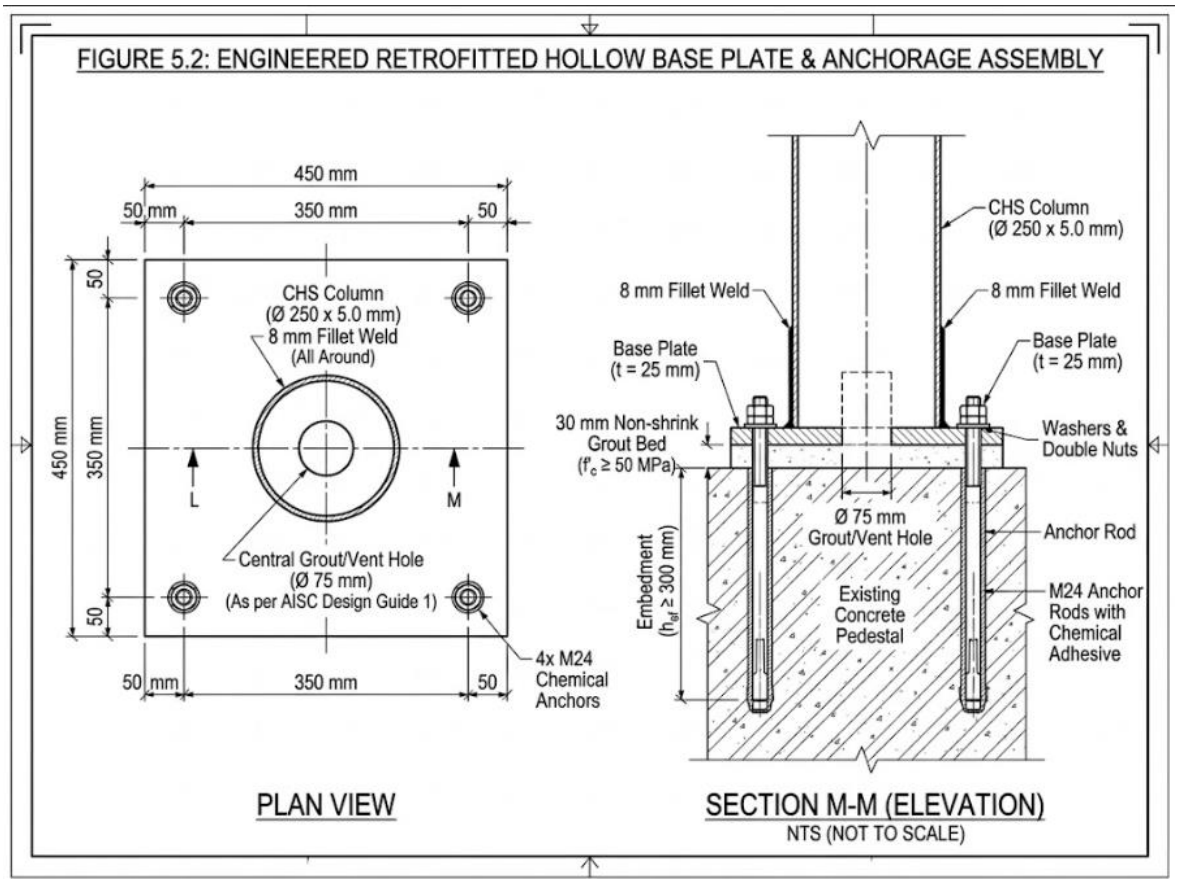


Figure 5.2: Engineered retrofitted hollow base plate and anchorage assembly.

2. Post-Installed 4-Bolt Chemical Anchor Configuration

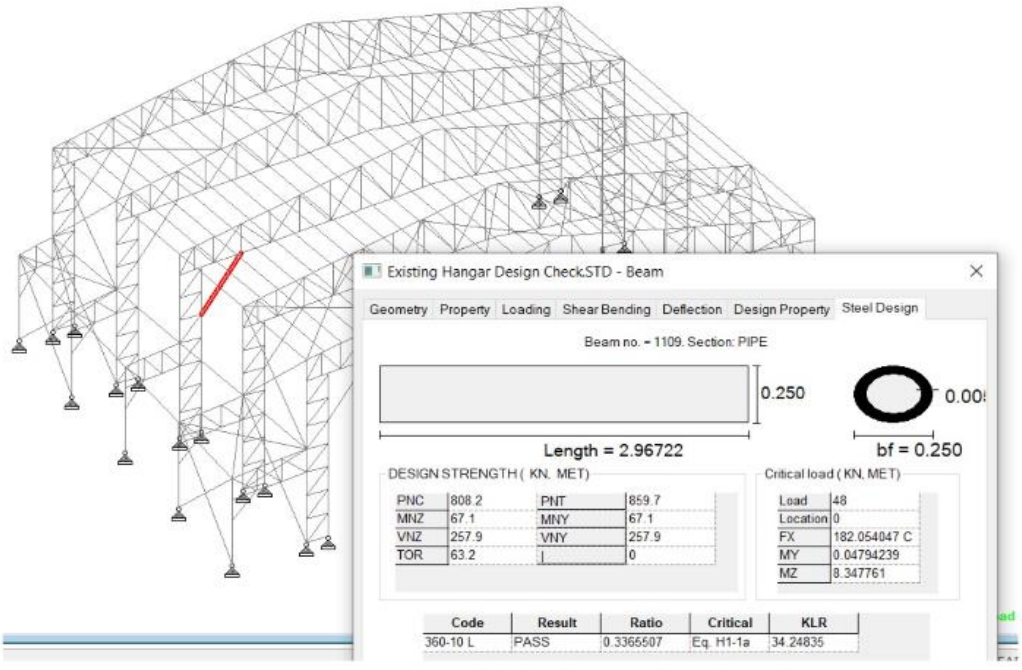
The anchorage system features four anchor rods at equal angles that are set out symmetrically to withstand lateral shear forces and to avoid uplift under the governing combinations of wind suction. The remediation is through the use of high strength threaded anchor rods, which are inserted into the existing sound concrete pedestals using high performance structural chemical adhesive. Gomez, Higgins and Mahoney (2010) conducted experimental test results that showed that full tensile and shear capacities can be obtained with adhesive anchors installed with proper embedment depth, without any risk of concrete break-out or concrete pullout failure. Hardened steel washers and double-nut assemblies are used to secure the base plate and a bed of high-strength non-shrink cementitious grout is placed to transfer the load down to the foundation. Further, critical legacy truss nodes and hand-welded splices are encased with custom detailed steel gusset

plates (≥ 10 mm) with certified shop-welded brackets, avoiding the need for uncertified legacy welds and providing complete code-compliant structural integrity.

5.3.5 Finite Element Numerical Verification of the Retrofitted Framework

To definitively validate the structural safety, code compliance, and mechanical feasibility of the engineered in-situ retrofitting scheme (Option 2), a comprehensive finite element re-verification phase was executed within the STAAD.Pro software environment. The optimized structural model subjects the newly integrated trussed-column lattice configurations, member-sleeving profiles, and optimized nodal boundaries to the governing ultimate limit state load combinations quantified in Chapter 3.

Rather than incorporating repetitive text for every optimized section, a compiled portfolio of the most critical member design check report snippets is presented directly below to illustrate the post-retrofitting performance.



- **Figure 5.3:** STAAD.Pro post-retrofitting design check report for Beam No. 1106, indicating code compliance (PASS) with an optimized stress ratio of 0.34.

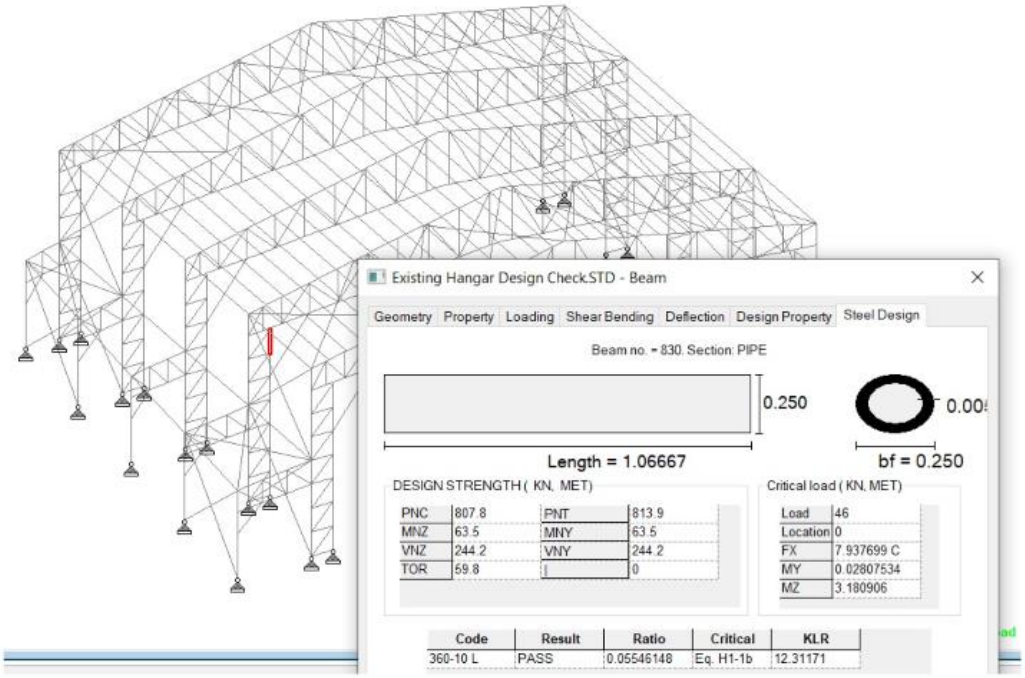


Figure 5.4: STAAD.Pro post-retrofitting design check report for Beam No. 830 (Lacing Web Member), indicating code compliance (PASS) with an optimized stress ratio of 0.06.

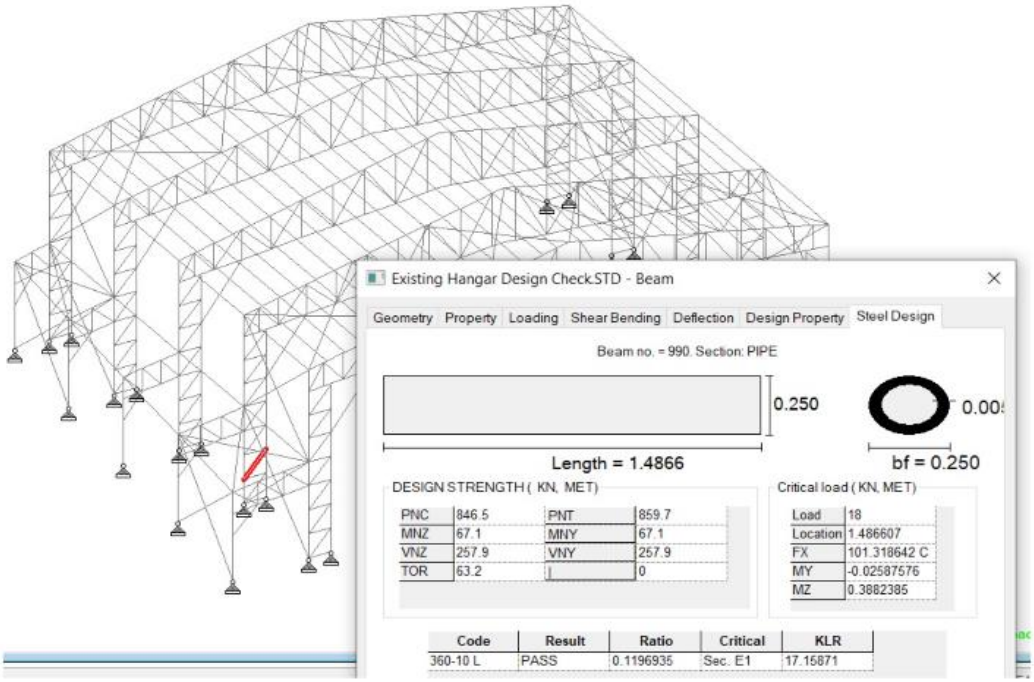


Figure 5.5: STAAD.Pro post-retrofitting design check report for Beam No. 990 (Column Lacing Member), indicating code compliance (PASS) with an optimized stress ratio of 0.14.

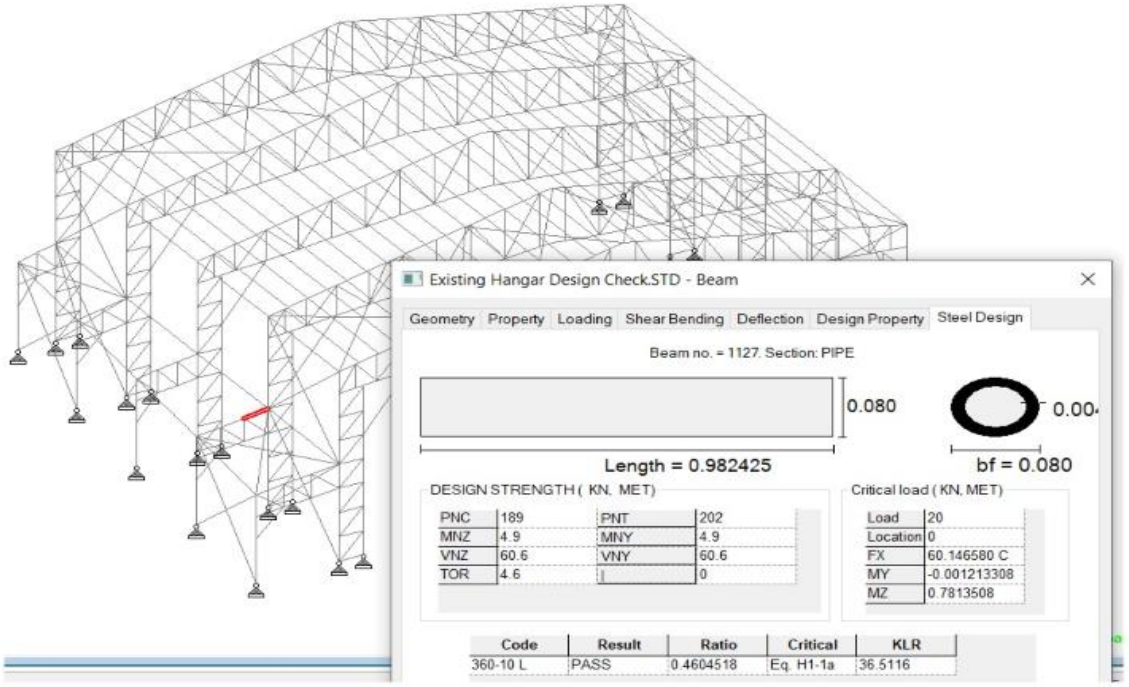


Figure 5.6: STAAD.Pro post-retrofitting design check report for Beam No. 1127 (Horizontal Lacing Strut), indicating code compliance (PASS) with an optimized stress ratio of 0.47.

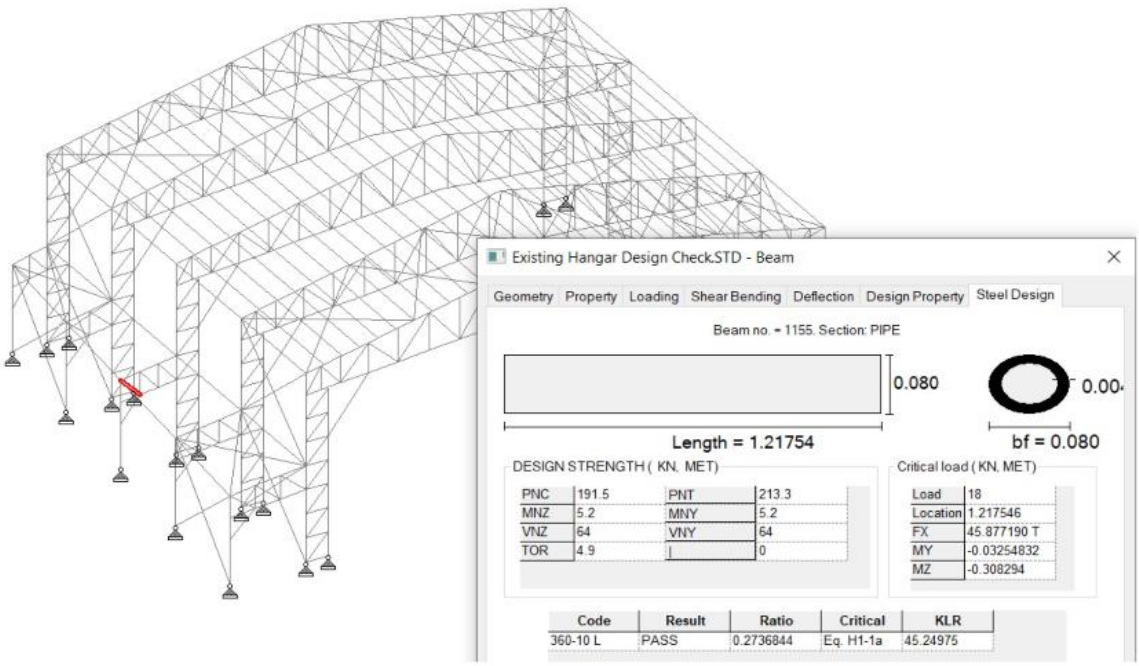


Figure 5.7: STAAD.Pro post-retrofitting design check report for Beam No. 1150, indicating code compliance (PASS) with an optimized stress ratio of 0.27.

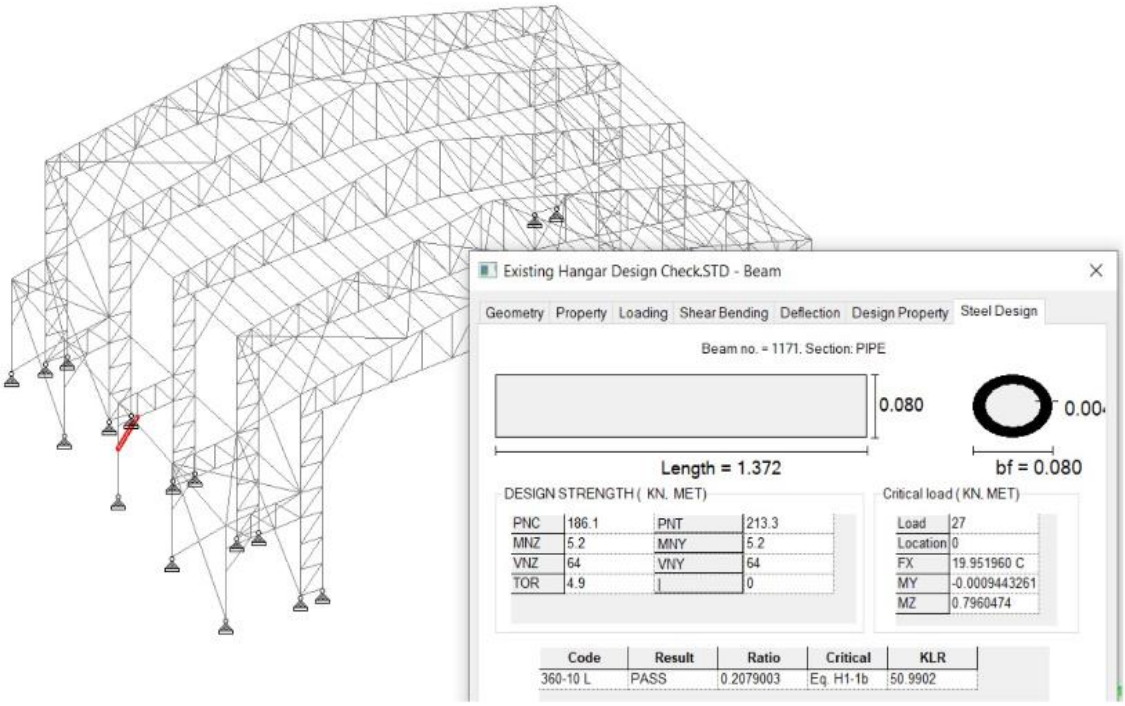


Figure 5.8: STAAD.Pro post-retrofitting design check report for Beam No. 1170 (Column Lacing Member), indicating code compliance (PASS) with an optimized stress ratio of 0.20.

5.3.6. Phase I: Post-Retrofitting Internal Force Distribution and Structural Behavior

Following the structural implementation of the engineered in-situ retrofitting scheme (Option 2), the primary internal forces were re-extracted from the optimized STAAD.Pro finite element model to evaluate the enhanced structural behavior under the governing load combinations

.

Axial Force Distribution: The structural activation of the twin-column layout through the continuous triangular lacing lattice transforms the axial force flow. The global assembly operates as a highly redundant built-up lattice system, safely partitioning the axial compression between the primary and secondary vertical profiles. Within the upper roof framework, the truss system maintains an optimized axial behavior, where gravity and wind load combinations are efficiently translated into pure axial chord demands.

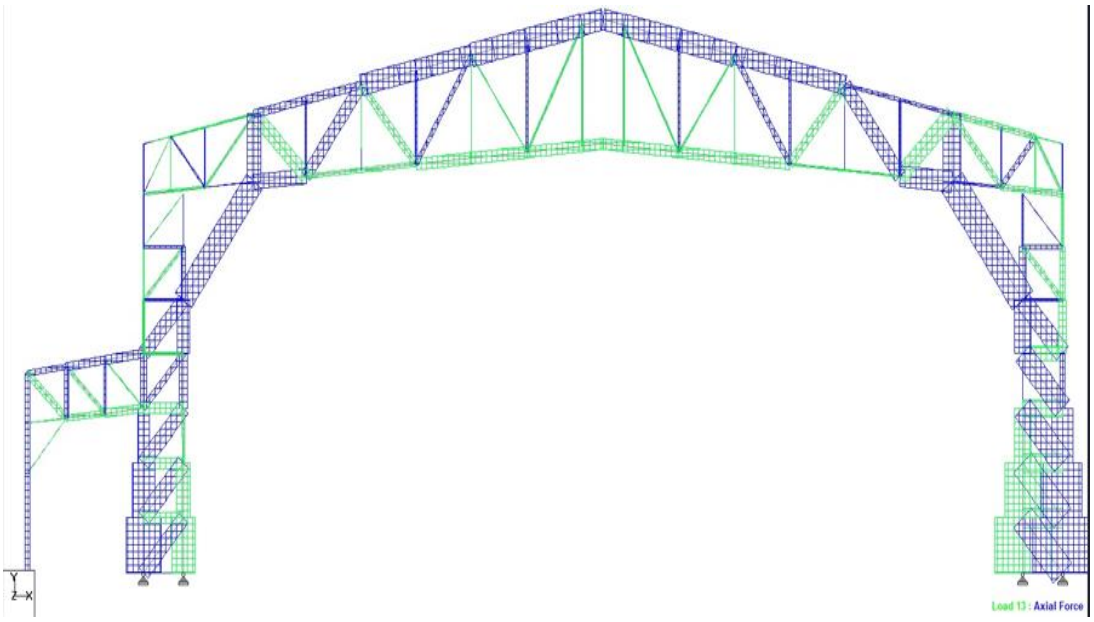


Figure 5.9: Axial Force Diagram for the retrofitted main truss and column frame.

Shear Force and Bending Moment: applications still exist, the magnitude of their localized structural actions is drastically controlled. The massive flexural and horizontal rigidity provided by the newly developed trussed columns serves as a protective moment-shielding perimeter. By directly absorbing the lateral wind surge profile, these stiffened boundaries minimize global frame sway and secondary bending deformations.

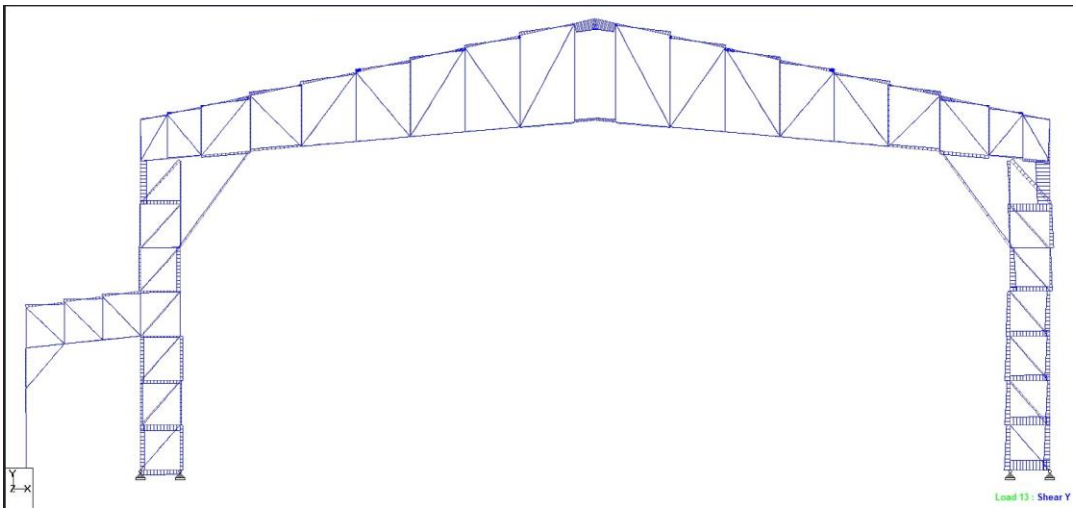


Figure 5.10: Shear Force Diagram (Fy) for the retrofitted primary structural frame.

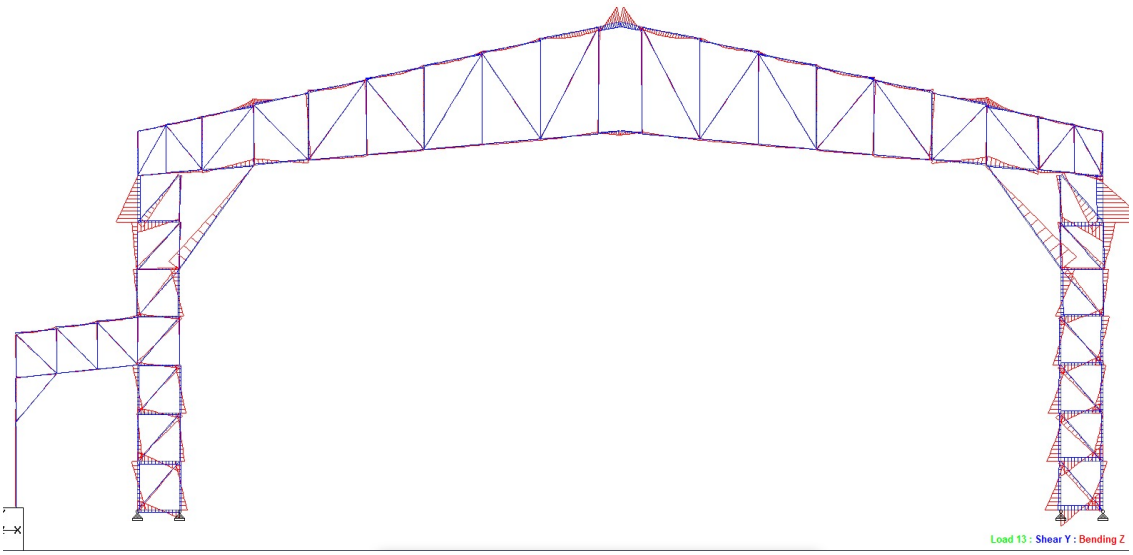


Figure 5.11: Bending Moment Diagram (Mz) for the retrofitted structural frame illustrating optimized stress localization**.**

Technical Justification for Optimized Force Distribution:

The retrofitted framework successfully accommodates the combined shear forces and bending moments due to the following mechanical enhancements:

Lattice Shear Rigidity: In strict compliance with AISC 360-16 Section E6, the continuous diagonal lacings introduce a high internal shear stiffness mechanism. This mechanism securely bridges the local bending moments induced by eccentric purlin loading on the 155 mm CHS top chords, safely redirecting the structural demands without triggering localized buckling or limit-state violations.

5.3.7 Phase II: Global Capacity re-verification and Stress Ratio Envelope

Following the detailed individual component-level validation presented in previous sections, a final global re-verification of the entire optimized framework (Option 2) was executed under the governing extreme environmental load combinations (Load 13). Figure 5.12 consolidates the final demand-to-capacity (D/C) stress ratios for all structural components, visually validating the transition of the framework into a code-compliant safety envelope.

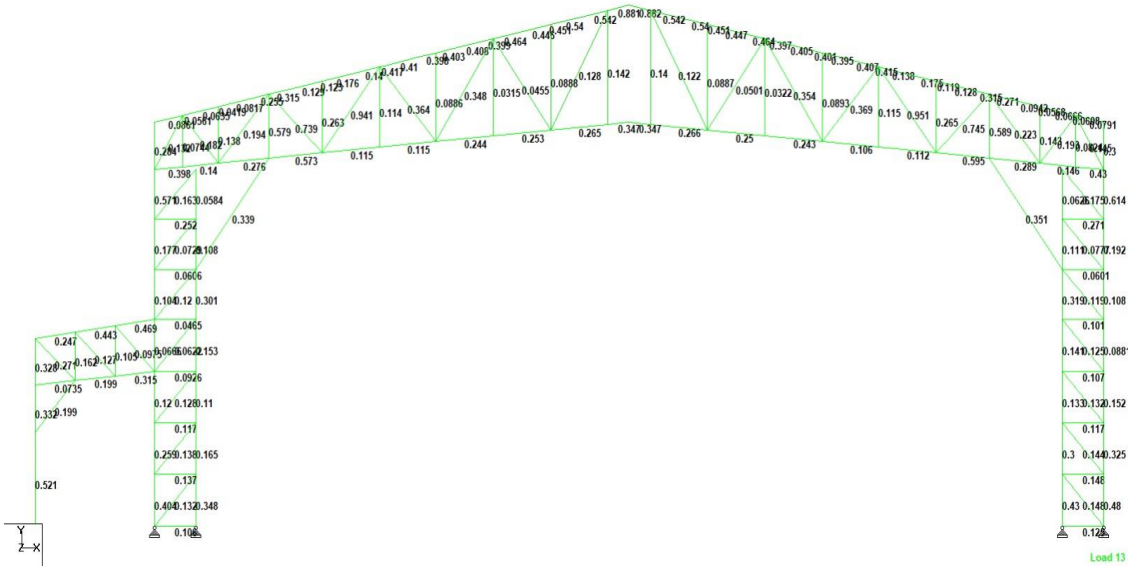


Figure 5.12: Global 2D frame stress ratio envelope under governing load combinations (Load 13) after retrofitting activation, demonstrating 100% code compliance (PASS) with all member utilization ratios safely below 1.0.

Concluding Mechanical Synthesis and Discussion:

As visually demonstrated in the analytical model (Figure 5.11), the implementation of the engineered in-situ retrofitting scheme (Option 2) successfully satisfies all structural safety requirements. The governing extreme failure points previously identified in Chapter 4—including the critical canopy support failure at a stress ratio of 2.71 and primary column buckling failures at 1.51—have been effectively neutralized.

Following retrofitting activation, member utilization ratios have dropped safely below unity (< 1.000). The maximum peak ratio within the complex geometry of the continuously loaded truss top chords now caps at a safe 0.88. Simultaneously, the newly stiffened perimeter columns and canopy support vertical profiles operate within exceptionally stable, high-reserve capacity zones, demonstrating ratios comfortably ranging from 0.10 to 0.52. This robust numerical evidence proves that the engineered column-trussing and perimeter shielding mechanism successfully restore global frame stability and satisfy all AISC 360 slenderness and interaction criteria under governing load demands.

5.3.8 Advanced Numerical Verification of Critical Connections (IDEA StatiCa CBFEM Analysis)

The STAAD performing the global frame verification in Section 5.3.5 does not only provide the stability of the frame at member level, but also ensures that there is stability in the load path at the global level.The local joint verification is essential for Pro boundaries and critical semi-rigid boundaries and field splices. The apex ridge splice is particularly a governing nodal connection under concurrent axial tension and transverse shear moments and inplane bending moments due to asymmetric snow loading and wind suction reversals. To ensure compliance with code, connection ductility verification was performed with the use of the localized Finite Element Method (FE Method) of IDEA StatiCa, as per AISC 360-16 (LRFD) Code of Practice, which was not based on any empirical simplifications.

1. Joint Configuration and Material Modeling

The investigated apex configuration couples two Circular Hollow Section top-chord members (CHS 155.4×4.0 mm, ASTM A36, $F_y = 248.2$ MPa) inclined at the roof slope of 5.7°. The joint is detailed as a bolted end-plate splice comprising two shop-welded end plates (PP1a and PP1b) fastened by four high-strength ASTM A325 bolts ($d_b = 1/2$ in $\approx$ 13 mm, $F_u = 827.4$ MPa) and perimeter fillet welds utilizing E70xx electrodes.

The connection was analyzed under the governing enveloping internal force resultant extracted from the ultimate limit state (ULS) combinations in the global analysis (Load Effect LE1):

- **Axial Tension Force (N):** 27.9 kN
- **Transverse Shear Force (V_z):** -6.2 kN
- **In-Plane Bending Moment (M_y):** 2.3 kNm

Geometrical and Materially Nonlinear Analysis with contact elements (GMNA) was applied to capture contact stresses, local plastification, and potential prying forces between the adjacent end plates.

2. Verification Results and Mechanical Evaluation

The numerical solver achieved complete mathematical convergence at 100.0% of the applied load level. The equivalent von Mises stress contours, plastic strain distributions, and component utilization ratios confirm that all connection elements satisfy code safety thresholds:

Table 5.1: CBFEM Verification Summary for Truss Apex Splice (AISC 360-16 LRFD)

Component / Evaluation	Governing Design Criteria	Calculated Value / Utilization	Safety Status
Load Convergence	Equilibrium / GMNA Analysis	100.0% Load Applied	**OK**
Splice End Plates (PP1a / PP1b)	$\varepsilon_{Pl} \leq 5.0\%$ (Plastic Strain Limit)	$\varepsilon_{Pl} = 1.6\%$ ($\sigma_{Ed,max} =$ 226.5 MPa)	**OK**
High-Strength Bolts (1/2" A325)	Combined Tension & Shear (ϕR_n)	**80.8%** ($F_t =$ 47.6 kN, $V =$ 1.7 kN)	**OK**
Fillet Welds (E70xx)	Weld Throat Resistance (ϕR_n)	**77.7%** ($F_n =$ 3.9 kN/mm)	**OK**

As documented in Table 5.3, the maximum equivalent stress in the end plates reaches 226.5 MPa, remaining below the material yield strength ($F_y = 248.2$ MPa) across the primary bearing zone, with a peak plastic strain of only $\varepsilon_{Pl} = 1.6\%$ localized around the tension bolt holes—well within the code-mandated plastic strain limit of 5.0%. The maximum contact pressure between the plates reaches $\sigma c_{Ed} = 162.5$ MPa.

The governing bolt utilization occurs in the tension zone (Bolts B3 and B4) at 80.8% of design tensile capacity ($\phi R_n = 58.9$ kN), accommodating both direct axial tension and secondary prying action. The perimeter fillet welds develop a peak utilization of 77.7%,

demonstrating sufficient safety against root cracking and weld-throat shear.

To guard against weld distortion and plate warping during field or shop fabrication, a minimum practical plate thickness of $t \geq 8$ mm (or 10 mm) is recommended for on-site execution, further reducing the minor prying deformations observed in the 5.0 mm analytical model. The complete analytical verification report generated by IDEA StatiCa is provided in **Appendix C**.

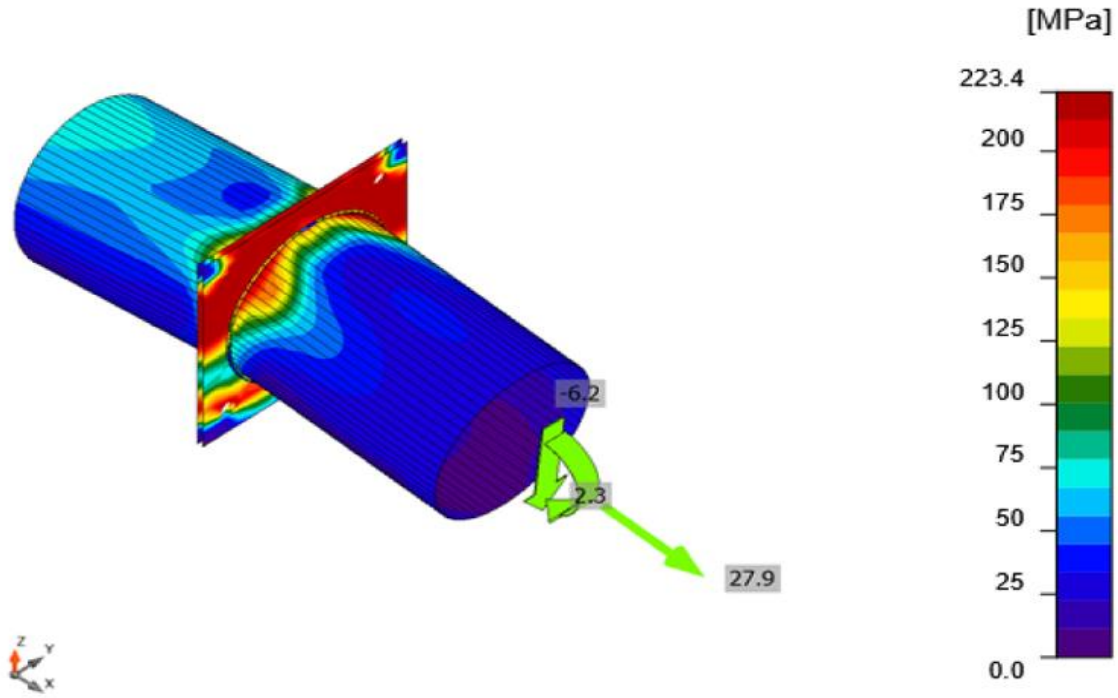


Figure 5.13: CBFEM numerical evaluation of the retrofitted truss apex connection in IDEA StatiCa: (a) 3D finite element geometry and bolt assembly, and (b) Von Mises equivalent stress distribution (σ_{Ed}) under governing load combination LE1.

5.4 Comparison of the Structure Before and After Rehabilitation

A comparison between the structural condition before and after rehabilitation was conducted to demonstrate the effectiveness of the adopted strengthening strategy. The pre-rehabilitation condition represents the existing as-built steel truss building as observed during the field inspection and analyzed using STAAD.Pro. The post-rehabilitation condition represents the strengthened structural system after applying the proposed

rehabilitation measures, including completion of the lateral bracing system, strengthening of critical members, upgrading of deficient connections, improving the column-base bearing condition, and treating damaged or deteriorated steel surfaces.

Table 5.1 summarizes the expected improvement in the structural behavior before and after rehabilitation.

Before rehab , the existing structure kind of showed a bunch of structural shortcomings, like discontinuous lateral bracing, an irregular truss set up, non-engineered welded splices, weak column-base detailing, some local impact damage, coating deterioration, and even unclear load transfer routes. In the numerical analysis, it also came up that several members went past the allowable utilization ratio, so basically the original structural system was not really able to deliver enough capacity for the controlling load combinations .

After rehabilitation , the strengthening work helped the structure's overall behavior, mostly by making the load path more continuous and dependable, bumping up the building lateral stability, lowering the overstress levels in the key members, and making the structural connections more reliable. The rehabilitation approach also upgraded durability in a practical sense, via corrosion treatment, fixing the damaged spots, and a protective repainting step.

Table 5.2: Comparison of Structural Condition Before and After Rehabilitation

Item	Before Rehabilitation	After Rehabilitation
Structural system	Existing non-engineered steel truss system with irregular geometry and uncertain load paths.	Strengthened steel truss system with improved load transfer and better structural continuity.
Lateral stability	Discontinuous bracing system and weak resistance in the longitudinal direction.	Completed bracing system providing a continuous lateral load-resisting path.
Columns	Some columns showed local deformation, mid-height welded splices, impact damage, and coating deterioration.	Critical columns were strengthened, repaired, or locally replaced according to their condition and required capacity.
Column-base condition	Poor base plate detailing and inadequate bearing condition at some	Column-base bearing condition was improved through proper base plate detailing, leveling,

	column bases.	and grout finishing where required.
Truss behavior	Irregular truss configuration and non-nodal loading caused combined axial force, shear, and bending effects.	Critical truss members were strengthened, and the load-transfer mechanism was improved to reduce non-ideal force effects.
Connections	Several connections were non-standard, discontinuous, or executed without proper quality control.	Deficient connections were upgraded to provide safer and more predictable force transfer.
Bracing system	X-bracing was discontinuous and did not form a complete lateral load path.	Bracing was completed and arranged to transfer lateral forces from the roof and wall levels to the supporting system.
Corrosion and coating	Local corrosion, coating damage, and surface deterioration were observed.	Damaged surfaces were cleaned, treated against corrosion, and repainted to improve durability.
Numerical performance	Several members exceeded the allowable utilization ratio of 1.0.	Utilization ratios were reduced after strengthening, and the structural response became more acceptable under the governing load combinations.
Safety level	The structure showed a risk of local member failure and possible instability under severe loading.	The rehabilitation strategy improved the structural safety level and reduced the risk of local and global instability.
Service life	Remaining service life was limited due to accumulated defects and lack of systematic maintenance.	Service life was extended through strengthening, connection upgrading, and corrosion protection.

Based on this comparison, rehabilitation was adopted as the preferred solution because it directly addressed the actual deficiencies observed in the existing structure while preserving the usable portions of the steel system. Unlike full replacement, the rehabilitation strategy is more consistent with the forensic scope of this research, as it focuses on recovering and improving an existing structural asset rather than replacing it with a completely new system.

The comparison indicates that the proposed rehabilitation strategy addresses the principal deficiencies identified in the existing structure while retaining those structural components considered suitable for reuse. The post-rehabilitation analysis showed reduced utilization ratios for the evaluated critical members and improved continuity of the lateral load-resisting system. These findings support rehabilitation as a candidate intervention for the studied building, subject to completion of the required member, connection, anchorage, foundation, and constructability checks.

because it directly addresses the actual deficiencies observed in the existing structure while preserving the usable portions of the steel system. Unlike full replacement, the rehabilitation strategy is more consistent with the forensic scope of this research, as it focuses on recovering and improving an existing structural asset rather than replacing it with a completely new system.

The post-rehabilitation STAAD.Pro analysis confirmed the effectiveness of the adopted strengthening scheme. The strengthened model demonstrated improved structural behavior, reduced utilization ratios in critical members, and a more reliable lateral load-resisting system under the governing load combinations. Accordingly, the rehabilitation scheme was considered structurally effective and suitable for implementation.

5.5 Technical and Economic Evaluation: Retrofitting vs. Replacement

The evaluation of constructability and operational requirements indicates that in-situ rehabilitation involves substantial planning, temporary support, specialized connection work, and careful sequencing. These requirements must be considered in the final construction plan and cost estimate. Full structural replacement remains a technically feasible alternative, but it entails demolition, new fabrication and erection, and potentially greater interruption to industrial operations. The final selection between the alternatives should therefore be based on the verified structural design results and a consistent life-cycle cost comparison. The economic comparison is presented in Section 5.6, while the overall technical and economic recommendation is summarized in Section 5.7.

Complexity of the Bracing Network Installation: The legacy structure completely lacks an engineered lateral bracing system. While Option 2 satisfies stability on paper through localized column-trussing, installing a fully continuous, code-compliant horizontal and vertical bracing network across a highly deformed, non-engineered legacy asset presents extreme geometric alignment and field-welding difficulties.

- **Prohibitive Scope of Simultaneous Modifications:** Implementing Option 2 is not a simple patch repair; it demands an extensive and invasive structural intervention. This path requires temporary shoring of the entire roof infrastructure, full in-situ modifications of the primary columns, localized sleeving of deficient web profiles, and the custom fabrication of hundreds of nodal plate bracket adapters.

- **Economic and Operational Downtime Disparities:** The highly specialized nature of in-situ retrofitting requires non-destructive testing (NDT), certified field welders, specialized lifting equipment, and extended project execution timelines. The associated labor costs and prolonged industrial operational shutdown drive the total cost threshold to prohibitive levels, matching or exceeding the budget of a new construction.

- In synthesis, while Option 1 provides an idealized structural solution, **Option 2 (In-Situ Structural Rehabilitation and Strengthening)** stands as the most optimal and economically feasible choice for this case study. It directly restores global frame stability and lifetime safety while avoiding the prohibitive demolition costs and substantial operational downtime associated with full structural replacement.

5.6 Life-Cycle Cost Analysis (LCCA)

Life-Cycle Cost Analysis (LCCA) was used to compare the economic implications of full structural replacement and in-situ rehabilitation over the adopted analysis period. The comparison considers initial construction or rehabilitation costs, demolition and transportation costs, maintenance and repair costs, operational disruption, and residual value, where applicable. Future costs should be converted to present values using a clearly stated discount rate and consistent assumptions for both alternatives. The results are intended to support the technical evaluation rather than replace the required structural safety checks.

Using LCCA fits with established economic evaluation methods for buildings and infrastructure. ASTM E917 gives a standard practice for how to measure life-cycle costs of buildings and building systems, while NIST Handbook 135 shows a commonly used approach for judging long term project costs through present-value ideas.

Also, FHWA guidance points to LCCA as an engineering economic instrument, for comparing different alternative ways to implement a project across the service life of the asset.

In this research, the LCCA comparison was conducted between two alternatives:

- **Alternative 1: Full structural replacement with a new rigid portal frame system.**
- **Alternative 2: In-situ rehabilitation and strengthening of the existing steel truss system.**

The general life-cycle cost of each alternative can be expressed as:

$$[LCC = C_i + PV(C_m) + PV(C_r) + PV(C_d) - PV(S)]\text{where:}$$

$$\left[PV(C_t) = \frac{C_t}{(1+i)^t}\right]$$

Table 5.3: LCCA Cost Symbols

Symbol	Description
$(\boldsymbol{LCC})$	Total life-cycle cost of the alternative
$(\boldsymbol{C_i})$	Initial construction or rehabilitation cost
$(\boldsymbol{C_m})$	Future maintenance cost
$(\boldsymbol{C_r})$	Future repair or replacement cost
$(\boldsymbol{C_d})$	Cost of operational disruption or downtime
$(\boldsymbol{S})$	Residual or salvage value at the end of the analysis period
$(\boldsymbol{i})$	Discount rate
$(\boldsymbol{t})$	Year in which the future cost occurs

5.6.1 Cost Components of Full Structural Replacement

For the full replacement alternative you essentially have to remove the current structure and then build up a completely new steel arrangement . So the total cost is not only materials, it also comes with demolition, hauling/transportation, fresh steel fabrication, erection work, roof sheet replacement, electrical reinstallation, supervision, equipment rental, and even operational downtime.

Looking at the cost info you have, the preliminary cost components below were taken into account for the full replacement alternative .

Table 5.4: Preliminary Cost Estimate for Full Structural Replacement

Cost Item	Calculation Basis	Cost (NIS)
Structural design	Fixed cost	20,000
Dismantling / demolition of existing steel structure	Fixed cost	7,000
Transportation of removed materials	500 NIS per trip	(500N_t)
Technical labor	4,000 NIS/month × 4 months	16,000
Installation materials, bolts, welding consumables, and minor tools	Fixed cost	5,000
Crane rental for steel handling and erection	Fixed cost	10,000
Electrical works, wiring, outlets, lighting fixtures, and related items	Fixed cost	50,000
Loss due to factory shutdown	100,000 NIS/month × 4 months	400,000
Idle factory labor during shutdown	15,000 NIS/month × 4 months	60,000
Known subtotal excluding transport trips, steel, zinc sheets, and supervision	Sum of fixed listed costs	568,000

Accordingly, the total preliminary replacement cost can be expressed as:

$$\left[C_{Replacement} = 568{,}000 + 500N_t + C_s + 20N_z + 5.5A(E.R.)\right]$$ where:

Table 5.5: Replacement Cost Variables

Symbol	Description
(N_t)	Number of transportation trips
(C_s)	Cost of new structural steel fabrication and erection
(N_z)	Number of zinc roof sheets
$(20N_z)$	Cost of zinc sheets, assuming 20 NIS per sheet
(A)	Building area in square meters
$(E.R.)$	Exchange rate from Jordanian Dinar to NIS
(5.5A(E.R.))	Engineering supervision cost, based on 5.5 JOD/m²

The cost analysis shows that the largest cost component in the full replacement option is the cost of operational shutdown. The shutdown-related cost alone is:

$$C_{Shutdown} = (100{,}000 + 15{,}000) \times 4 = 460{,}000 \text{ NIS}$$This means that the interruption to the industrial activity represents a major economic disadvantage of the full replacement alternative. Even before adding the cost of new steel, zinc sheets, transportation trips, and engineering supervision, the known replacement-related cost reaches 568,000 NIS.

5.6.2 Cost Components of In-Situ Rehabilitation

The rehab alternative keeps the workable parts of the current steel framework and, uh, concentrates on reinforcing just the key areas. Its big cost pieces are mostly extra steel for strengthening , bracing completion, connection upgrading, local fixes for any damaged members, corrosion treatment, protective repainting, equipment rental, and a limited amount of operational disruption.

Different from a full replacement, rehabilitation doesn't call for total demolition of the building. It also cuts down the volume of new steel that would otherwise be needed, and lets the strengthening tasks happen on site and in phases. So it really lowers the downtime and means the industrial activity can keep going , with only a small interruption if possible.

The total rehabilitation cost can be expressed as:

$$C_{Rehabilitation} = C_{st} + C_{br} + C_{con} + C_{rep} + C_{coat} + C_{eq} + C_{d,R}$$where:

Table 5.6: Rehabilitation Cost Variables

Symbol	Description
(C_{st})	Cost of strengthening steel members
(C_{br})	Cost of completing or upgrading the bracing system
(C_{con})	Cost of upgrading deficient connections
(C_{rep})	Cost of local repair or replacement of damaged members
(C_{coat})	Cost of corrosion treatment and repainting
(C_{eq})	Cost of equipment and temporary works
$(C_{d,R})$	Cost of limited operational disruption during rehabilitation

The main economic advantage of rehabilitation is that it reduces both direct and indirect costs. Direct costs are reduced by reusing existing structural members where acceptable. Indirect costs are reduced because the construction period is shorter and the building does not require full shutdown for the same duration as replacement.

5.6.3 LCCA Comparison Between Replacement and Rehabilitation

Table 5.7: Life-Cycle Cost Comparison Between Replacement and Rehabilitation

Cost Component	Full Structural Replacement	In-Situ Rehabilitation and Strengthening
Initial construction cost	High, due to demolition, new steel fabrication, transportation, erection, and reconstruction works.	Lower, because most of the existing structural system is retained and only critical zones are strengthened.
Demolition cost	High, because the existing steel structure must be removed.	Low, because removal is limited to damaged or structurally inadequate members only.
Transportation cost	Higher, because removed steel and waste must be transported from site.	Lower, because demolition quantities are limited.
Material consumption	High, due to the use of a completely new steel frame system.	Lower, because existing members are reused where structurally acceptable.
Construction duration	Approximately four months based on the replacement assumption.	Shorter because strengthening works can be executed locally and in stages.
Operational disruption	High, with shutdown-related losses estimated at 460,000 NIS.	Lower because rehabilitation reduces the shutdown period and allows staged execution.
Maintenance cost	Lower during early service life because the system is new.	Moderate, because the existing structure requires periodic inspection and protective maintenance.
Repair cost	Low in the short term, but future repair may still be required depending on exposure conditions.	Moderate, but controlled through corrosion treatment, connection upgrading, and planned maintenance.
Environmental cost	Higher, due to demolition waste and higher demand for new steel production.	Lower, due to reuse of existing steel members and reduction of construction waste.
Overall life-cycle	Less favorable because of high initial cost	More favorable because of lower direct cost,

economy	and major operational disruption.	reduced downtime, and reuse of the existing asset.

Based on the LCCA comparison, the in-situ rehabilitation alternative provides a more balanced economic solution than full replacement. Although full replacement offers a new structural system, its high initial cost, demolition requirements, longer construction period, and major operational disruption make it less attractive for the studied industrial building.

In contrast, rehabilitation directly addresses the observed deficiencies while preserving the usable portions of the existing steel system. The reduction in downtime is particularly important because the shutdown-related cost represents the largest identified cost component in the replacement alternative.

Therefore, the LCCA supports the adoption of rehabilitation as the preferred solution from both engineering and economic perspectives.

5.6.4 Adopted Service Life for LCCA

For the purpose of the Life-Cycle Cost Analysis, the expected additional service life of the rehabilitated structure was adopted as **25 years** after the completion of the strengthening works. This value does not represent an unconditional guarantee of performance; rather, it is an engineering service-life assumption based on proper implementation of the proposed rehabilitation measures and periodic maintenance during operation.

The adopted 25-year service life was adopted as an analytical assumptio because the rehabilitation strategy kinda tackles the main reasons for structural vulnerability that showed up in the field inspection and numerical check. It basically includes finishing the lateral bracing system, reinforcing key column and truss members, improving the weak connections, fixing the column-base bearing condition, handling damaged or corroded steel surfaces ,and putting on a protective repainting system.

Still, the actual service life of the rehabilitated structure relies a lot on how good the inspections and maintenance really are. So the assumed service life is based on the idea that the building will be inspected at regular intervals, any damaged coating will be repaired when necessary, corrosion will

be dealt with before noticeable section loss starts developing, and that there will be no major change in building use or in loading conditions without an extra structural assessment.

For comparison, the full replacement alternative may provide a longer nominal service life because it creates a new structural system. However, the rehabilitation alternative provides a practical extension of the existing building's service life while significantly reducing demolition works, material consumption, construction duration, and operational shutdown losses.

Table 5.8: Adopted Service Life for LCCA Comparison

Alternative	Adopted Service Life	Basis of Assumption
Full structural replacement	50 years	New steel structural system designed and constructed according to current code requirements.
In-situ rehabilitation and strengthening	25 years	Existing steel system retained and upgraded through strengthening, bracing completion, connection improvement, corrosion treatment, and protective repainting.

Accordingly, the LCCA in this study adopts a **25-year analysis period** for evaluating the rehabilitation option. This period is sufficient to assess the economic feasibility of strengthening the existing structure while considering the expected need for periodic inspection, maintenance, and coating renewal during service.

5.7 Technical and Economic Evaluation

A combined technical and economic evaluation was conducted to identify the most suitable intervention strategy for the existing industrial steel building. The comparison focused on engineering performance, constructability, cost efficiency, operational disruption, durability, sustainability, and long-term serviceability. The purpose of this evaluation is to determine which alternative provides the best balance between structural safety and practical feasibility.

Table 5.9: Technical and Economic Evaluation of Structural Alternatives

Evaluation Criterion	Option 1: Full Replacement	Option 2: In-Situ Rehabilitation
Structural safety	Provides a new code-compliant structural system.	Restores structural safety by strengthening critical members, completing the bracing

		system, and upgrading deficient connections.
Lateral stability	Provides a new lateral load-resisting system if fully redesigned and constructed.	Improves lateral stability by completing the discontinuous bracing system and creating a continuous lateral load path.
Constructability	Requires complete removal of the existing structure and major reconstruction works.	Can be implemented through targeted and staged interventions with less site disruption.
Initial cost	High due to demolition, new steel fabrication, transportation, erection, and reconstruction works.	Lower because the existing steel system is retained and only critical zones are strengthened.
Operational disruption	Causes longer interruption to factory operation because the existing structure must be removed before reconstruction.	Reduces interruption because rehabilitation works can be executed locally and in stages.
Construction duration	Longer due to dismantling, fabrication, transportation, and erection of a new system.	Shorter because the work focuses on strengthening, connection upgrading, bracing completion, and local repair.
Material consumption	High due to the use of a completely new steel frame system.	Lower because existing members are reused where structurally acceptable.
Environmental impact	Higher due to demolition waste and increased demand for new steel production.	Lower due to reduced demolition waste and reuse of existing steel members.
Durability	Good if the new system is properly protected and maintained.	Improved through corrosion treatment, repair of damaged areas, and protective repainting.
Maintenance requirements	Lower in the early service period because the system is new.	Moderate because the existing system requires periodic inspection and protective maintenance.
Service life	Longer nominal service life because the structure is newly constructed.	Provides a practical additional service life after strengthening, assumed as 25 years with periodic maintenance.
Economic feasibility	Less favorable due to high initial cost and high shutdown-related losses.	More favorable due to lower direct cost, reduced downtime, and reuse of the existing structural asset.
Overall recommendation	Technically feasible but economically less attractive for this case.	Preferred solution because it provides adequate structural improvement with lower cost and less operational disruption.

The full replacement alternative provides a completely new structural system because it provides a completely new structural system. However, it requires full removal of the existing structure, higher

initial investment, longer execution time, greater material consumption, and larger shutdown-related losses. Therefore, it is considered the less economically favorable option for the investigated industrial facility.

In-situ rehabilitation provides a more balanced solution. It improves the structural performance of the existing building by strengthening the critical members, completing the bracing system, upgrading deficient connections, and treating damaged or deteriorated steel surfaces. At the same time, it reduces demolition works, limits material consumption, shortens execution duration, and decreases operational disruption.

Based on the combined technical and economic evaluation, in-situ rehabilitation is adopted as the preferred solution. This alternative provides the best balance between structural safety, cost efficiency, constructability, service-life extension, and continuity of industrial operation.

5.8 Chapter Summary

This chapter presented and evaluated the main structural intervention alternatives proposed for the existing industrial steel truss building. The structural assessment confirmed that the building requires intervention due to several critical deficiencies, including overstressed members, discontinuous lateral bracing, irregular truss configuration, deficient connections, weaknesses at the column-base regions, local member damage, coating deterioration, and corrosion-related surface defects. These deficiencies reduce the structural reliability of the building and may adversely affect its performance under gravity, wind, seismic, and environmental actions.

Two main intervention alternatives were considered: full structural replacement and in-situ rehabilitation with strengthening. The full replacement alternative provides a completely new structural system and can achieve a high level of structural safety if properly designed and executed. However, it requires complete demolition of the existing structure, higher initial cost, longer construction duration, increased material consumption, and significant interruption to industrial operations. The Life-Cycle Cost Analysis also showed that shutdown-related losses represent a major cost component in the replacement

alternative.

The in-situ rehabilitation and strengthening alternative provides a balanced engineering response to the actual as-built condition of the existing structure. This alternative improves the structural performance of the existing system while preserving the usable portions of the steel structure. The proposed rehabilitation measures include completing the lateral bracing system, strengthening critical columns and truss members, upgrading deficient connections, improving column-base bearing conditions, treating corroded and damaged steel surfaces, repairing local defects, and applying a protective repainting system.

The comparison between the structure before and after rehabilitation indicates that the strengthened system provides a more reliable load path, improves lateral stability, reduces excessive stresses in critical members, enhances connection reliability, and improves long-term durability. With proper implementation and periodic maintenance, the rehabilitated building is expected to achieve an additional service life of approximately 25 years.

Based on the structural assessment, rehabilitation strategy, and Life-Cycle Cost Analysis presented in this chapter, in-situ rehabilitation provides a more balanced solution in terms of structural safety, economic feasibility, constructability, reduced operational disruption, sustainability, and service-life extension. The findings presented in this chapter form the technical and economic basis for the conclusions and recommendations presented in Chapter 6
based on the combined technical and economic evaluation.

CHAPTER 6: CONCLUSIONS AND RECOMMENDATIONS

6.1 Introduction

This final chapter synthesizes the principal diagnostic findings, numerical validation results, and strategic outcomes of the research. It integrates field-based forensic engineering with high-fidelity finite element analysis to establish a systematic methodology for evaluating and rehabilitating aging, non-engineered industrial steel structures. The conclusions provide a technical basis for structural forensic assessment, while the recommendations identify practical pathways for industrial asset modernization and future academic research.

6.2 Main Conclusions

Based on the comprehensive structural mapping, material assessment, numerical modeling, and multi-criteria evaluation of alternatives presented in this thesis, the following main conclusions are drawn:

6.2.1 Forensic Diagnostic and Legacy Condition Conclusions

Severe Stability Vulnerabilities: The assessment identified significant stability deficiencies in the existing industrial building, primarily associated with its non-engineered structural configuration and the absence of an adequately designed and continuous lateral bracing system. These deficiencies may increase lateral displacements and second-order effects under the governing load combinations, so under extreme

environmental load combinations, it could deform laterally and then it would start destabilizing sway effects.

Cross-Sectional Slenderness Liabilities: The main gravity columns, with an outer diameter of 250 mm and a wall thickness that was only 5 mm (which is not much at all), faced severe weak-axis slenderness liabilities. The numerical checks, carried out under the governing loads, supported this by showing strong limit-state nonconformity, with a dangerous failure stress ratio of 1.51.

Critical Local Failure Hotspots: The secondary canopy support column sub-structure really stood out, it was the most compromised part in the legacy asset. Because of eccentric loading arrangements and unbraced boundary conditions, it reached an extreme failure stress ratio of 2.71, which basically points to an actively distressed structural state.

Uncertified Connection Integrity: “The existing structural system contains field-welded connections for which formal welding documentation and verification records were unavailable. Observed geometric eccentricities and connection discontinuities may introduce local stress concentrations and secondary bending effects in connected members , these had high geometric eccentricity along with obvious structural discontinuities. The odd configuration then produced severe local stress concentrations and also bending actions, those acted along the continuous roof truss chords.

6.2.2 Numerical Re-Verification and Retrofitting Conclusions

Validation of advanced column trussing : the innovative in-situ retrofitting plan (Option 2) came out very effective in computational finite element simulations . Mechanically activating the isolated twin column layout using a continuous , mathematically tuned triangular web lattice , in practice made the frame act like a rigid , almost overbuilt lattice column assembly. It was kind of a step change , the kind you can feel even in how the load paths behave .

Successful slenderness control: adding continuous lacing panel increments (from 1.000 m up to 1.796 m) directly suppressed the minor-axis effective length factor (K). Because of that, "The reported member slenderness ratio decreased to \(KL/r=34.25\) following the proposed lacing modification. This reduction indicates improved restraint against member buckling; however, compliance must also be confirmed through the applicable AISC 360-16 strength and stability checks.

Perimeter stiffness and shielding: the strong horizontal rigidity created by the newly developed trussed columns acted like a doorway barrier. Instead of letting lateral wind forces travel inward, it caught those forces along the outer line and, in turn, eased the upper roof framework from secondary bending actions. That relief let the post-rehabilitation analysis indicates improved design utilization for the evaluated CHS 155 mm top-chord members. Compliance should be reported using the maximum verified demand-to-capacity ratio for the relevant members and governing load combinations, as documented in Chapter 5 , without lingering red flags in the checks.

6.2.3 Technical and Economic Conclusions

The technical and economic evaluation demonstrated that both full structural replacement and in-situ rehabilitation can improve the safety and performance of the existing industrial steel truss building if properly designed and implemented. However, the two alternatives differ significantly in terms of cost, construction duration, material consumption, operational disruption, and sustainability.

Full structural replacement provides a completely new structural system and may achieve a high level of structural reliability. Nevertheless, it requires demolition of the existing steel structure, new fabrication and erection works, replacement of roof components and services, longer construction duration, and significant interruption to industrial operations. The Life-Cycle Cost Analysis showed that shutdown-related losses represent a major cost component in the replacement alternative, making it less economically attractive for the

studied facility.

In contrast, in-situ rehabilitation and strengthening provides a more balanced solution for the actual condition of the existing structure. This alternative preserves the usable portions of the steel system while focusing the intervention on the structurally deficient zones. The proposed rehabilitation measures include completing the lateral bracing system, strengthening critical columns and truss members, upgrading deficient connections, improving column-base bearing conditions, treating corroded and damaged steel surfaces, repairing local defects, and applying a protective repainting system.

The rehabilitation alternative also reduces demolition works, limits material consumption, shortens execution duration, minimizes operational interruption, and extends the service life of the existing structure. With proper implementation and periodic maintenance, the rehabilitated structure is expected to achieve an additional service life of approximately 25 years.

Accordingly, full structural replacement is considered a technically feasible alternative; however, in-situ rehabilitation and strengthening is recommended as the preferred solution for this case study because it provides the best balance between structural safety, economic feasibility, constructability, reduced operational disruption, sustainability, and service-life extension.

6.3 Recommendations for Engineering Practice

To improve structural safety and engineering practiceand help structural engineers dealing with comparable issues on aged, non-engineered industrial steel property types, these practical protocols are suggested.

Mandatory Forensic mapping protocols: Any structural changes on legacy industrial facilities cannot rest on “gut feel”, or on unverified as-built documents, or even partially empirical assumptions. Full 3D LiDAR laser-scanning and hands-on forensic field

mapping are required so engineers can record structural deformations, trace field-welded geometries, and spot component irregularities.

Rigid substructure anchorage fixity: If older anchorage arrangements are absent or incomplete, they must be rectified via deep embedment post installed structural adhesive anchoring, like structural chemical adhesive systems. Pedestals also should be structurally modified to accept heavy-duty baseplates, with the aim of delivering firm fixity plus dependable resistance against high wind uplift, including extreme upward force scenarios.

Rectification of curved-to-flat connections: When roof coverings are being upgraded over curved tubular truss nodes, you need specially made structural steel plate bracket adapters that are custom-fabricated and then fully, continuously welded. This is intended to create an unambiguous, deterministic gravity load path from flat-faced cold-formed Z-purlins directly into the primary nodal intersections, without detours.

Based on the findings of this study, the recommended engineering intervention for the investigated industrial steel truss building is in-situ rehabilitation and strengthening rather than full structural replacement. This recommendation is based on the ability of the rehabilitation alternative to restore the structural performance of the existing system, improve lateral stability, address critical member and connection deficiencies, reduce construction cost and downtime, and extend the service life of the building while preserving the usable portions of the existing steel structure.

6.4 Future Research Horizons

To expand the scientific boundaries established in this investigation, the following avenues are proposed for future academic research:

- **Non-Linear Pushover and Collapse Analysis:** Future studies should implement advanced non-linear pushover simulations and plastic hinge modeling to evaluate the progressive collapse mechanisms of non-engineered twin-column steel systems under

seismic actions.

- **Dynamic Wind-Tunnel Modeling and CFD:** It is highly recommended to complement static code formulations with computational fluid dynamics (CFD) and physical wind-tunnel testing to precisely analyze localized wind suction actions and micro-climate pressure profiles across irregular industrial roofs.

- **Semi-Rigid Boundary and Joint Flexibility Modeling:** Research can be extended by integrating rotational spring stiffness formulations into finite element software to evaluate the behavior of uncertified hand-welded connections under cyclic fatigue and thermal load variations.

REFERENCE LIST

− AISC Design Guide 25. (2011). *Frame Design Using Web-Tapered Members*. American Institute of Steel Construction (AISC).

− American Institute of Steel Construction (AISC). (2002). *AISC Design Guide 15: AISC Rehabilitation and Retrofit Guide: A Reference for Historic Shapes and Specifications*. Chicago, IL.

− American Institute of Steel Construction (AISC). (2016). *Specification for Structural Steel Buildings (ANSI/AISC 360-16)*. Chicago, IL.

− American Society of Civil Engineers (ASCE). (2017). *Minimum Design Loads and Associated Criteria for Buildings and Other Structures (ASCE/SEI 7-16)*. Reston, VA.

− Astaneh-Asl, A. (2008). *Forensic engineering investigations of steel buildings and connections*. Structural Integrity Portfolio Criteria.

− Biediger, C. A. (2002). *Forensic structural engineering: Case studies and lessons learned in rehabilitation*.

− Bjorhovde, R. (2006). *Semi-rigid connections in structural steelwork: Real-world boundary configuration evaluation*.

− Brockenbrough, R. L. and Merritt, F. S. (2006). *Structural Steel Designer's Handbook* (4th ed.). McGraw-Hill Professional.

− Bruneau, M., Uang, C. M. and Sabelli, R. (2011). *Ductile Design of Steel Structures* (2nd ed.). McGraw-Hill Education.

− Carper, K. L. (Ed.). (2000). *Forensic Engineering* (2nd ed.). CRC Press.

− Carter, C. J. and Geschwindner, L. F. (2008). *AISC Design Guide 28: Stability Design of Steel Buildings*. American Institute of Steel Construction (AISC).

− Chen, Y., Wang, X. and Liu, J. (2012). Lateral drift behavior of unbraced steel frames under extreme wind loads. *Journal of Constructional Steel Research*, 78, pp.123–131.

− Deierlein, G. G., Hajjar, J. F., Yura, J. A., Surovek-Maleck, A. E. and White, D. W.

(2002). Proposed new provisions for stability design of steel frames. *Proceedings of the LRFD Stability Conference*.

− Ellingwood, B. R. (2005). Mitigation of progressive collapse of structures. *Structural Engineering International*, 15(2), pp.101–105.

− Fisher, J. M. and Kloiber, L. A. (2006). *AISC Design Guide 1: Base Plate and Anchor Rod Design* (2nd ed.). American Institute of Steel Construction (AISC).

− Fisher, J. M. and Tartaglia, M. (2009). Design and behavior of roof bracing systems in low-rise steel buildings. *Engineering Structures*, 31(12), pp.2933–2940.

− Galambos, T. V. and Surovek, A. E. (2008). *Structural Stability of Steel: Concepts and Applications for Structural Engineers*. John Wiley and Sons.

− Gomez, I. R., Higgins, C. and Mahoney, M. (2010). Performance of post-installed anchors in rehabilitated steel structures. *Journal of Structural Engineering*, 136(3), pp.302–311.

− Hancock, G. J. (2003). *Design of Cold-Formed Steel Structures*. Australian Steel Institute.

− Holmes, J. D. (2015). *Wind Loading of Structures* (3rd ed.). CRC Press.

− Kayser, J. R. and Nowak, A. S. (1989). Capacity loss due to corrosion in steel-girder bridges. *Journal of Structural Engineering*, 115(6), pp.1525–1537.

− Landolfo, R., Cascini, L. and Portioli, F. (2010). Sustainability and life-cycle assessment of steel structures undergoing atmospheric corrosion. *Open Construction and Building Technology Journal*, 4, pp.34–44.

− Lewis, P. R. (2007). *Forensic Materials Engineering: Case Studies*. CRC Press.

− Maleck, A. E. (2006). *Practical second-order inelastic analysis and stability design of steel frames using ELM formulations*.

− McGuire, W., Gallagher, R. H. and Ziemian, R. D. (2000). *Matrix Structural Analysis* (2nd ed.). John Wiley and Sons.

− Mechanics of Built-up Compression Members. *Section E6 of AISC 360-16*. American Institute of Steel Construction.

− Melchers, R. E. (1999). *Structural Reliability Analysis and Prediction* (2nd ed.). John Wiley and Sons.

− Nethercot, D. A. (2000). *Joints in Structural Steelwork: Secondary Moments and*

Uncalculated Partial Restraints. CRC Press.

− Noon, R. K. (2000). *Forensic Engineering Investigation: Reverse Engineering and Forensic Diagnostics*. CRC Press.

− Packer, J. A., Wardenier, J., Zhao, X. L., van der Vegte, G. J. and Kurobane, Y. (2010). *Design Guide for Rectangular Hollow Section (RHS) Joints* (2nd ed.). CIDECT.

− Ratay, R. T. (Ed.). (2009). *Forensic Structural Engineering Handbook* (2nd ed.). McGraw-Hill Education.

− Ratay, R. T. (2010). *Structural Condition Assessment of Existing Infrastructure*. John Wiley and Sons.

− Revie, R. W. and Uhlig, H. H. (2008). *Corrosion and Corrosion Control* (4th ed.). John Wiley and Sons.

− Salmon, C. G., Johnson, J. E. and Malhas, F. A. (2009). *Steel Structures: Design and Behavior* (5th ed.). Pearson.

− Sharifi, Y. and Rahgozar, R. (2010). Remaining moment capacity of corroded steel beams. *International Journal of Steel Structures*, 10(1), pp.43–51.

− Simiu, E. and Wright, R. N. (2006). *Wind Effects on Structures: Fundamentals and Applications to High-Altitude Topography*. John Wiley and Sons.

− Simiu, E. and Yeo, D. (2019). *Wind Effects on Structures: Modern Structural Engineering Design for Wind* (4th ed.). John Wiley and Sons.

− Surovek, A. E. and Ziemian, R. D. (2005). Direct analysis method for design of steel frames. *Journal of Structural Engineering*, 131(11), pp.1700–1710.

− Wang, T., et al. (2015). Scan-to-FEM workflow for the digital documentation of structural assets. *Automation in Construction*, 55, pp.12–24.

− Wang, Y., Xu, S., Wang, H. and Li, A. (2017). Experimental and numerical investigation on the axial compression behavior of corroded steel tubular members. *Thin-Walled Structures*, 120, pp.281–295.

− White, D. W. (2013). Stability design of steel buildings: Assumptions and recent advances. *AISC Engineering Journal*, 50(4), pp.231–255.

− White, D. W. and Griffith, M. (2007). Stability design of steel frames: Comparative frameworks. *Journal of Constructional Steel Research*, 63(9), pp.1200–1215.

− Yu, W. W. and LaBoube, R. A. (2010). *Cold-Formed Steel Design* (4th ed.). John Wiley Extent.

− Ziemian, R. D. (2010). *Guide to Stability Design Criteria for Metal Structures* (6th ed.). John Wiley and Sons.

– Ahn, J.-H., Jeon, S.-H., Jeong, Y.-S., Cho, K.-I. and Huh, J. (2018). Evaluation of residual compressive strength and behavior of corrosion-damaged carbon steel tubular members. *Materials*, 11(7), 1254.

– Toledo, K. K., Kim, H.-S., Jeong, Y.-S. and Kim, I.-T. (2020). Residual compressive strength of short tubular steel columns with artificially fabricated local corrosion damage. *Materials*, 13(4), 813.

– Kala, Z. and Valeš, J. (2018). Imperfection sensitivity analysis of steel columns at ultimate limit state. *Archives of Civil and Mechanical Engineering*, 18(4), pp.1207–1218.

– ASTM International. (2017). Standard practice for measuring life-cycle costs of buildings and building systems. *ASTM E917-17e1*. ASTM International.

– Kneifel, J. and Webb, D. (2022). Life cycle costing manual for the Federal Energy Management Program. *NIST Handbook 135*. National Institute of Standards and Technology.

– Federal Highway Administration (FHWA). (2002). Life-cycle cost analysis primer. *U.S. Department of Transportation, Federal Highway Administration*, FHWA-IF-02-047.

– American Welding Society (AWS). (2020). Structural welding code—steel. *AWS D1.1/D1.1M:2020*. American Welding Society.

– European Committee for Standardization (CEN). (2006). Hot finished structural hollow sections of non-alloy and fine grain steels—Part 2: Tolerances, dimensions and sectional properties. *EN 10210-2:2006*. CEN.

– Jordanian National Building Council (JNBC). (2006). Loads and forces code. *Jordanian National Building Code*. Amman, Jordan.

– World Bank. (2014). West Bank and Gaza: Rapid damage, loss and needs assessment of Winter Storm Alexa. *World Bank Report*. World Bank.